Defense Nuclear Agency
6801 Telegraph Road
Alexandria, Virginia 22310-3398

OPSSI

1 March 1996

MEMORANDUM FOR DISTRIBUTION

SUBJECT: Declassification Review of Operation BUSTER-JANGLE Test Reports

The following 100 reports concerning the atmospheric nuclear tests conducted during Operation BUSTER-JANGLE in 1951 have been declassified and cleared for open publication/public release:

WT-301 thru WT-306, WT-309 thru WT-319, WT-321 thru WT-351, WT-353, WT-354, WT-356 thru WT-370, WT-372, WT-374 thru WT-385, WT-388 thru WT-390, WT-392, WT-393, WT-396, WT-398 thru WT-402, WT-405 both volumes thru WT-407, WT-409, WT-410, WT-412, WT-415, WT-417, Wt-418, WT-422 and WT-423

An additional 12 WTs from BUSTER-JANGLE have been re-issued with deletions and are identified with an "EX" after the WT number. These reissued versions are unclassified and approved for open publication. They are:

WT-308, WT-320, WT-371, WT-373, WT-386, WT-391, WT-394, WT-395, WT-397, WT-404, WT-414 and WT-425

This memorandum supersedes the Defense Nuclear Agency, ISTS memorandum same subject dated August 22, 1995 and may be cited as the authority to declassify copies of any of the reports listed in the first paragraph above.

RITA M. METRO
Chief, Information Security Section

A Facsimile Report

Reproduced by
UNITED STATES
ATOMIC ENERGY COMMISSION
Division of Technical Information
P.O. Box 62 Oak Ridge, Tennessee 37831

WT

368

1 OF 7

LEGAL NOTICE

This report was prepared as an account of Government sponsored work. Neither the United States, nor the Commission, nor any person acting on behalf of the Commission:

A. Makes any warranty or representation, expressed or implied, with respect to the accuracy, completeness, or usefulness of the information contained in this report, or that the use of any information, apparatus, method, or process disclosed in this report may not infringe privately owned rights; or

B. Assumes any liabilities with respect to the use of, or for damages resulting from the use of any information, apparatus, method, or process disclosed in this report.

As used in the above, "person acting on behalf of the Commission" includes any employee or contractor of the Commission, or employee of such contractor, to the extent that such employee or contractor of the Commission, or employee of such contractor prepares, disseminates, or provides access to, any information pursuant to his employment or contract with the Commission, or his employment with such contractor.

UNCLASSIFIED
SECRET

WT-368

[redacted]

Copy 171 of 243 copies, Series B

OPERATION JANGLE

BLAST AND SHOCK MEASUREMENTS III

Project 1.5a	Transient Ground Displacement Measurement (WT-382)
Project 1.5b	Detection of Time of Arrival of First Earth Motion (WT-386)
Project 1.6	Earth Displacements (Shear Shafts) (WT-353)
Project 1.7	Ground Acceleration (Shock Pins) (WT-357)
Project 1(9)a	Ground Acceleration, Ground and Air Pressures for Underground Test (WT-380)
Project 1(9)b	Base Surge Analysis for Nuclear Tests (WT-390)

SECRET
UNCLASSIFIED

UNCLASSIFIED

SECRET

WT-382

OPERATION JANGLE

Project 1.5a

TRANSIENT GROUND DISPLACEMENT MEASUREMENT

By

W. E. Morris

U. S. Naval Ordnance Laboratory
White Oak
Silver Spring 19, Maryland

Classification cancelled or changed to UNCLASSIFIED
by authority of Lt. Jr. Capt. J. L. W. Pritchard, DASA, dated Sept. 16, 1959
by [illegible] TID date 10/6/59

SECRET

RESTRICTED DATA
ATOMIC ENERGY ACT 1946

UNCLASSIFIED

SECRET

PROJECT 1.5a

CONTENTS

SECRET

RESTRICTED DATA
ATOMIC ENERGY ACT 1946

ILLUSTRATIONS

TABLES

[redacted]
PROJECT 1.5a

PREFACE

This project was carried out essentially as a part of Project 1.1 For administrative details and acknowledgements, reference may be made to the Project 1.1 report, Measurement of Acceleration.

ABSTRACT

An attempt was made to measure the transient ground displacement for the surface and underground shots of Operation JANGLE. The method of high speed photography of the ground motion is described. Negative results were obtained for both the surface and underground shots. This method does not appear promising for any future nuclear surface tests. With good photography, this method has considerable promise for underground nuclear explosions and is recommended for future tests.

CHAPTER 1

INTRODUCTION

1.1 OBJECTIVE

The objective of this project was to measure the transient ground displacement produced by the surface and underground explosions of atomic weapons and to correlate this displacement with ground acceleration and damage to structures.

1.2 HISTORICAL

In the planning stages of medium measurements it was recognized that ground motion was an important parameter that should be measured. While it was determined that major emphasis would be placed on ground acceleration and pressure measurements, it was decided that ground displacement measurements would also be included in the program.

Along with the method of high speed photography which was adopted and is described in this report, some thought was given to measuring ground displacement by means of a displacement gage. Preliminary plans for such a gage were drawn up, but due to the stringent time schedule, personnel were not available for further work, and this effort was suspended.

CHAPTER 2

THEORY AND PREDICTIONS

2.1 LAMPSON THEORY

The only available theory on transient displacement resulting from underground explosions was that of C. W. Lampson[1], who derived empirical formulae for displacement from data on small charge work. Lampson's formulae for maximum transient displacement are as follows:

$$D_H = \frac{FW^{1/3}}{17.2} K^{1/3}(3.94\lambda^{-3} + .0018\lambda^{-1})$$

$$D_V = \frac{FW^{1/3}}{17.2} K^{1/3}(1.05\lambda^{-3} + .0027\lambda^{-1})$$

where D_H and D_V are the maximum horizontal and vertical transient displacement respectively (ft)

W = weight of TNT (lbs)

K = soil constant and is equal to $1/25\,\rho\,v^2$,

where ρ is the soil density ($\frac{\text{lbs}}{384\ \text{in}^3}$)

and v is the velocity (in/sec)

F = coupling factor determined by the depth of burial of the charge

F = 0.21 for a charge on the surface

F = 0.32 for $\lambda_c = 0.135$, where λ_c is equal to the depth of burial (ft) divided by $W^{1/3}$. This is the λ_c value for a 1 KT bomb at a depth of 17 ft

$\lambda = r/W^{1/3}$ where r is the distance from the center of the charge (ft).

1 C. W. Lampson, Final Report on Effects of Underground Explosions NDRC Report No. A-479, OSRD Report No. 6645.

2.2 PREDICTIONS FOR THE AMCHITKA SITE

In the original planning for the Amchitka site, predictions were made on the basis of a 20 KT weapon and a soil constant of 43,000. For these assumptions, the Lampson formulae predicted a maximum displacement of 25 feet for the first station planned at 1,000 feet and a displacement of 0.2 feet at the farthest station at 5,000 feet. This anticipated displacement influenced the location of the first accelerometer station, since such large displacements would most certainly break any cable transmitting information from a close-in station.

2.3 PREDICTIONS FOR THE NEVADA SITE

When the site was moved to the Yucca Flats site at the Nevada Proving Grounds, the ground displacement predictions were revised (Table 2.1) to conform with a 1 KT weapon and a soil constant of 8,000 for distances close in and 18,000 for distances far out. The displacement stations are identical with the accelerometer stations of Project 1.1, since correlation of acceleration and displacement was desired. The maximum displacement is given by the equation for the horizontal component, so this equation was used for predicting the maximum transient displacement. Also the predictions are for the underground shot. For a surface shot the theory predicts that the displacement should be two thirds that of the underground shot.

TABLE 2.1

Maximum Transient Ground Displacement Predictions for the Underground Nuclear Test at Yucca Flats

Station	Distance from Zero (ft)	Predicted Maximum Displacement (ft)
1	275	17
2	340	8.5
3	420	4.1
4	520	3.4
5	642	1.7
6	794	1.0
7	982	0.5
8	1213	0.3
9	1500	0.2
10	1890	0.1

2.4 EFFECT OF HE TESTS AT YUCCA FLATS

The HE tests at Yucca Flats prior to the nuclear shots indicated that the acceleration results did not agree with the Lampson formula for acceleration. In particular, the acceleration followed a different attenuation curve[2] and predictions close in were a factor of four greater than realized in the results. This would indicate that the displacement would follow a similar pattern, but lacking definite information, it was decided to use the Lampson predictions. Time was not taken to make more exact estimates to conform to the HE results, since the method of measurement could cover a wide latitude.

---

[2] Ground Acceleration Measurements, Project 1.1, Operation JANGLE, Chap. 2, Section 2.4.

CHAPTER 3

PROCEDURE

High speed photography of ground motion was adopted as a direct and convenient method of measuring transient ground displacement. Fiducial markers, 3' x 3' in area and painted in alternate black and white squares, were installed on telephone poles at a height of 10 feet above the ground. The movement of these markers, representing the motion of the ground, was to be recorded by high speed photography. The fiducial markers were installed at the accelerometer stations, and the telephone poles were buried to a depth of 10 feet, the depth of most of the accelerometer gages; thus, ground motion at the location of the acceleration measurements would be obtained, enabling direct comparison of acceleration and displacement. Cameras were located 5,000 feet from ground zero (Fig. 3.1) and were to record the radial and vertical motion of the ground of the first ten accelerometer stations.

The photography was carried out by the Sandia Photographic Laboratory. Predicted maximum displacement (Table 2.1) and location of the fiducial markers were supplied to Sandia along with specifications for Mitchell cameras to be operated at 100 fps and with 100 cps timing.

Sandia estimated that with the arrangement of Fig. 3.1, the lower limit of displacement that could be detected would be of the order of 0.1 feet. For this reason it did not appear feasible to attempt to measure ground motion beyond station 10.

The films were to be analyzed by the Sandia Laboratory for horizontal and vertical ground motion as a function of time, and this data was to be transmitted to the NOL for further analysis.

Identical procedures were followed on both the surface and underground shots.

CHAPTER 4

RESULTS

4.1 SURFACE SHOT

Inspection of the films revealed that the fiducial markers were clearly visible prior to the time of detonation. Because the cameras were not set for exposure to bomb light, the film is overexposed immediately after detonation, and by the time the bomb light has diminished sufficiently, the air blast and ground shock have passed and dust has obscured the markers. For these reasons ground motion was not observed on the surface shot.

It might be mentioned that the air blast, which arrived ahead of the ground shock out to 420 ft (λ = 3.3), was of considerable magnitude, and all of the fiducial markers and some of the poles for the first five stations were blown down.

4.2 UNDERGROUND SHOT

Better results were anticipated for the underground shot because (1) the bomb light would be much less and (2) the air shock would be greatly diminished and should lag further behind the ground shock than on the surface shot. Unfortunately, no results on transient ground displacement were obtained from the photographic films of the underground shot. According to the Sandia Photographic Analysis Report, only four of the ten fiducial markers could be identified on the film. The first four stations, where appreciable displacement was expected, were among those missing. The stations that were identified were stations 4 to 7 (520 ft to 982 ft) and for these no motion was detected. The reasons for lack of film data are not known to the author. In viewing the several films identified with the photography of the ten stations, only one fiducial marker was visible to the author.

The reduced air blast effect was evident from the fact that all of the fiducial markers were still standing after the explosion.

CHAPTER 5

CONCLUSIONS AND RECOMMENDATIONS

5.1 CONCLUSIONS

5.1.1 Surface Shot

If the cameras had been set for bomb light exposure, some motion might have been detected for the close-in stations. The ground motion observed would have been due principally to air induced ground shock, since it preceded the directly propagated ground shock, and most of the latter ground shock motion would have been obscured by the dust raised by the air blast. Further out where the true ground shock overtook the air blast, there was probably insufficient ground movement to be detected by the photographic method.

In general, the photography of ground motion for a nuclear surface shot does not appear promising for future tests. The difficulty arises from the effect of the considerable air blast; preceding the arrival of the ground shock at the close-in distances, this air blast disturbs the fiducial markers prior to ground shock arrival, induces a ground shock of its own, and produces a dust which quickly obscures any target. If any future attempts are made to photograph ground motion from a surface shot, exposure for bomb light is essential.

5.1.2 Underground Shot

It is quite probable that with good photography ground motion could be detected for an underground nuclear explosion of the same scale depth as that of the JANGLE shot. The factors contributing to this conclusion are: (1) the bomb light is greatly reduced over that of the surface shot, (2) the air blast is much less than that for the surface shot and its effect on ground motion and targets is considerably decreased relative to displacement produced by ground shock, (3) the ground shock arrives prior to the air blast, and (4) ground motion could probably be observed before dust, reduced and delayed compared to that from a surface shot, would obscure a target.

As the depth of burial increases, detection of ground motion by photography becomes more and more certain, inasmuch as the air blast becomes negligible and at the same time the magnitude of the ground displacement increases.

For a larger charge at the same scale distance (λ), the displacement should increase as $W^{1/3}$, so a larger bomb would be more favorable for ground motion measurement.

5.1.3 Estimate of Permanent Displacement

It is certain that from post observation of the area and from the shear shaft results that the permanent displacement was very much less than predicted from Table 2.1. The post test survey, which is not available at the time of writing, will give an accurate measurement of permanent displacement, and this will indicate the order of magnitude of the transient displacement. As a guess it appears that the transient displacement at the nearest station (λ = 2.2) was not over a foot at most.

5.2 RECOMMENDATIONS

Recommendations for future atomic tests are as follows:

(1) Measurement of transient ground displacement by means of high speed photography of ground motion is recommended for underground explosions of atomic weapons of 1 KT yield or greater. This method is particularly recommended for weapons of yield larger than 1 KT and for charges buried at a scale depth deeper than the JANGLE underground shot.

(2) Measurement of transient ground displacement by high speed photography is not recommended for any atomic weapon detonated at the surface.

(3) High speed photography of ground displacement starting at zero distance and proceeding out to the limits of detection are recommended for future tests.

(4) A ground displacement gage should be developed for future tests in order to supplement photographic measurements.

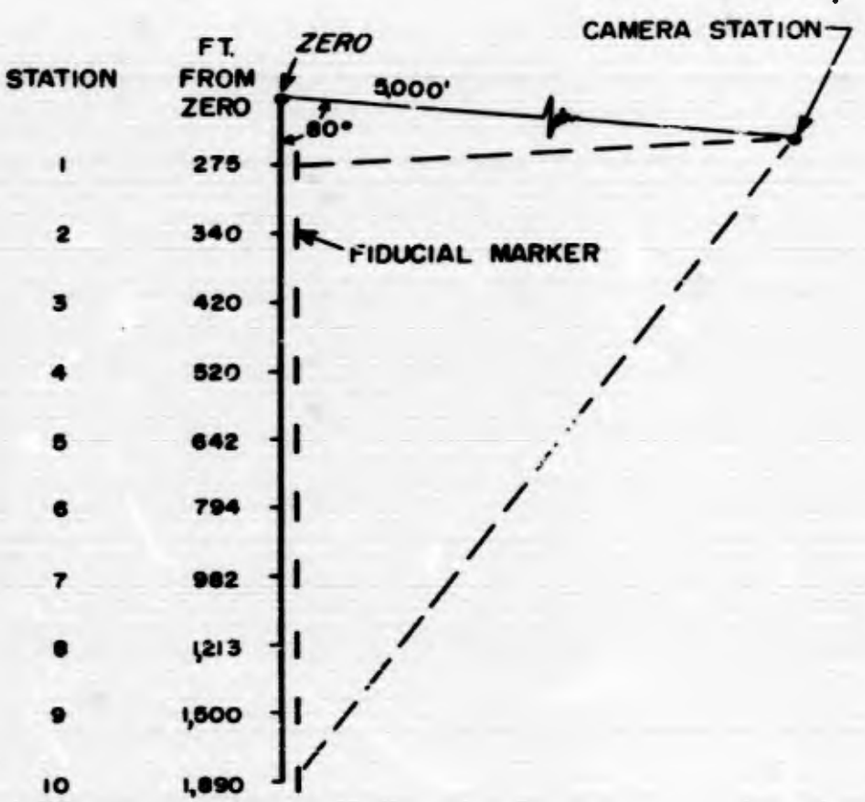

Fig. 3.1 Location of Fiducial Markers and Camera Station for the Surface and Underground Tests

OPERATION JANGLE

PROJECT 1.5b

Detection of Time of Arrival of First Earth Motion

by

George W. Cook

and

W.P. Kiley

1 April 1952

DAVID W. TAYLOR MODEL BASIN

Washington 7, D.C.

CONTENTS

ILLUSTRATIONS

TABLE

ABSTRACT

Under JANGLE Project 1.5b, necessary instrumentation was developed and measurements were made on the underground burst of time of arrival of the first detectable earth motion at each of ten stations located between 100 feet and 600 feet from ground zero. The instrumentation consisted of seismic detectors which triggered electronic flash lamps; the time sequence of the lamp flashes was recorded photographically from a remote camera station.

The data obtained shows the time of arrival at Station 1 (100 feet) to be 26.6 milliseconds and to increase somewhat linearly to 234 milliseconds at Station 10 (542 feet). This report presents the data in both tabular and graphical form and discusses the instrumentation and methods developed to carry out the measurements.

ACKNOWLEDGMENTS

In addition to the authors, other members of the David Taylor Model Basin staff involved in the work of Project 1.5b were:

Frederick B. Bryant

Willis S. Campbell

Vernon E. Benjamin

Henry B.O. Davis

Maxwell E. Graybill

The preliminary test of the system on the HE-2 Shot was conducted by the authors.

CHAPTER 1

INTRODUCTION

1.1 OBJECTIVE

The objective of Project 1.5b was to obtain a measurement of time of arrival of the first detectable earth motion at each of ten stations located on a radial line outward from ground zero on the underground burst. These stations were located at points between 100 ft. and 600 ft. from ground zero, covering the region between the "close-in" measurements of Project 1.2b and the "farther-out" measurements of Projects 1.1 and Project 1.2a.

A secondary objective of the project was to evaluate a method of recording such data by photographing, from a remote station, signals from high-speed electronic flash lamps located at each measurement station, thus eliminating the need for an interconnecting wire or radio link.

1.2 DESIGN OF INSTRUMENT

Instrumentation to accomplish these objectives was designed at the David Taylor Model Basin during July and August 1951. The proposed method of measurement involved the use of a seismic detector and an electronic flash lamp unit, for each station. Photography of the flash lamp signals from a remote camera station was to be performed by the Sandia Corporation under Project 4.1, and the photographic instrumentation is therefore not discussed in this report.

Three prototype units were installed at selected representative locations on the HE-2 shot fired 3 September 1951, for the purpose of proof-testing the instruments. In this test, the sensitivity of the seismic detectors was set at 0.9 "g". The results obtained indicated that this sensitivity was much too poor to give an accurate indication of time of arrival of earth motion, due apparently to the relatively slow buildup of acceleration caused by the motion. It was decided, therefore, to design a new detector having a sensitivity as great as 0.01 "g", for use on the underground burst.

At this same time the possibility of the electronic flash tubes being prematurely triggered by radiation was discussed and it was decided that the electronic units should be located underground so that at least three feet of earth would be interposed between the flash lamp and

the initial burst of the bomb. This decision necessitated complete redesign of the apparatus originally planned.

This report describes the instrumentation designed for the project and presents the data obtained on the test, in both graphical and tabular form. The analysis of the data is not a part of this project.

CHAPTER 2

INSTRUMENTATION

2.1 GENERAL

The instrumentation for Project 1.5b was located at ten stations on the main blast line of the underground burst at distances of 100, 125, 150, 178, 217, 262, 314, 378, 456 and 542 feet from ground zero. At each station there was a seismic detector, or gage, an electronic flash unit, and a storage battery for supplying power to the electronic unit.

2.2 SEISMIC DETECTOR

The detector shown in Figure 2.1 is fundamentally a seismic switch the sensitivity can be adjusted after it has been installed in the ground in its final position. The functional parts of the switch consist of a stationary electrically insulated contact, and a pendulum. The electrical conductivity between the two is determined by the physical shape of the points of contact and the force holding them together. This force is directly proportional to the weight of the pendulum times the sine of the angle by which the pendulum deviates from true vertical. When an acceleration equal to the sine of this angle is applied in a horizontal plane, from the proper direction, the force holding the contacts together disappears and the electrical contact is open. It can readily be seen by referring to Figure 2.1 that the topside adjustment of the sensitivity is made by rotation of the lead screw, which raises or lowers the pendulum.

The sensitivities used for the underground burst were set so that a horizontal acceleration of 0.02 "g" would open the switch which, in turn, initiated the operation of the Electronic Flash Unit.

2.3 THE ELECTRONIC FLASH UNIT

The Electronic Flash Unit is shown in Figure 2.2 and schematically in Figure 2.3, and is basically similar to several types of commercial battery-operated flash units. The unit is made up of a vibrator type power supply, two energy-storage capacitors, an FT-220 flash tube, and the thyratron-triggering circuit. The two 25 ufd storage condensers are

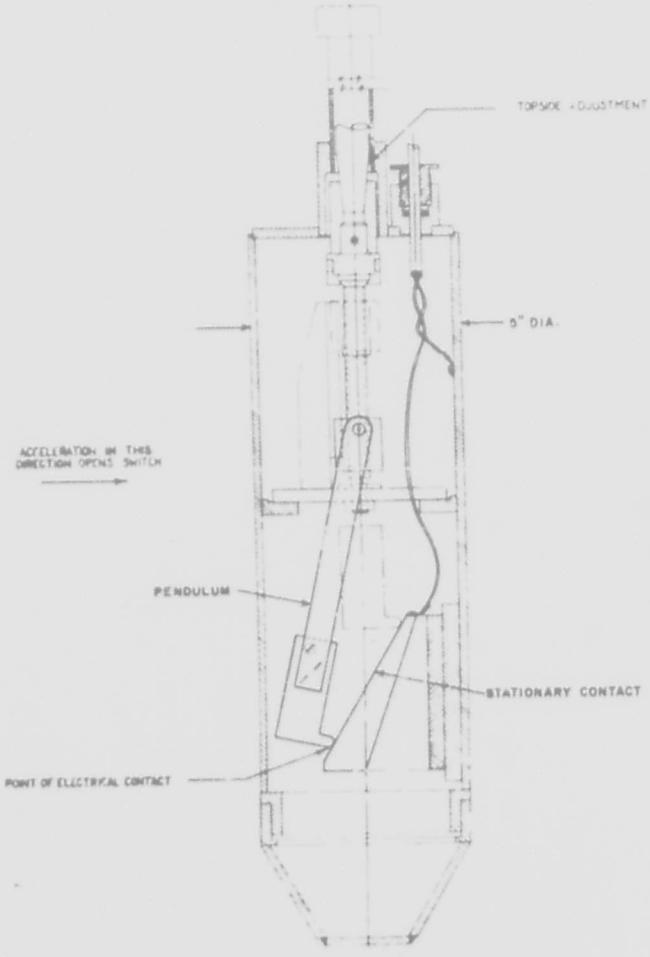

Figure 2.1 Seismic Detector

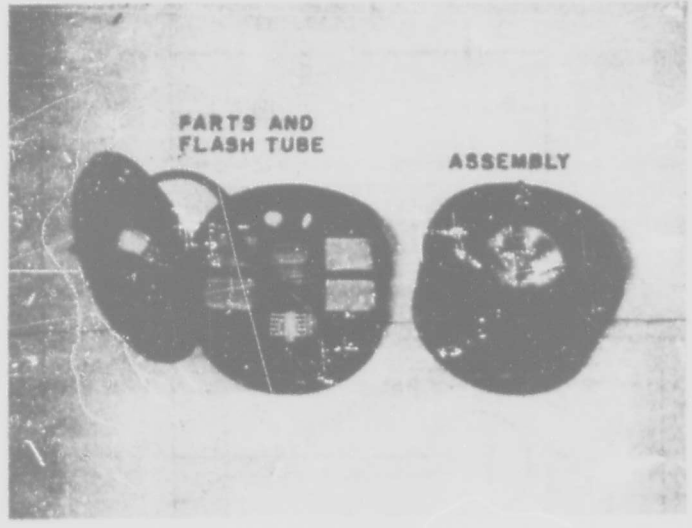

Figure 2.2 Electronic Time Unit

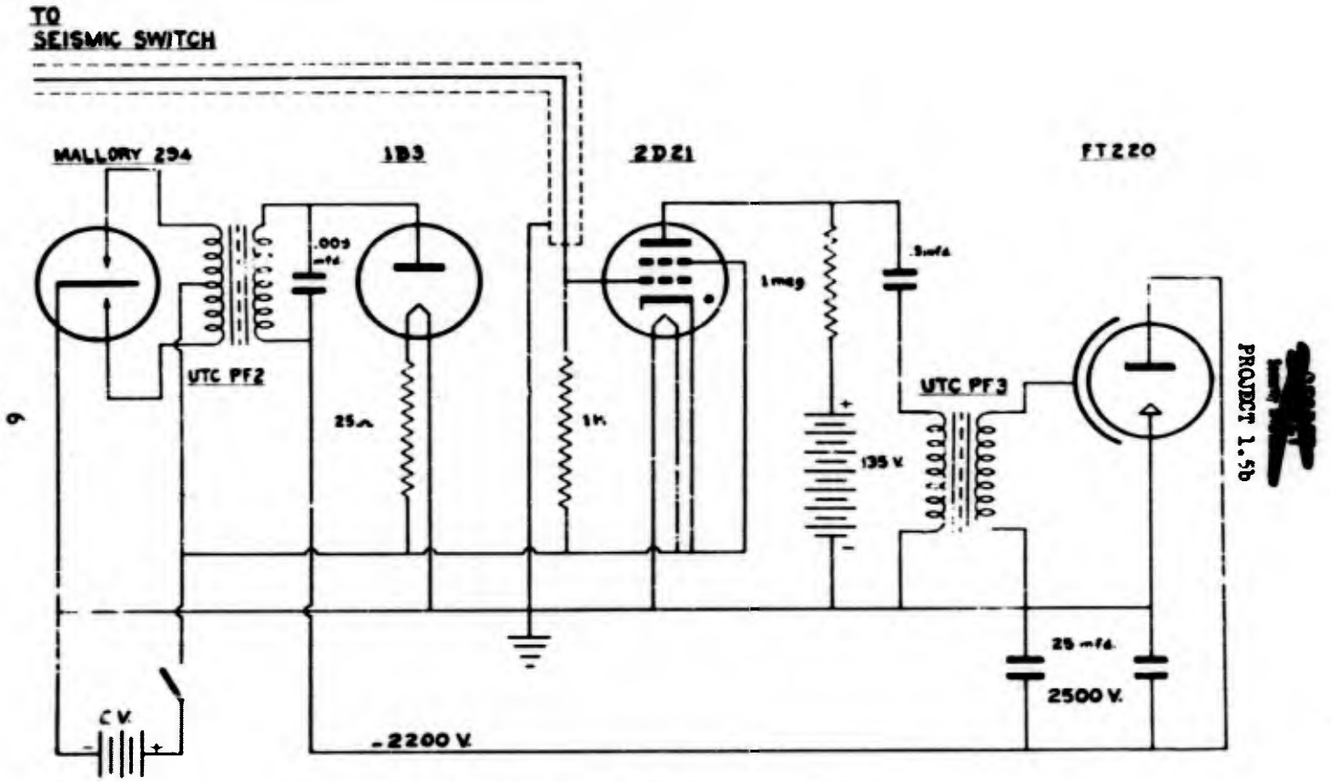

Figure 2.3 Electronic Flash Unit

charged up to 2200 volts within about 30 seconds after the unit is turned on. The electrodes of the flash tube are connected directly across these two storage condensers and the flash tube is then ready to flash whenever it is triggered by the thyratron circuit. The six volts from the storage battery is utilized to bias the thyratron and keep it in a nonconducting state. This biasing voltage is removed whenever the normally closed seismic switch circuit is opened and the electronic flash tube is immediately triggered. The energy of the resulting flash is approximately 200 watt seconds and the intensity reaches a maximum in about 40 microseconds.

2.4 INSTALLATION AND OPERATION

A typical instrumentation setup for any one of the ten stations is shown in Figures 2.4 and 2.5. The gage was buried to a depth of five feet allowing about a foot of the pipe to protrude above the surface of the ground. Adjustment of the sensitivity of the gage was made by means of a long wrench inserted in this pipe after the gage was placed in the ground. The gage cable was buried at a depth of about a foot and a half and connected to the electronic flash unit which was located at a nearby location having a clear line of sight to the camera tower. The flash unit was located in the bottom of a large cylindrical container which extended about four feet underground and about one foot above ground. This container and the mirror housing mounted on top of the cylinder were made of 1/16 in. furniture steel. The 12 inch square mirror located directly above the flash lamp was mounted at 45 degrees from vertical and was adjustable in both the vertical and horizontal planes permitting easy direction of the flash beam to the camera.

The storage battery was a conventional automobile type having a capacity of one hundred ampere hours.

The remainder of the instrumentation required for these measurements was installed and operated by the Sandia Corporation under Project 4.1 and consisted of two remote recording camera stations. All ten of the flash units were visible at one of the camera stations and five were visible at the other. The main recording was made at the camera tower located at about 9000 ft. east of ground zero. The camera used was an aerial type camera modified to record as a streak camera and was operated at an approximate film speed of 32 feet per second.

The results obtained agreed substantially for the five stations recorded simultaneously by both cameras.

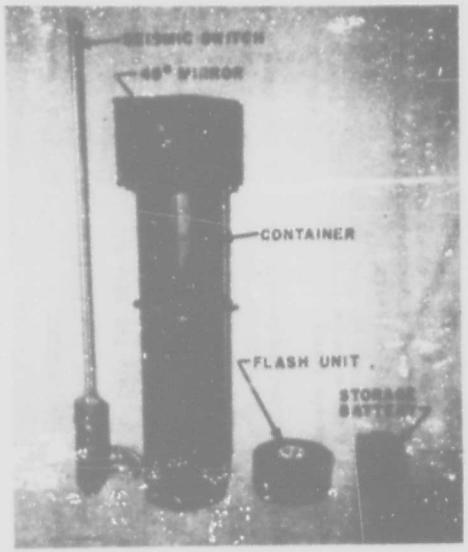

Figure 2.4 Parts for Instrumentation Used at Each Measurement Station

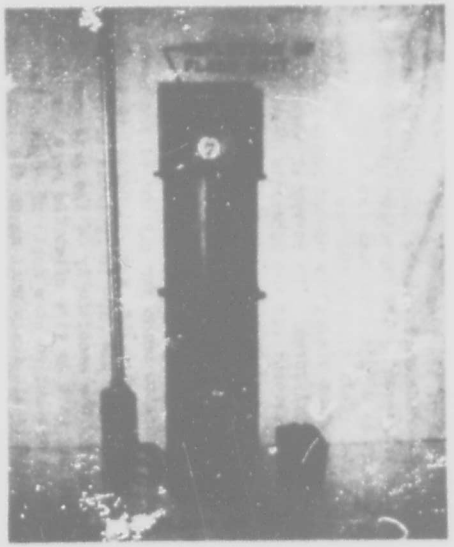

Figure 2.5 Partial Assembly of Instrumentation Used at Each Measurement Station

CHAPTER 3

TEST RESULTS

3.1 GENERAL

The test results are tabulated in Table 3.1 and shown graphically in Figure 3.1. All ten of the Electronic Flash Units operated, but, for reasons unknown to the authors, the switch at Station 6 (262 ft.) and the switch at Station 8 (378 ft.) were both actuated at times inconsistent with the time of activation of the other switches.

TABLE 3.1

Time of Arrival of First Earth Motion

Station	Distance from Ground Zero feet	Time from Zero Time milliseconds
1	100	26.60
2	125	33.90
3	150	38.90
4	178	44.60
5	217	57.60
6	262	7.40*
7	314	82.70
8	378	65.60*
9	456	107.40
10	542	133.60

*These two readings appear inconsistent with the readings from the other eight stations and are, therefore, not considered valid.

SECRET

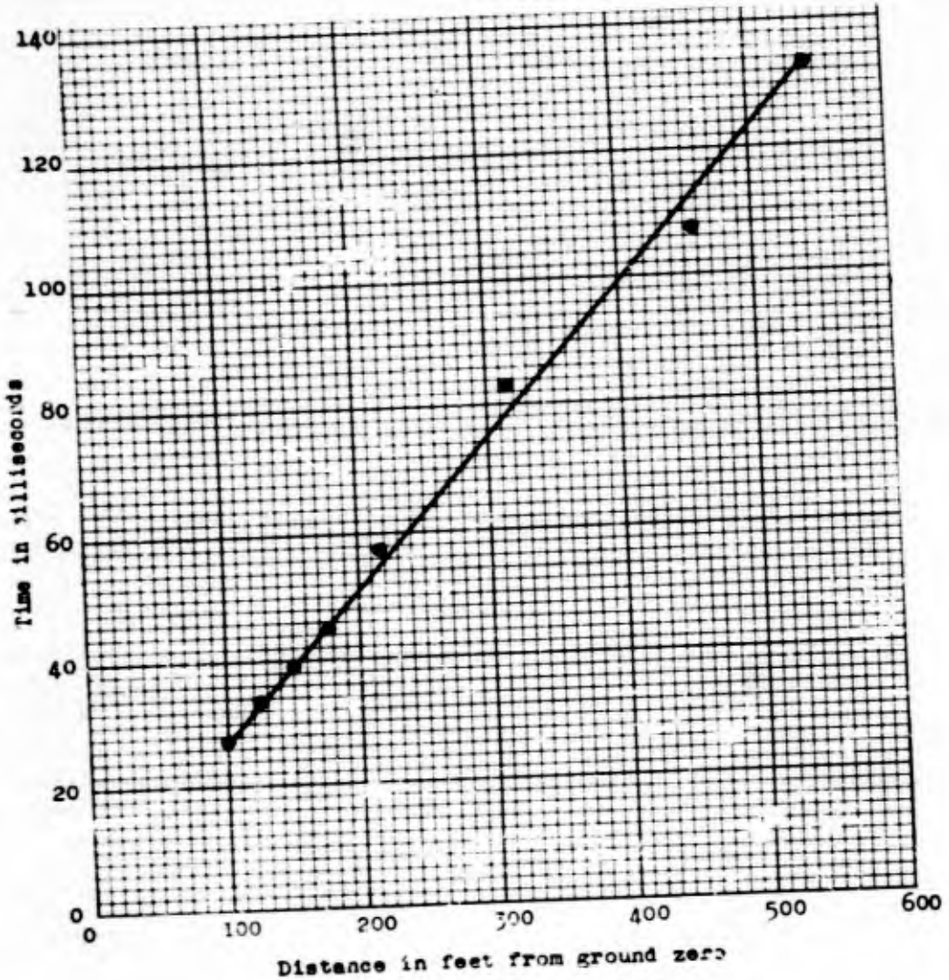

Figure 3.1 Time of Arrival

CHAPTER 4

DISCUSSION

4.1 SUCCESS OF RECORDING METHOD

The method of recording time of arrival of earth motions employed by this project could very easily be adapted to the recording of other types of phenomena wherein an indication of a certain condition at successive stations, as a function of time, is the information desired. Recording by this means has both desirable and undesirable features. Each station is a simple, complete, self-powered, integral unit requiring no timing signals or connecting cables and can be installed in an hour or two. Once it is installed it requires no further attention except to turn it on a few hours prior to zero time. On the other hand great care must be taken in the placing of the flash units relative to ground zero to prevent the outburst of light of the explosion from obscuring the flashes from the close-in stations. It is also necessary to place the electronic flash units underground to avoid the possibility of ionization of the flash tube by radiation. It is the opinion of the authors that, if due precautions are taken, these dangers can be avoided.

[redacted]

OPERATION JANGLE

PROJECT 1.6

EARTH DISPLACEMENT

(SHEAR SHAFTS)

April 1952

Prepared by
The Ohio River Division Laboratories
Mariemont, Ohio
for
Office of the Chief of Engineers
Engineering Division
Civil Works

[redacted]

[redacted]

PREFACE

This report contains methods of tests and test data for permanent displacements in the ground at various distances from ground zero of a surface and a shallow underground explosion of atomic bombs. Each bomb had a computed radiochemical yield of about one and two-tenths (1.2) kilotons.

The necessity for early completion of the report precludes incorporation of data pertaining to precise permanent displacements, and engineering properties of the soil at the Nevada Test Site. This information, requested of others, is expected to be available at a later date.

Conclusions and recommendations are predicated on permanent displacement information obtained from pre- and post-shot test data.

ACKNOWLEDGMENTS

The Ohio River Division Laboratories, Corps of Engineers, U. S. Army, Mariemont, Ohio, have designed, developed and tested the special instruments needed, and were responsible for the field surveys, analysis of data and preparation of reports. Mr. Henry J. Kurtz, Chief of the Electrical Measurements Branch, and his assistant, Mr. Curtis A. Anderson, were in charge of this work at the Laboratories and in the field, under the direction of the Project Officer, Mr. Harald J. Sundstrom of the Office of the Chief of Engineers.

[redacted]

RESTRICTED DATA
ATOMIC ENERGY ACT 1946

PROJECT 1.6

CONTENTS

ILLUSTRATIONS

ABSTRACT

No significant permanent movement, either vertically or radially, was observed for any of the shafts in the surface shot area. In the underground shot area, definite and significant movements were observed only for the two innermost shafts (at 250' and 312.5') on the main (south) blast line, each shaft being displaced radially outward less than a foot at the ground surface. Vertical movements of the tops of the shafts at these same locations were considerably less and of the order of 0.75 to 1.5 inches downward. The horizontal and vertical movements observed were due principally to rotation and translation of the top five foot segment of pipe and should not be interpreted as applicable to the entire shaft as a unit. For the conditions and locations in effect in these tests, it appears that major permanent displacements will not extend beyond approximately two and three lambda for surface and shallow underground shots, respectively, except for possible local disturbances very near the ground surface. There is considerable asymmetry in permanent displacements about ground zero in the underground tests.

[redacted] Information

CHAPTER 1

INTRODUCTION

1.1 OBJECTIVE

The principal objective of Project 1.6 was to determine the approximate limits and amount of permanent displacements to be expected in the plastic zones surrounding the earth craters caused by surface and shallow underground explosions of atomic weapons. This type of information is needed in order to permit more realistic appraisals of probable structural damage in terms of differential displacements in all directions in soil masses; and would be of particular value in enhancing the accuracy and economy of plans for emergency restoration of strategic facilities. These data, when correlated with similar information from future tests in other types of foundation material, should permit reasonably accurate predictions of the effects of atomic bombing attacks occurring on or near rock-fill or earth dams, levees, and structural foundations, particularly for those structures requiring piling or caissons for stability.

Only permanent displacements were measured. Data on transient displacements of other installations in the areas may be available at a later date when the records and notes of other projects in Programs One and Three have been fully reduced; and should be analyzed in any future attempt to correlate transient and permanent displacements. There were also more than 100 concrete monuments constructed at each of the surface and underground areas by other projects and are to be used to determine permanent displacemen along at least eight radii. These displacements are currently being surveyed by the U. S. Coast & Geodetic Survey.

1.2 HISTORICAL

No information has been found of any previous attempts to determine permanent displacements at significant depths below the ground surface. Summary data on permanent displacements at the ground surface are available for a wide range of soil types and charges and may be found in reports dealing with the Camp Gruber tests under C. W. Lampson, the Dugway tests of the Corps of Engineers, the Third Isthmian Canal Studies (1947) for the Panama Canal, and summary reports of our foreign allies, such as A Second Survey of Ground Shock Effects (British Ministry of Home Security). However, very little of this work has been done at the shallow charge depths comparable to the JANGLE tests and no tests are known in soil similar to the Nevada Test Area media except

for the high explosive tests which preceded this Operation. The survey notes on permanent displacements from the high explosive tests at the Nevada Test Site have been examined but do not appear to scale when used as a basis for atomic predictions, if the conventional formulae now in general acceptance are applied. The high explosive test (No. HE-2) at the Nevada Test Site using 40,000 pounds of T.N.T. detonated at a lambda depth of 0.150 corresponds closer to the conditions of the underground atomic burst than any previous research.

1.3 BASIC THEORY

No theoretical analysis of crater formation or of displacements in the media surrounding an explosion is presented in this report, since the problem has been previously explored in numerous research projects having much greater scope. The shafts were designed to permit maximum economy of construction while still providing a flexible column whose segments could shift laterally and vertically so as to accurately register the differential displacements expected in the soil at various depths.

A search of literature on previous research in the United States and Britain indicates that the general practice in predicting permanent horizontal displacements in various types of soil, due to explosions occurring at various depths below the ground surface, has been to arbitrarily use one-third of the value of maximum transient displacements as computed by using the conventional formulae. Actually, it should be recognized that the ratio of maximum transient displacement to permanent displacement will vary between a value of one at the edge of the crater and a value of infinity in the elastic zone. Similarly the ratio of the permanent vertical displacement of a point to its permanent horizontal displacement will not be the same for any given value of lambda but will vary grossly due to factors such as the type of soil, position of explosive, and other like factors. Lambda is defined as the radial distance in feet from ground zero divided by the cube root of the equivalent energy release of the charge of T.N.T. in pounds.

In planning this project, it was hoped that the articulated shafts would suffer sufficient displacement to permit establishing a rough empirical rule for predicting permanent displacements in terms of distance and depth ratios for a range of soil conditions and weapons. However, due to the almost complete absence of movement, such rules cannot be reliably predicated except in the most general terms.

1.4 DESCRIPTION OF SHEAR SHAFTS

The shear shaft locations relative to ground zero at the surface shot test are are shown in Figure 1.1. Similarly, the locations of the shafts at the underground shot test area are shown in Figure 1.2. All completed shafts were identical, except for insignificant variations in deviations from the vertical. Offsets of the bottoms from the tops of the shafts varied from about 2 to 8 inches before the shots. All the shaft segments were roughly in a straight line however, so that in no instance was the line of sight obscured over the entire depth of the nine segments. Figure 1.3 shows a typical section of the installations.

Each shaft consisted of nine lengths of standard weight black steel pipe, each length 5-feet long and 6 inches in inside diameter. The segments were joined together at each junction with a metal sleeve tack-welded to the pipes. The sleeves were light enough to offer only very limited restraint but served to keep the pipe segments in line prior to testing and also kept sand from sifting through the joints and filling the pipes. Figures 1.4 through 1.7 show typical views of equipment used and methods of installation. The pipe segments were vibrated after being placed in the drill holes, and sand was packed around the pipes to assure full contact with the ground.

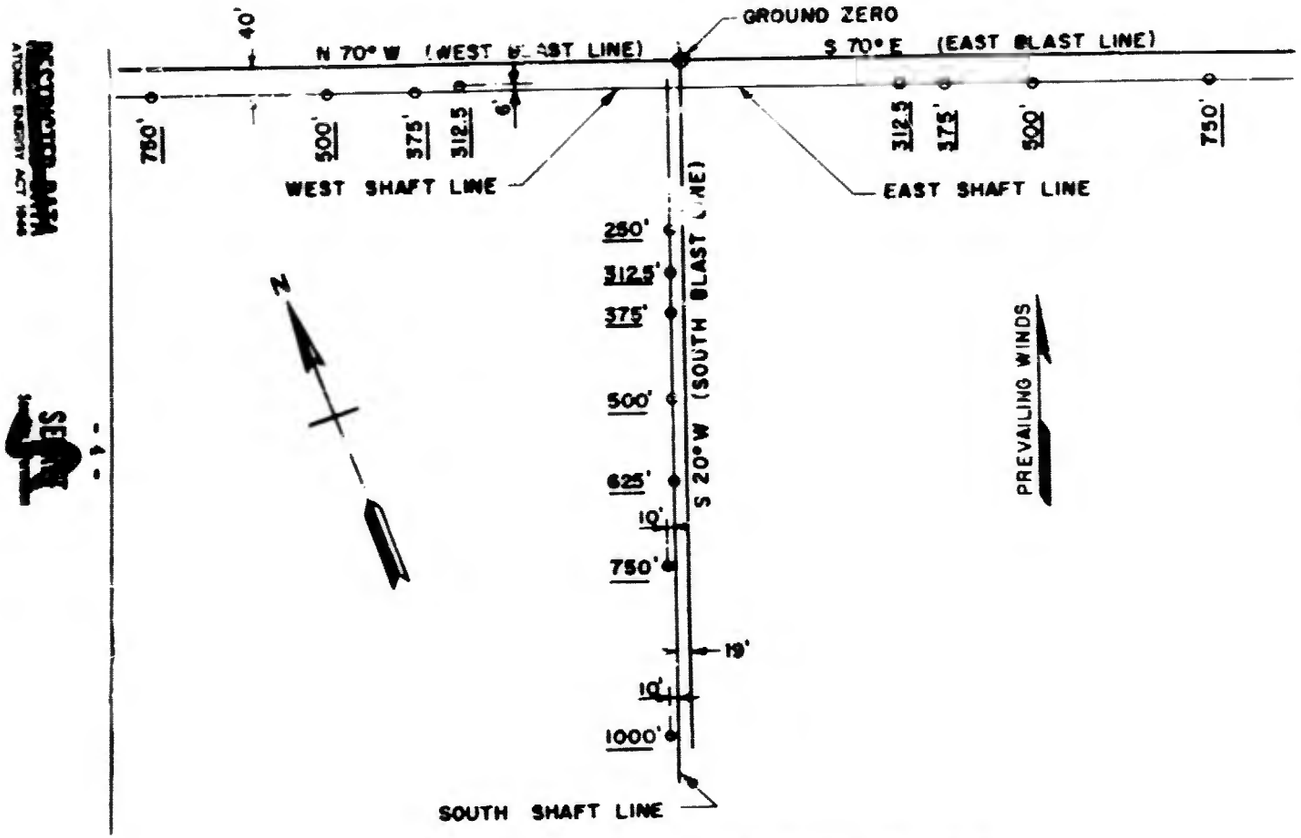

Fig. 1.1 Shear Shaft Layout, Surface Shot Site

Fig. 1.2 Shear Shaft Layout, Underground Shot Site

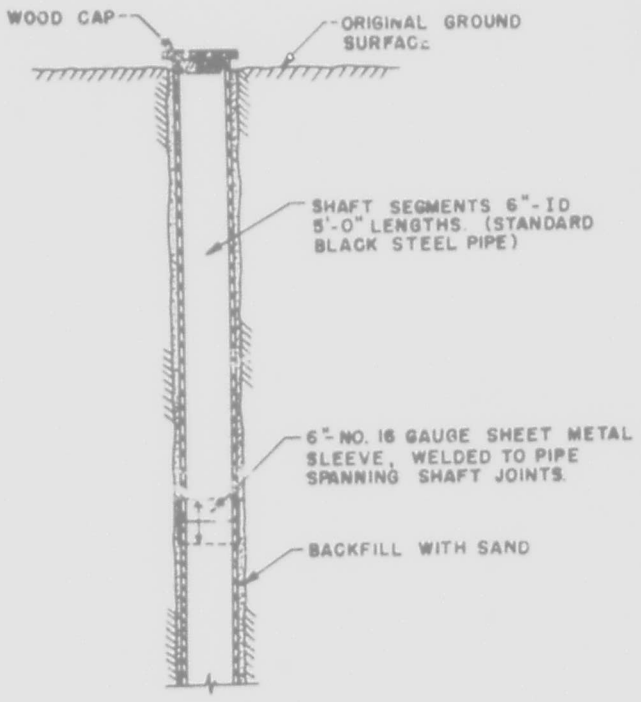

Fig. 1.3 Typical Shaft (Pre-Shot)

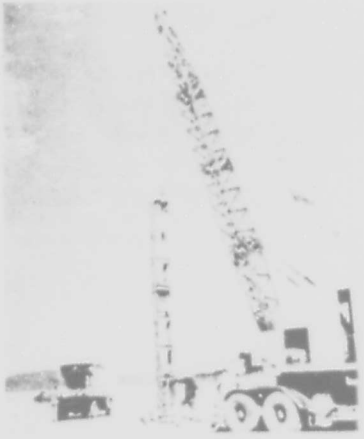

Fig. 1.4 Driving of Shear Shafts

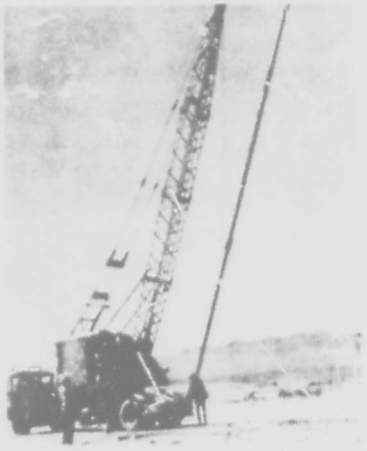

Fig. 1.5 Installation of Pipe Segments

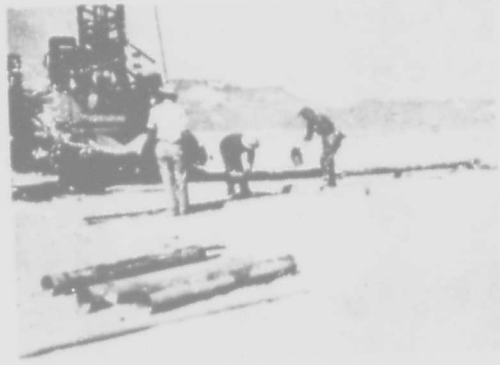

Fig. 1.6 Installation of Shear Shafts

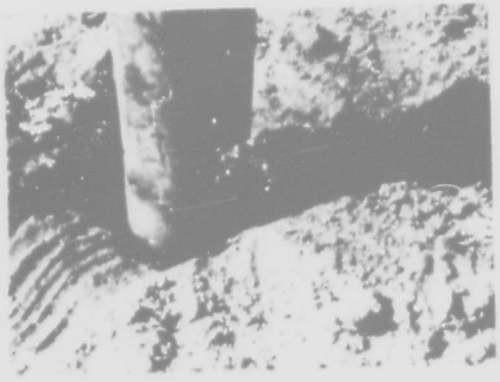

Fig. 1.7 Shaft and Welded Sleeve

CHAPTER 2

INSTRUMENTATION

2.1 GENERAL REQUIREMENTS

The instrumentation requirements of the problem were originally established to meet the worst possible conditions which might have to be met for the Amchitka Site of Operation WINDSTORM. Segmental shafts 6 inches in diameter and 70 feet deep were to be installed for tests involving 25 kiloton bombs and with predicted maximum transient displacement ranging up to approximately 100 feet near the crater. Instruments were desired which would be able to detect permanent displacements at the bottom of the 70-foot shaft with an accuracy of approximately 1 inch, assuming maximum relative displacement up to one-half diameter between the various pipe segments and possibly sufficient cumulative displacement to prevent line-of-sight instrumentation within the shaft.

An extensive search of technical articles and manufacturers' literature plus an actual field test using a special adaptation of electrical resistivity exploration methods demonstrated that the underground position of the pipe could not be established within a tolerance of 12 inches or more, by using external survey methods. A similar search of literature on sub-surface survey techniques and equipment used to trace the position of pipes and shafts by internally traversing the pipes, similar to practices used in oil field exploration, showed that special instruments would have to be designed to meet the conditions imposed for the shear shaft surveys.

Accordingly several instruments were developed to meet the special requirements of the shear shaft installations to determine separation of pipe segments and their changes in angle of inclination. These instruments are described in par. 2.2.

Operation JANGLE provided that the U. S. Coast and Geodetic Survey would make the ground control survey, both before and after each shot, to determine permanent movements of the tops of each shaft in the vertical, horizontal-radial, and horizontal-transverse directions due to the blasts. Inasmuch as this information has not been available in time for this report, rough chain and level data, secured by Project 1.6 personnel, are reported instead.

2.2 DESCRIPTION AND OPERATION OF INSTRUMENTS

2.2.1 Inclinometer

Essential details of the inclinometer design are shown in Figure 2.1. This instrument was used to determine change in the angle with the vertical of each shaft segment due to the shot-induced soil movements. The two permanent magnets together with gravity, served to orient the instrument in such a way that the bearing points were held against the inside surface of the segment under test, thus keeping the axis of the instrument parallel with the axis of the shaft segment. A selsyn motor is mounted inside the instrument with the axis of its rotor perpendicular to the axis of the instrument. A small weight suspended from the rotor serves to rotate the rotor an angle equal to that between the axis of the instrument and the vertical. By rotating the inclinometer about its axis in a shaft segment, a maximum angle is noted which is the deviation of the shaft segment with the vertical. Indications of this angle are shown on the inclinometer indicator (Figure 2.2). The indicator consists of another similar selsyn motor with a long pointer attached to its rotor, and a circular scale. It is electrically connected to the selsyn in the inclinometer so that each rotor rotates through angles of similar magnitudes. Thus deviations from the vertical can be determined for the most remote shaft segments. Figures 2.4, 2.5 and 2.7 illustrate the inclinometer and inclinometer indicator during actual tests, and calibrations.

2.2.2 Feeler Gage

The feeler gage, designed to determine the amount of vertical separation between the shaft segments, is shown in Figures 2.6 and 2.9. It consists of a plate 0.01 ft. in thickness coupled to removable pipe segments. A demountable scale is used at the ground level on a convenient pipe segment to measure the amount of shaft separation as the feeler is moved between the extreme limits of this separation.

2.2.3 Scales and Light Source

This device (Figure 2.10) was designed to measure deviation of the shaft segments from the vertical in those instances where the horizontal displacements did not interfere with the line of sight. The circular projections have electrical contacts which light a pilot lamp when in contact with the side of a shaft segment and insure that the axis of the apparatus is parallel to the axis of the segment under examination. The angle of deviation from the vertical is determined from the scalar difference read on the two scales when viewed with a vertical line of sight. Because of high electrical resistance developed by the layer of rust and

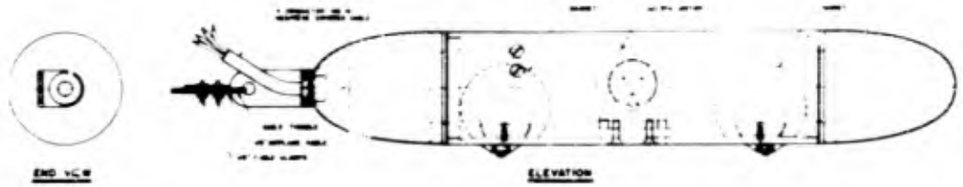

Fig. 2.1 Inclinometer

Fig. 2.2 Inclinometer Indicator

Fig. 2.3 Field Use of Instrumentation

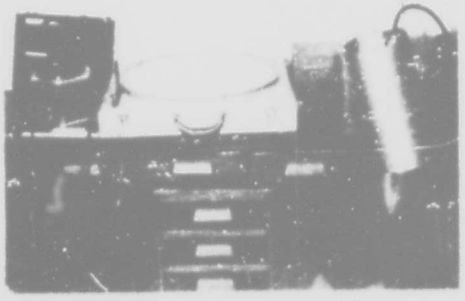

Fig. 2.4 Calibration of Inclinometer

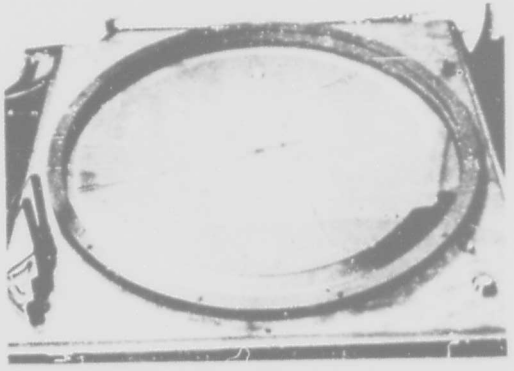

Fig. 2.5 Inclinometer Indicator

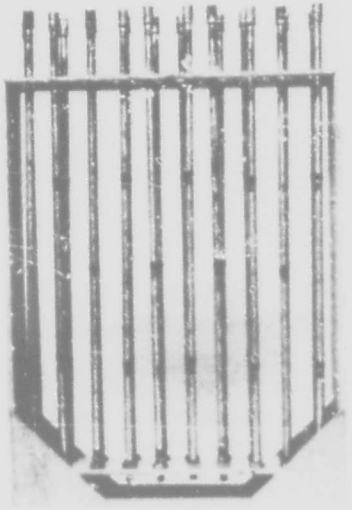

Fig. 2.6 Feeler-Pipe Segment

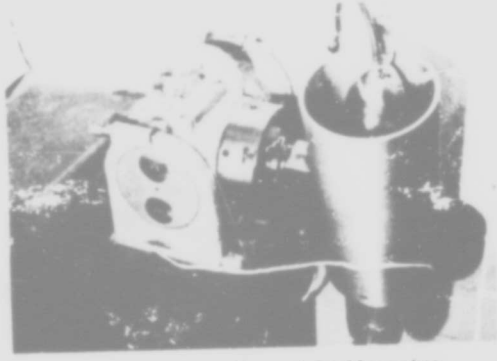

Fig. 2.7 Calibration of Inclinometer

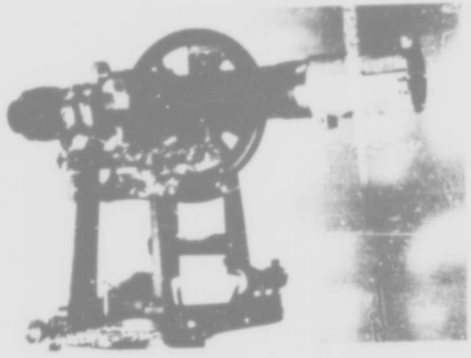

Fig. 2.8 Vertical View Attachment
To Transit

Fig. 2.9 Feeler Head

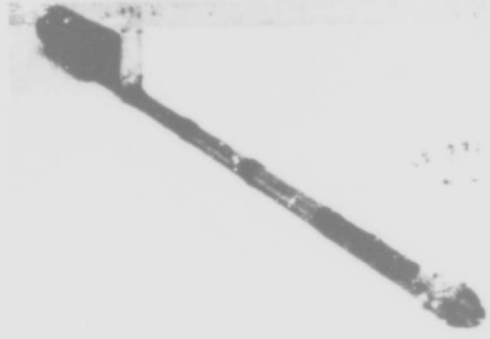

Fig. 2.10 Scales and Light Source

oil on the shear shafts it was impracticable to use this apparatus In its place a lamp suspended by a flexible cord was used, and the inclinometer, described above.

2.2.4 Vertical View Transit Attachment

In order to have easy reference to a vertical line of sight, a precision plane mirror was mounted at an angle of 45 degrees in the line of sight of a standard transit (Figures 2.3 and 2.8). Through the use of this adaptation, angles of deviation with the vertical and bearings can be made with one setting of the transit.

CHAPTER 3

OPERATIONS

3.1 SITE CONDITIONS

The geology of the general area has been described in the United States Geological Survey's report on Project 1(8)a, entitled "Operations WINDSTORM and JANGLE, Geologic, Hydrologic and Thermal Features of the Site", dated Feb. 1952. Data on a general seismic survey of the vicinity is available in the Project 1(8)a-1 report Seismic Refraction Survey for Navy Contract NOY 26616, Nye County, Nevada (United States Geophysical Company, Inc., 27 July 1951). Nevada State reports also contain general geologic information on this part of the state. In general, the valley fill at the surface and underground test areas can be described as an incoherent alluvium which originated in the siliceous volcanic formations forming the adjacent highlands. It is composed of fine to coarse sand and gravel with numerous, discontinuous layers of caliche of random depth.

No information has been received in response to a request for engineering properties of the soil representing the two sites, consequently no attempt has been made to predict probable effects of an atomic bomb in soils different from the rather unusual material of the Nevada Test Site.

3.2 FIELD LAYOUT

Locations of shear shafts at the surface and underground sites (Figures 1.1 and 1.2) were identical except for minor variations. Several shafts in the surface shot area were relocated in the field in order to clear incomplete shafts at the original positions which were abandoned due to excessive damage during construction. Whenever it was necessary to abandon a shaft, a new offset location was selected a few feet away, with the distance from ground zero remaining unchanged. Because of interference with the operation of other projects, the east line of shafts at the underground site was located on a line approximately 15° south of the original line.

3.3 CONSTRUCTION AND INSTALLATION

The shaft segments and mandrels were originally procured by the U. S. Navy, Bureau of Yards and Docks, for use at the Amchitka Site and were subsequently modified to suit the shallower shafts used at the

Nevada Test Site. The holes for the shafts were drilled by the Atomic Energy Commission's contractor, who also assembled and placed the pipe segments. The pipe segments were slipped onto a mandrel in a horizontal position and then joined by thin metal sleeves which were tack-welded to both segments at each joint. Construction equipment and sequence are illustrated by Figures 1.4 through 1.7 inclusive.

3.4 PRE-TEST SURVEYS

Complete surveys were made of all shafts in both test areas before the shots. This included, (a) inclinometer readings of the nine pipe segments of each shaft; (b) feeler tests of the junctions between the segments of each shaft; (c) offset observations of the bottom of each shaft relative to the top by means of a lamp and flexible cord; (d) bearings of offsets of the bottoms of the shafts, by means of a transit; and (e) rough chain and level surveys of all lines of shafts using the most remote shaft as a reference, in each instance.

3.5 POST-TEST SURVEYS

The post-test surveys were duplications of those made before the shots except that complete tests were made only of the shafts near ground zero, those including 312.5 ft. at the surface shot area, and those including 375 ft. at the underground shot area. Tests (b), (c) and (e) of paragraph 3.4, above were made on all shafts.

3.6 SALVAGE

Both of the mandrels, as well as the spare sections of steel pipe for the shear shafts, have been placed in the storage yard at the Mercury Camp, and are now available for use by other organizations or for disposal by the Test Command. The Office, Chief of Engineers, does not contemplate any further research which could utilize this material and the low value of the pipe and mandrels does not justify shipping them elsewhere for storage. Similarly no further work is planned for the future use, removal or salvage of any part of the shafts now in place at the test sites.

CHAPTER 4

TEST RESULTS

4.1 SURFACE TEST

Test results obtained from the pre-test surveys (see par. 3.4) were used as reference values for comparison with those obtained during the post-test surveys (see par. 3.5).

In no instance, of all the tests made at the surface site, was there any discernable permanent movement of the shafts which could be attributed to the effect of the shot. There were indications, however, of destructive effects of heat and air blast. Steel straps welded to the topmost pipe segment to hold wooden caps in place were ruptured out as far as 375 ft. from ground zero. Similarly the wooden caps were badly burned within the same distance.

4.2 UNDERGROUND TEST

The underground test results were obtained in a manner similar to that used in the surface tests, that of using the pre-test survey data as reference. Except for the 250 ft. and 312.5 ft. shafts of the south blast line, none of the shafts in the underground area showed any significant permanent displacement that can be attributed to the effects of the atomic explosion. Although permanent displacements, both radial and vertical, were determined from rough chainage and level surveys by project personnel, no significant differences are anticipated between these data and those which will be available later from the precise surveys of the U. S. Coast & Geodetic Survey.

The permanent displacements of the top pipe segments at the 250 ft. and 312.5 ft. shaft locations are presented graphically in Figure 4.1. The plan view shows the resulting radial permanent displacements as determined from the rough chainage surveys. The side view shows the radial horizontal and vertical permanent displacements after the shot as determined by the inclinometer tests together with the rough level surveys. The rough chainage surveys also indicate that the tops of the shafts on all three radii at 375 ft. moved approximately one inch toward ground zero. Since none of the precise survey data of the U. S. Coast and Geodetic Survey are available as yet, these apparent movements have not been verified at this date.

Referring again to Figure 4.1, the action of the ground waves was in evidence at the two locations shown, with rather divergent results:

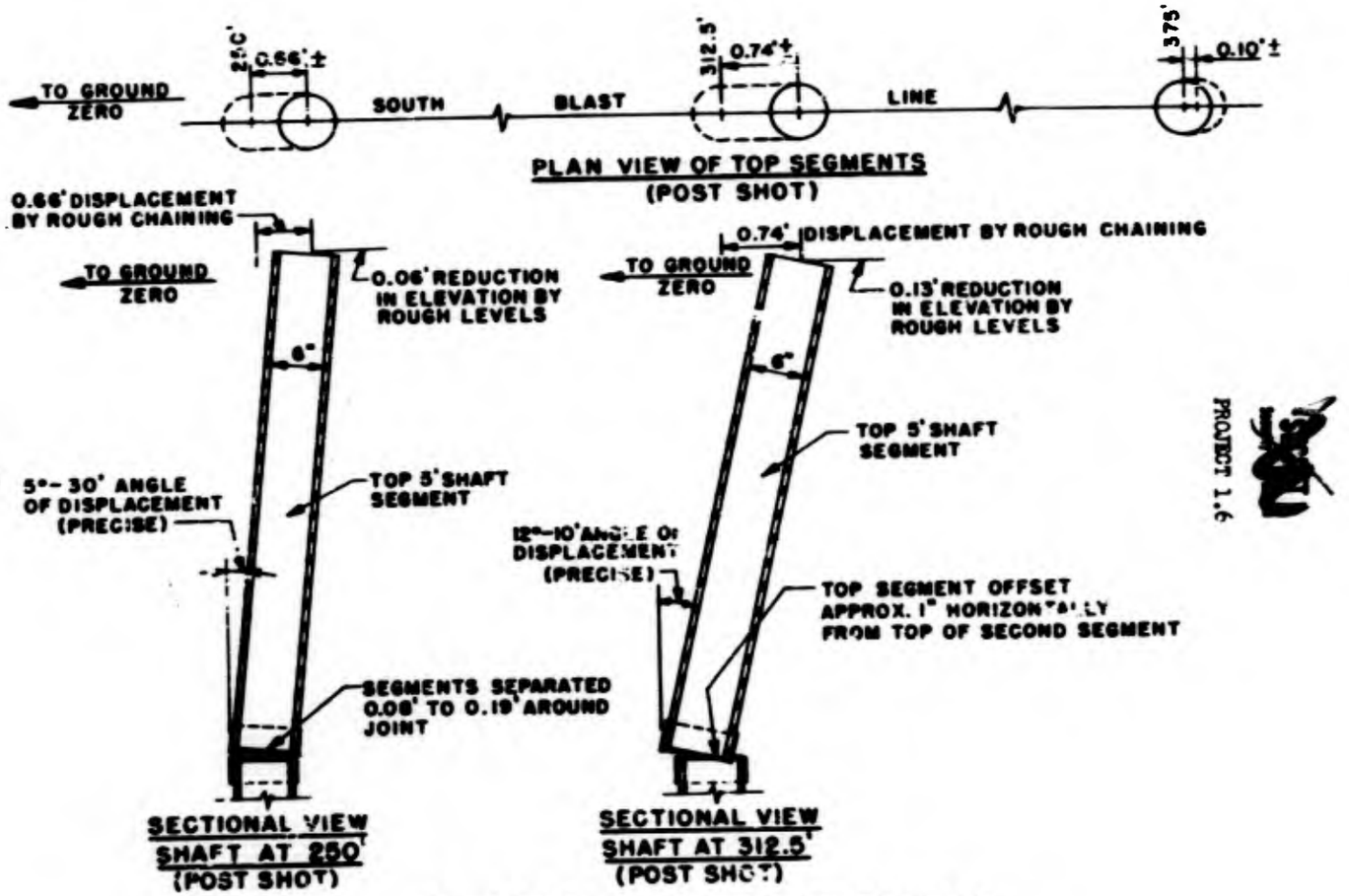

Fig. 4.1 Underground Site Displacement Studies

PROJECT 1.6

(a) The horizontal displacement of the top segment at ground level was greater at 312.5 ft. than at 250 ft. by 0.08 ft. away from ground zero.

(b) Horizontal shearing forces were in evidence at the 312.5 ft. shaft. The welded sleeve holding the top two segments together failed in shear, the relative horizontal movement between the bottom of the top segment and the top of the second segment being approximately one inch. There was no apparent horizontal shearing action between the first and second segments at the 250 ft. shaft. However, there was tensile stress at this junction sufficient to fail the spot welding of the sleeve on the pipes, and resulting in a joint separation of about 0.14 ft.

(c) Elevations at the top of the shafts were both lowered, the amount at the 312.5 ft. shaft being the greater of the two by approximately 0.07 ft. This appeared to be due principally to rotation of the top pipe segment, rather than to possible subsidence of the entire shaft.

(d) Angular displacement of the top segment at 312.5 ft. was about twice the amount at 250 ft.

(e) The top of the second segment at 250 ft. appears to have moved approximately two inches away from ground zero, whereas the top of the second segment at 312.5 ft. appears to have moved approximately two inches toward ground zero.

Some of the above results are derived from the rough chainage and level surveys and may need revision when the more precise survey data are available from the U. S. Coast and Geodetic Survey.

CHAPTER 5

DISCUSSION

5.1 GENERAL

Prior to the JANGLE test the best and most current predictions of maximum horizontal and vertical transient displacements anticipated at various distances from the surface and underground bursts were those shown on Fig. 1.1-3 of Report Three (Program One, August 1951). These curves apparently were derived by using the formulae found in Appendix "B" of The Effects of Atomic Weapons and using a seismic velocity of 4500 feet per second as selected from the latest seismic survey of the Nevada Test Site. For example, selecting a location on these curves representing points 250 feet from ground zero at the underground test, the maximum transient displacements predicted were about 30 feet and 8 feet in horizontal and vertical directions, respectively. Similarly corresponding displacements of the same point at the surface test would be about 20 feet and 5½ feet, respectively. By using the standard rule that, "---the permanent horizontal displacement is approximately one-third the maximum transient displacement ---," as given in paragraph B.26 of The Effects of Atomic Weapons the above referenced curves were converted into permanent displacement curves.

With the exception of two locations, the permanent displacements of all installations of project 1.6 were essentially zero. It is apparent that the best data and formulae now standard for predicting permanent displacements due to surface and shallow underground atomic explosions are of doubtful value for conditions similar to those of Operation JANGLE. In the absence of detail data on the properties of the soil at the site, it is suspected that factors such as the moisture content of the soil and the particle gradation characteristics within the soil mass may be responsible for a large share of the gross deviation from predicted values. When data and transient displacements of installations by other projects in the area becomes available, it will be possible to determine whether the lack of permanent displacement is due to high recovery properties of the soil or due to high energy absorption characteristics as suspected.

During installation of the shear shafts additional information became available from the high explosive tests at the Nevada Test Site. The high explosives test area was midway between the surface and underground atomic sites and was probably in soil with similar characteristics.

Both the underground atomic shot and the high explosive shot designated as HE-2 occurred at approximately the same charge depth ratio. Based on lambda values, projected permanent displacements of approximately 1.0 feet were recorded from the high explosives tests at a distance corresponding to 250 feet from ground zero at the underground atomic test. Test data from the underground atomic test showed permanent horizontal displacements approaching this value at 250 and 312.5 feet from ground zero but only along the south blast line. The east and west blast lines showed no significant permanent horizontal displacement.

5.2 CORRELATION WITH OTHER TESTS

The comments in paragraph 5.1 indicate that the HE-2 high explosive test shot came somewhat closer to the order of displacement measured in the underground atomic test shot than did predictions based on empirical formulae. Data being obtained at present in the Dugway high explosive tests should also be valuable, when available, for correlation purposes.

In both the atomic and the high explosive tests at the Nevada Test Site, it should be borne in mind that displacements of a small order should not be used to study trends of effects. The order of displacement measurement approaches or equals the probable order of accuracy of the measurements in many cases. An example having possible influence in these small displacements is the presence of existing bituminous roads meandering through the high explosives test area. These may have carried a relatively high order of wave transmission at the ground surface where the wood hubs for horizontal displacement measurements were located for the high explosives test.

When precise survey data for the atomic test sites become available from the U. S. Coast and Geodetic Survey, trends from displacements of small order at the ground surfaces may be more reliable.

5.3 WAVE PHENOMENA

The apparently unpredictable and inconsistent behavior of the top pipe segments at the 250 ft. and 312.5 ft. locations on the south blast line of the underground shot test may seem more logical if transmission of the energy waves through the soil is analyzed.

Seismic velocity variations with depth below the ground surface at the Nevada Test Site are considerable and could account for some very complex wave phenomena. For example, when it is considered that velocity near the surface is of the order of 1000 ft. per second and velocities at 20 or 30 ft. depths are approximately 2000 ft. per second it is reasonable to expect considerable wave distortion short distances from the energy source. It is possible for waves to travel through the deeper

strata at high velocities and arrive at approximately the same time as surface waves traveling a shorter distance but at a slower velocity. These waves traveling through different routes but arriving at the same point may tend to increase or decrease movement at that point depending upon the degree of phase displacement of the waves. If the waves are in phase the result will be maximum displacement; if 180° out of phase a cancellation effect will result with the more intense wave predominating. The effects of these complex waves will be evident not only in magnitude, but also, in direction of movement. If this analysis is applied to the south blast line of the underground shot at the 250 ft. and 312.5 ft. locations, the possibilities of variable results can be realized.

CHAPTER 6

CONCLUSIONS

This report is considered final insofar as project personnel are concerned, and no further reports are contemplated to cover the precise survey data on project 1.6 installations which may eventually be furnished by the U. S. Coast and Geodetic Survey. All statements apply only to test conditions similar to those of Operation JANGLE and the Nevada Test Site unless specifically stated otherwise:

1. Due to the almost complete absence of permanent movement of project 1.6 installations at both the surface and underground tests, it is inadvisable to attempt correlations or interpretation of project data now available except in the most general terms. It is apparent that the conventional formulae and methods now in use for predicting permanent displacements are grossly inaccurate for conditions similar to those prevailing for Operation JANGLE.

2. Revisions of existing formulae and methods for predicting permanent displacements, and any correlations with data from previous related research cannot be profitably attempted until the engineering properties of the soil at the Nevada Test Site are available in detail throughout the range of test installations.

3. Detailed soil data, such as moisture content, density, porosity, grain size and gradation, plasticity, and elasticity are needed for improving existing formulae in order to more accurately predict movement in other type soils.

4. Gross asymmetry of test effects can be expected in underground explosions research but it probably can be reduced if a site could be obtained which has a more homogeneous soil than found at the Nevada Test Site.

CHAPTER 7

RECOMMENDATIONS

The following recommendations are based upon the experience gained at the test site and on the very limited data obtainable to date from Operation JANGLE. While several recommendations are not directly related to the research objectives of project 1.6 they have been included because of their importance to the economy, efficiency and success of future projects:

1. When data on both transient and permanent displacements are to be obtained in the same test, it is suggested that all work on displacements be done by one project or organization in order to obtain the best economy and efficiency and to provide the most reliable correlations and coverage.

2. Complete engineering soil data should be obtained at the Nevada Test Site for correlation with similar information from other test sites.

3. When all data becomes available on the transient and permanent displacements measured by the numerous projects of Operation JANGLE, it should be analyzed, together with all related data from the major high explosives tests, (such as Dugway, Camp Gruber, Panama, etc), to determine whether present formulae and methods for predicting displacements can be improved. In particular, factors such as moisture content, ground water levels, and soil gradation should be scrutinized to see if their influence on displacements is adequately covered by the seismic velocity terms as used in present formulae. The gross deviation between actual values and the best possible predicted values obtained by using existing formulae suggests that simpler formulae, in both the terms and coefficients, but providing predictions having the same order of accuracy should be established for general use until the knowledge and accuracy of test data and its application will justify or require more complex formulae.

4. Further effort should be made to obtain a test site having a more homogeneous medium, preferably one more representative of soil conditions in probable target areas.

BIBLIOGRAPHY

C. W. Lampson, Final Reports on Effects of Underground Explosions OSRD Report No. 6645. 1946

D. C. Campbell, LCDR, USN, Program One, Report Three, with supplements. Technical Operations Squadron (Prov) Aug. 1951.

AFSWP. Capabilities of Atomic Weapons. July, 1951.

AFSWP. Windstorm Handbook. Nov. 1950.

A. F. Spilhaus, Operation JANGLE, Weapons Effects Tests, Preliminary Report. Jan. 1952.

E. B. Doll, and D. C. Sachs. HE Tests - Operation JANGLE, Interim Report, Stanford, Cal.; Stanford Research Institute, Oct. 1951.

E. B. Doll, HE Tests - Operation JANGLE, Interim Report - Part II. Stanford, Cal.; Stanford Research Institute, Oct. 1951.

E. B. Doll, Underground Explosion Tests at Dugway, Interim Report. Stanford, Cal., Stanford Research Institute, July 1951.

ERA, INC., Instrumentation for Underground Explosion Test Program, Interim Technical Report No. 1, Dry Clay, Dugway, St. Paul, Minn.: Engineering Research Associates, Inc., 1 Aug. 1951.

ERA, INC., Instrumentation for Underground Explosion Test Program, Interim Technical Report No. 2, Dry Sand, Dugway, St. Paul, Minn.: Engineering Research Associates, Inc., 1 Oct. 1951.

ERA, INC., Instrumentation for Underground Explosion Test Program. Interim Technical Report No. 3, Wet Clay, Dugway, St. Paul, Minn.: Engineering Research Associates, Inc., 1 Nov. 1951.

E. R. Shepard, Subsurface Explorations by Geophysical Methods. Philadelphia, Pa. American Society for Testing Materials, 1949.

F. J. Crandell, Ground Vibration Due to Blasting and its Effect Upon Structures. Journal of the Boston Society of Civil Engineers, April 1949.

A. M. Rugg, Seismic Refraction Survey for Navy Contract NOY 26616, Nye County, Nevada. United Geophysical Company, Inc., 27 July 1951.

SECRET

PROJECT 1.6

F. Walley, A Second Survey of Ground Shock Effects, British Ministry of Home Security, Research and Experiments Department.

Isthmian Canal Studies - 1947, Appendix 6 of the Report of the Governor of the Panama Canal.

O. B. Maxey & C. H. Jameson, Water Resources Bulletin No. 5 State Engineer, State of Nevada.

SECRET

SECRET

OPERATION JANGLE

PROJECT 1.7

GROUND ACCELERATION

(Crook Line)

by

Robert J. Parr

and

[illegible]

June 47

MASSACHUSETTS INSTITUTE OF TECHNOLOGY

CAMBRIDGE, MASSACHUSETTS

[illegible]

SECRET
Security Information

PREFACE

Project 1.7 was originally planned for the Amchitka site of Operation WINDSTORM. The purpose of the project was to determine whether simple installations of this type would furnish reasonably reliable data regarding magnitudes of ground shock associated with nuclear explosions. The approximate data obtained using shock pins could then be correlated with the precise records obtained from the relatively few electronic devices which could be installed at that very isolated site.

Abandonment of the Amchitka site in favor of the Nevada Test Site reduced the overall supply and construction problems to such a great extent that many additional recording channels could be added. Installations like those required for shock pins, which do not require timing or remote recording channels and equipment, were therefore of less relative value at Nevada than at Amchitka. They were retained in the operation, however, because of the low cost involved, the advanced state of procurement and the desire to establish the capabilities, limitations, and possible applications of this type of instrumentation.

ACKNOWLEDGEMENTS

The Department of Civil and Sanitary Engineering of the Massachusetts Institute of Technology has been responsible for the project, under the direction of the Project Officer, Harald J. Sundstrom of the Office, Chief of Engineers.

The project was carried out by the Structural Dynamics Research Section of the Department of Civil and Sanitary Engineering, Massachusetts Institute of Technology, headed by Dr. Robert J. Hansen. Dr. John G. Archer was project supervisor, and was assisted by Messrs. Fujio Matsuda and Harry C. Saxe.

CONTENTS

ILLUSTRATIONS

CHAPTER 2 INSTRUMENTATION

ABSTRACT

The purpose of the project was to determine the feasibility of using shock pins for measuring the approximate magnitudes of acceleration of a transmitting medium at varying distances from an atomic explosion.

The report contains the development of a theoretical equation for the determination of the horizontal acceleration required to overturn shock pins having varying physical dimensions. In addition, the report describes the laboratory calibration procedure performed in order to determine the validity of the theoretical relationship. Charts comparing the theoretical and experimental results are given.

The use of shock pins at the JANGLE tests is then discussed. Descriptions of the field test procedure together with sketches and photographs are given, and the results of both tests are presented in tabular form.

Experimental values of horizontal acceleration as obtained using shock pins are plotted against the appropriate lambda values and presented in graphical form. To serve as a basis of comparison with the more exact instrumentation methods, preliminary data of the Naval Ordnance Laboratory and the Stanford Research Institute are also presented on these graphs.

PROJECT 1.7

NOTATION

Symbol	Description	Units
a	Radial horizontal acceleration of ground in gravity units	g
A_a	Radial horizontal acceleration of ground	ft/sec/sec
C_1	Constant of integration	
C_2	Constant of integration	
d	Shock pin diameter	in
g	Acceleration of gravity	32.2 ft/sec/sec
h	Shock pin height	in
I	Mass moment of inertia of shock pin	slug-ft sq
M	Arbitrary constant	
N	Arbitrary constant	
r	Eccentricity of cam of shock pin calibration device	in
s	Diagonal distance from center of gravity of shock pin to toe	in
t	Time	sec
t_o	Correction applied to make $\emptyset = 0$ at $t = 0$	sec
T_a	Period of initial acceleration cycle	sec
W	Weight of shock pin	lb
$\ddot{x}$	Radial horizontal acceleration of shock pin	in/sec/sec
α	Stability constant for shock pin = $\sqrt{\frac{3g}{2h}}$	$\frac{1}{sec}$
λ	Scaled [illegible] distance from Ground Zero	

PROJECT 1.7

Symbol	Description	Units
$\emptyset$	Angle of rotation of shock pin about toe of pin	radians
τ	Stability constant " α " multiplied by time "t"	
τ_o	Stability constant " α " multiplied by time "t_o"	
θ_o	Angle between the diagonal "s" and side of pin	radians
θ	Angle between the diagonal "s" and side of pin when pin is in unstable equilibrium	radians
ω	Circular frequency	radians/sec
Ω	Circular frequency "ω" divided by the stability constant "α"	radians

CHAPTER 1

INTRODUCTION

1.1 OBJECTIVE

The objective of the project was to determine the feasibility of using simple devices, such as free-standing steel rods, to determine the shock an atomic explosion can transmit through the ground. These approximate data could then be used as a rough measure of the damage to structures to be expected at various distances from a shot point. In addition, the precise records secured by the remotely controlled or remote-recording electrical gauges must usually be very limited in numbers and in locations around a test shot. Therefore, if reasonable accuracy could be obtained using these shock pins, they would provide a low-cost method of supplementing the precise records.

1.2 HISTORICAL

It is probable that crude devices have been employed to measure ground shock since the earliest days when man first evidenced a scientific curiosity in earthquake phenomena. It is known that powder manufacturers, mining companies and quarrying interests in the United States have used sets of cylindrical steel pins of various heights for more than thirty years in determining probable damage to structures in the vicinity of their blasting.[1,2] An instrument known as a falling pin seismometer, consisting principally of cylindrical steel pins on a plate, has been found to have definite utility in this type work. In some instances, seismographs have been used in conjunction with the pin sets or seismometers to obtain correlated data, and rough rules of probable structural damage have been established for applying the pin data in the range of charge sizes and distances generally associated with quarry and mine blasting.

---

[1] Don L. Leet, Vibrations from Blasting (Wilmington, Delaware: Hercules Powder Company, 1946).

[2] Edward H. Rockwell, "Vibrations Caused by Quarry Blasting and Their Effect on Structures", The Explosives Engineer, (March and April 1927).

PROJECT 1.7

Mr. Tetsuo Akimo of Japan recently performed a series of experiments with cylindrical steel pins,[3] and in the course of his research discovered instances of shock pins being used in Japan for earthquake research as early as 1899.

The use of "Energy Ratio" as a criterion of ground shock damage, which the latest (1951) edition of the Capabilities of Atomic Weapons considered as the most desirable, has been developed through earlier studies of damage due to commercial blasting.[4]

[3] Tetsuo Akimo, "Experiments on the Overturning of Circular Columns by the Aid of a Shaking Table", Bulletin of the Earthquake Institute, (Tokyo University, 1950).

[4] F. J. Crandell, "Ground Vibration Due to Blasting and its Effect Upon Structures", Journal of the Boston Society of Civil Engineers, (April 1949).

CHAPTER 2

INSTRUMENTATION

2.1 GENERAL

Let us consider a shock pin resting on a flat plate. If the base plate is accelerated, a relative translation and rotation of the pin with respect to the base will tend to occur. The force which is applied to the pin will depend on the static coefficient of friction, and will be a maximum when sliding is impending. Up to this point, the force applied to the pin will be a function of the acceleration of the base. If the acceleration increases, the pin will begin to slide, and the force then acting on the pin depends on the relative velocity between the surfaces, and not upon the acceleration of the base. Therefore, if the pin is free to slide, the maximum acceleration that can be detected will be about 0.15 g (static coefficient of friction, steel on steel is approximately 0.15). If, however, relative translation between the plate and the pin is prevented at the contact surface, then the range may be increased. This may be accomplished by placing some type of tapered stop or shoulder in contact with the toe of the pin. In the analysis it was assumed that such a shoulder was provided.

2.2 MOTION OF BASE PLATE

2.2.1 Horizontal Acceleration

In our analysis it was assumed that the base plate was undergoing simple harmonic motion or:

$$\frac{d^2x}{dt^2} = A_m \sin \omega t \qquad (2.1)$$

where A_m = Radial horizontal acceleration of the ground

ω = Circular frequency = $\frac{2\pi}{T_A}$

T_A = Period

Although the type of ground motion anticipated was more of the

nature of a damped sinusoid, rather than a forced vibration as inferred here, a pure sinusoidal motion was assumed in order to simplify the analysis.

2.2.2 Vertical Acceleration

As a further simplification, the effect of vertical acceleration was neglected. This component of the acceleration was neglected for the following reasons:

1. Inclusion of vertical motion in the analysis unduly complicated the theoretical analysis.

2. It was observed from previous tests that the frequency of the vertical acceleration was greater than that of the horizontal acceleration, although the relative magnitude of the acceleration was of the same order. This higher frequency was expected to produce an averaging out of the effect of the vertical acceleration, resulting in the same net effect as if vertical motion were not present.

3. The uncertainties regarding the nature of the vertical motion were somewhat greater than for the horizontal motion.

2.3 THEORETICAL CONSIDERATIONS

On the basis of these assumptions, the following equation for the horizontal acceleration required to overturn a given shock pin was obtained:

$$a = \frac{d}{h}\sqrt{1+\Omega^2} \qquad (2.2)^1$$

where:
- d = Pin diameter
- a = Horizontal acceleration of medium in g's
- h = Pin height
- Ω = ω/α where ω = Circular frequency, α = Stability constant = $\sqrt{3g/2h}$
- g = Acceleration of gravity

A plot of the theoretical relationship between the horizontal acceleration and the term Ω is given in Figure 2.1. Ranges of h/d

[1] See Appendix A for derivation.

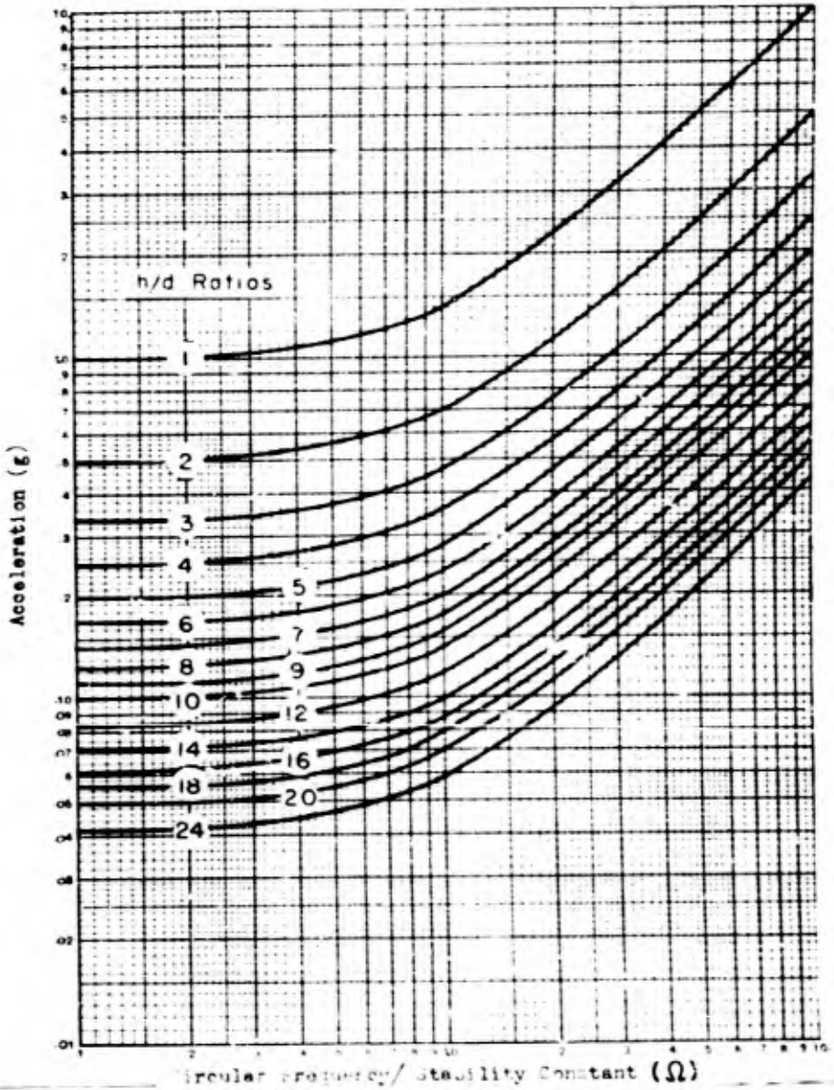

Fig. 2.1 Theoretical Plot of Ω vs Acceleration for Various h/d Ratios

values from 1 to 24 are included in the figure. From this figure and Eq. 2.2 it can readily be seen that the magnitude of acceleration required to overturn a given size pin is dependent not only upon the diameter/height ratio of the pin, but also upon the actual height of the pin, and the frequency of the ground motion. That is to say we cannot arbitrarily state that a pin having a diameter to height ratio of say 1/10, will require an acceleration of 0.1g to overturn. This would be reasonably accurate for the very low frequency ranges, but for the operating ranges experienced in the JANGLE tests this was decidedly in error.

Upon examining the plot of Fig. 2.1, it will be noted that the acceleration required to overturn a given pin increases as ω increases. This is due to the fact that for the lower frequency ranges, the natural period of overturning motion of the pin comes closer to the natural period of the ground, thus increasing its susceptibility to overturning. However, as the frequency is increased, the natural frequency of the pin deviates more sharply from the frequency of the ground motion, the tendency to overturn is further damped, and an increasing acceleration is required to cause the pin to fall. By similar reasoning, if we take two pins having the same h/d ratio but of different physical dimensions, and subject them to external motion of a given frequency, the taller pin will require a greater value of horizontal acceleration to cause overturning. This is graphically illustrated in Fig. 2.2 showing plots of acceleration versus circular frequency for the 3 and 12 inch pins used in the JANGLE Tests.

Further it can readily be seen from Eq. 2.2 that if a set of pins of a given height but varying diameter is used as shock pins, the period of ground motion must be known in order to come to any conclusion as to the magnitude of acceleration occurring at the test point. This could be overcome by using several sets of pins each set having different heights and solving simultaneously for the horizontal acceleration.

In planning for the JANGLE tests, the above was used in selecting pin sizes. It was decided to use pin heights of 3 and 12 inches with diameters compatible with the magnitudes and frequencies of the accelerations anticipated. The anticipated values of acceleration and period for various lambda values are shown in Figs. 2.3 and 2.4 respectively. Pin diameters were selected so as to obtain an approximate spread of ± 25% of the anticipated accelerations in the positive phase, and ± 50% in the negative phase at each installation.

The 3 and 12 inch heights were selected because they appeared to give well defined intersections in the range of frequencies anticipated when plotted as in Fig. 2.2. Upon examining this figure it

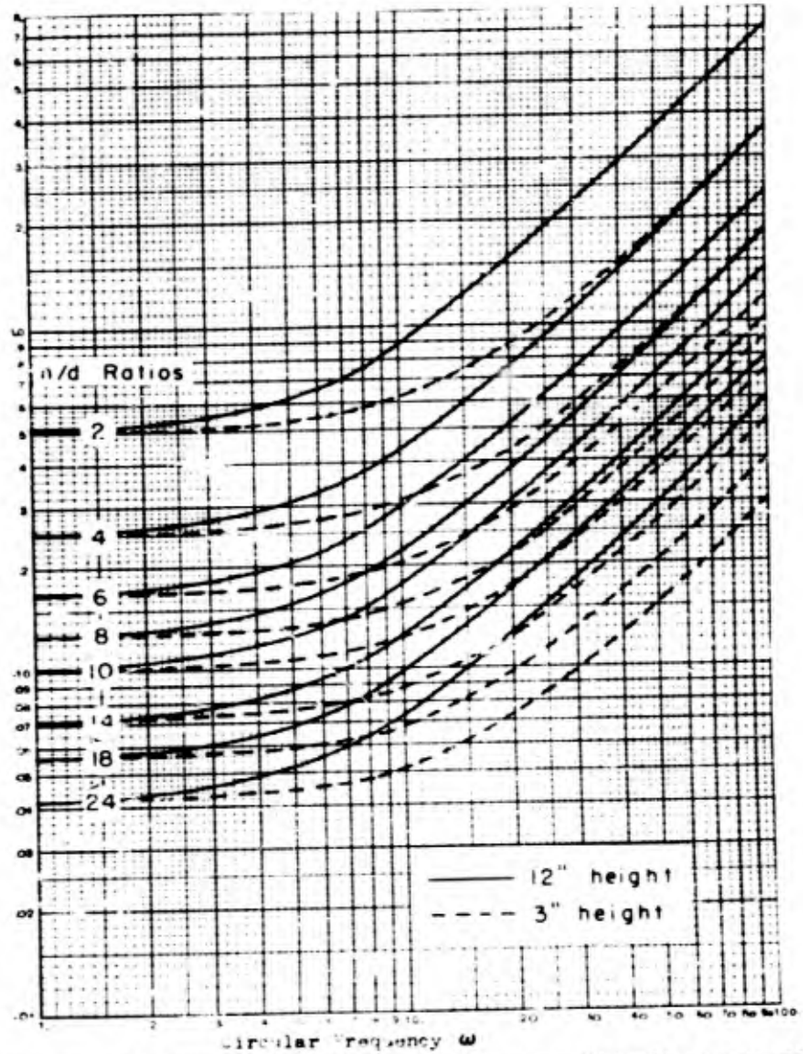

Fig. 2.2 Theoretical Plot of Circular Frequency ω (radians per sec) vs Acceleration for 3 and 12 Inch Pins Having Various h/d Values

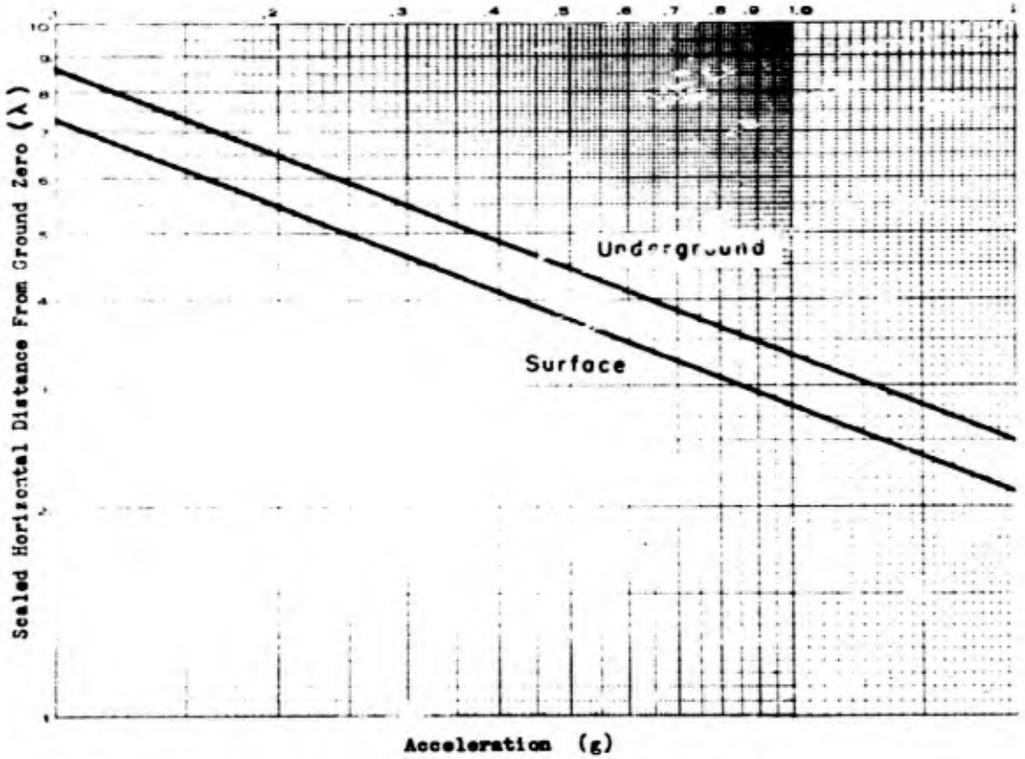

Fig. 2.3 Predicted Maximum Horizontal Acceleration as a Function of Distance from Charge

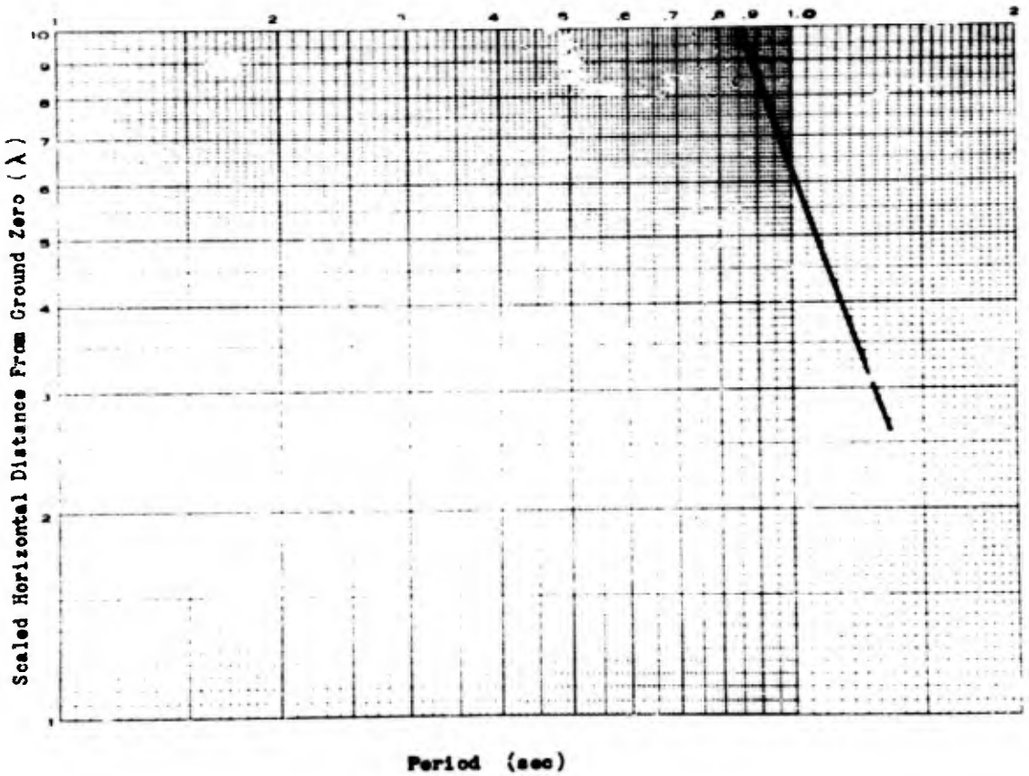

Fig. 2.4 Predicted Period of Initial Acceleration Cycle as a Function of Distance from Charge

w l be observed that the curves for the two pin heights selected i..ersect quite sharply in the vicinity of $\omega = 2\pi$. In line with this reasoning, if we knew the h/d values of the 3 and 12 inch pins which had just overturned due to a given acceleration, we could refer to the plot of Fig. 2.2, and by locating the intersection of the corresponding h/d curves we could quantitatively determine the accelerations and characteristic frequencies that had occurred at the test points.

2.4 SHOCK PIN CALIBRATION

In the theoretical analysis , it was assumed that

$$\frac{d^2x}{dt^2} = A_m \sin \omega t \qquad (2.1)$$

To conform to this assumption it was necessary to provide for simple harmonic motion in the design of the shock pin calibration device. This requirement ruled out the possibility of using a standard slide crank mechanism. It was decided to obtain the desired motion by using a circular cam of variable eccentricity. (See Fig. 2.5). The circular frequency could be varied from approximately $2\pi/3$ to a maximum of $20\pi/3$ using a power unit with variable speed drive. The cam was connected to the shaft by adjustable glands. The amplitude could be varied merely by loosening the connecting bolts on these glands and sliding the cam to the desired eccentricity. A variation of from zero inches to approximately ten inches eccentricity was possible.

To insure that sliding did not occur between pin plate and the bottom of the shock pins, adjustable toe strips were installed on the shaking table of the calibration device. (See Fig. 2.6).

To prevent the pin from falling before the calibration device had reached a state of uniform circular frequency, a pin release mechanism was mounted above the shock pin. (See Fig. 2.7). This trigger-like device consisted of a steel rod held against the top of the pin by a spring, the tip of the rod fitting in a small recess in the top of the shock pin to prevent slippage. This steel rod could be withdrawn by a solenoid actuated by a micro-switch set for release at the center of the next stroke. (The point of zero acceleration).

In order to be provided with an accurate measurement of the acceleration occurring during a given test run, a Statham Accelerometer of ± 2 g range was mounted on the underside of the shake table. This was in turn connected to a Hathaway control unit and Oscillograph shown in Fig. 2.8, thus permitting an accurate representation

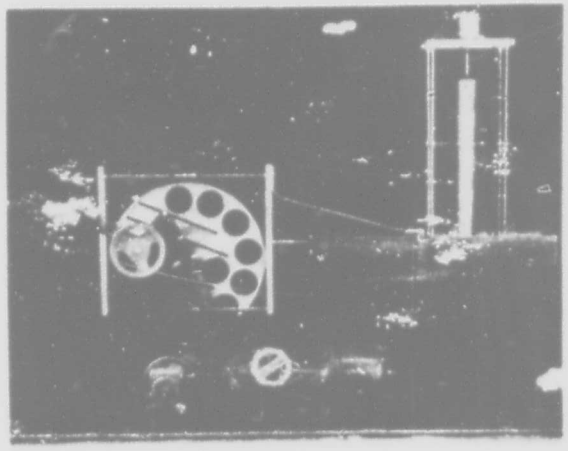

Fig. 2.5 View of Calibration Device Showing Eccentric Cam

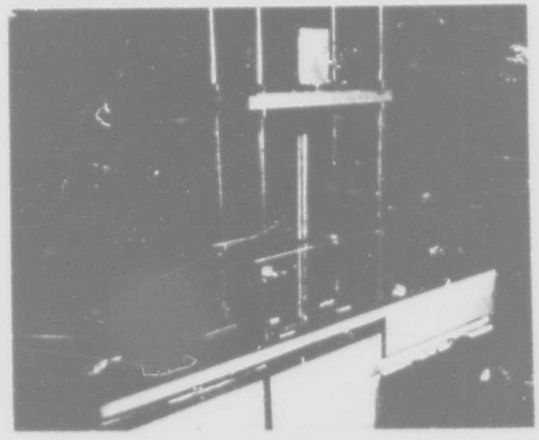

Fig. 2.6 View of Shake Table Showing Adjustable Toe-Strips

of the motion of the shake table. A typical photographic trace obtained using this procedure is shown in Fig. 2.9. The operator while conducting a test had merely to adjust the speed of the machine until the particular pin being tested was at the point of incipient overturning. While the machine was running he would then start the photographic trace on the oscillograph, and release the pin by actuating the pin release mechanism. By keeping the switch for the pin release mechanism engaged for a few cycles of motion, a slight pip would be registered on the trace (see "A" of Fig. 2.9). In this manner an accurate measure of the period of oscillatory motion was obtained.

It might be pointed out that, for consistency of test procedure, we adopted a standard criterion for deciding whether or not a pin had overturned in a given trial run. It was arbitrarily assumed that if a pin had not overturned in the second cycle, it was for all practical purposes standing at the acceleration and frequency of the test run. This was necessary because the continued shaking motion would eventually throw the pin violently about thus nullifying our test results. As was pointed out previously, the anticipated ground motion in the field test was more the form of a damped sinusoid. Consequently it was considered that a long continued forced vibration would not occur and that the criterion for overturning in the test procedure was valid.

As a means of positively determining exactly in what cycle a pin had overturned, a microswitch was mounted adjacent to the pin and on the side toward which the pin was to fall. (See Fig. 2.7) In this manner when a pin had definitely overturned it struck the microswitch and a small pip was registered on the oscillograph trace. (See "B" of Fig. 2.9)

In this method of graphic presentation of the transient motion of the pin, a complete pictorial record of the test run was obtained eliminating many human errors and considerably reducing the paper work involved.

The equation for the circular cam was, of course:

$$\ddot{x}_{max} = r\,\omega^2 \qquad (2.3)$$

where: $\ddot{x}$ = acceleration (in/sec/sec)
r = eccentricity (in)
ω = circular frequency (radians/sec)

Thus it was necessary merely to hold either r or ω constant and vary the remaining term accordingly. In the calibration tests, it

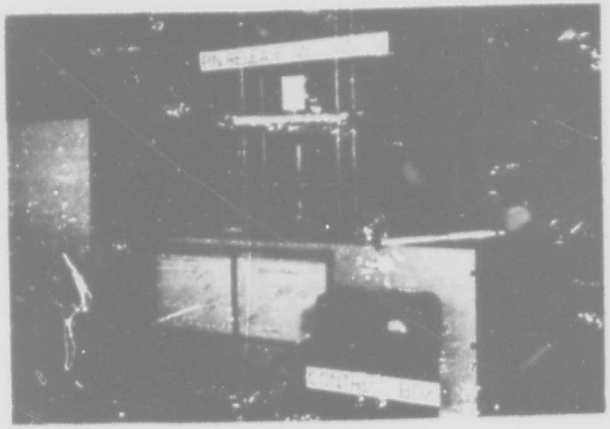

Fig. 2.7 View of Pin Release Mechanism and Shock Pin in Position

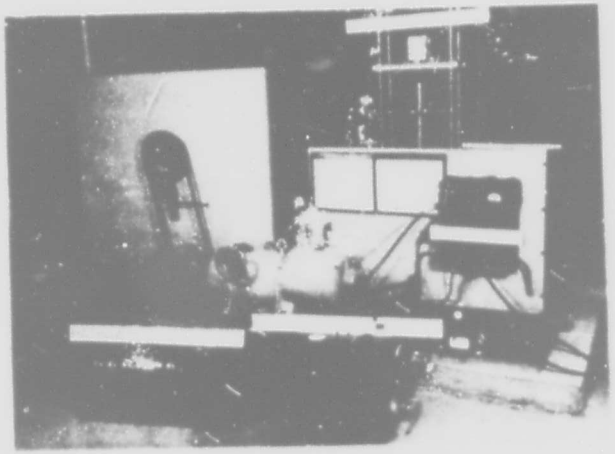

Fig. 2.8 View of Hathaway Control Unit and Oscillograph Connected to Control Box

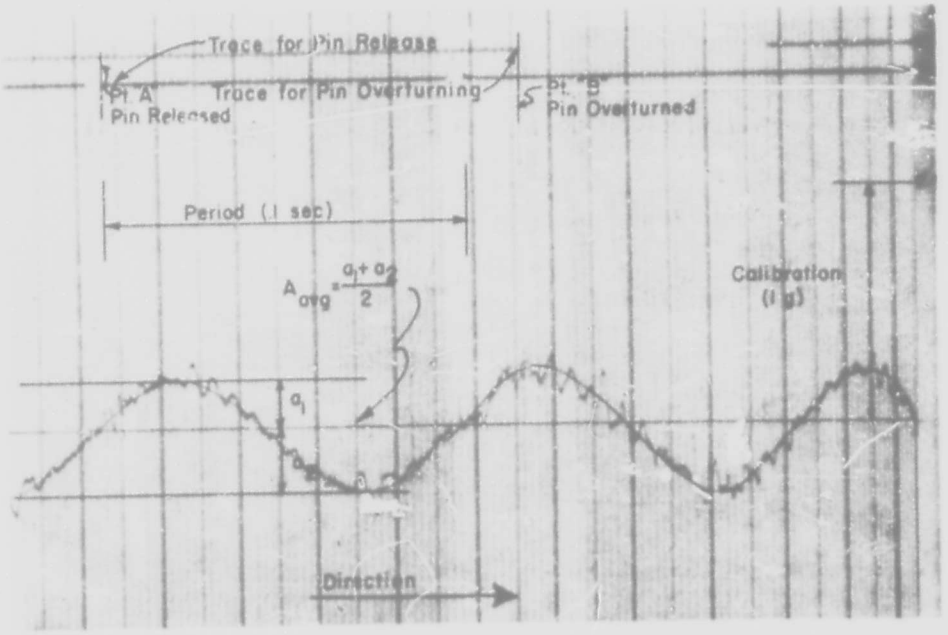

Fig. 2.9 Typical Trace Obtained Using Hathaway Oscillograph

was decided to set the cam at a constant eccentricity, r, and vary the circular frequency. This was increased until an acceleration of sufficient magnitude to overturn a given pin was attained. The photographic trace of the motion was obtained as previously explained. and a similar procedure repeated for the next larger size pin. When this had been completed for a complete set of pins, the eccentricity was changed by an arbitrary amount and the same sequence of tests repeated.

In all, four sets of steel shock pins of 3, 9 1/2, 12, and 22 inch heights respectively, and having diameters varying from 3/16 to 3 inches were fabricated. The ranges of heights were selected in order to determine whether the $\frac{h}{r}$ term of Eq. 2.2 actually entered into the picture as the theory predicted. Pins were squared and faced at both ends to within $\pm$ .001 inches, with one end center-drilled to receive the tip of the pin release mechanism.

2.5 RESULTS OF CALIBRATION

Some results of the calibration tests as compared to the theoretical results are plotted in Figs. 2.10 through 2.13. Since standard diameters of steel bars were used in the test pins, odd values of h/d could not be avoided.

In general the experimental results appear to be in fair agreement with the theoretical curves. The general shapes of both the experimental and the theoretical curves appear to be very similar, although the experimental data appear consistantly lower throughout. The reasons for this variance might be:

1. The shock pin machine might be imparting other than pure sinusoidal motion to the shake table.

2. Imperfection in machining the shock pins and roughness of the shake table surface. In this regard the effects of such imperfections would be more obvious in the more slender pins. This appears to be in agreement with the results, as the variance between the experimental and theoretical results appears greater for the higher h/d ratios.

3. The approximate nature of the solution.

4. Possible error in the accelerometer used. This is, however very unlikely.

2.6 FIELD RESULTS

Tabulations of all shock pin surveys for both the surface and underground tests are given in Tables 2.1 through 2.6.

Fig. 2.14 is included in the report to serve as an aid in visualizing the respective positions of pins, A through M in a typical shock pin installation. Note that pins at locations A through H are for measurement of the positive phase of the earth acceleration, while pins at locations J through M are for measurement of the negative phase of the earth acceleration.

Fig. 2.10 Comparison of Theoretical and Experimental Relationships Between Acceleration and Ω (Circular Frequency/ Stability Constant) for Several h/d Values

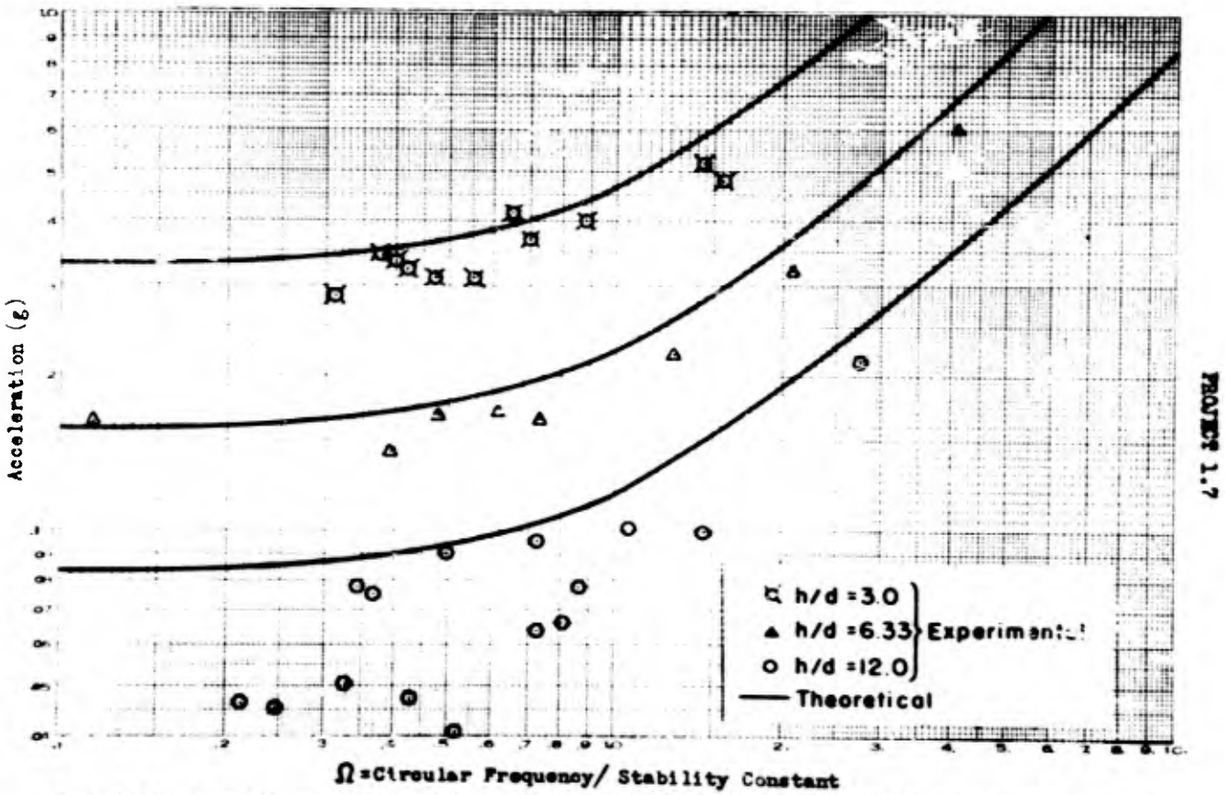

Fig. 2.11 Comparison of Theoretical and Experimental Relationships Between Acceleration and Ω (Circular Frequency/ Stability Constant) for Several h/d Values

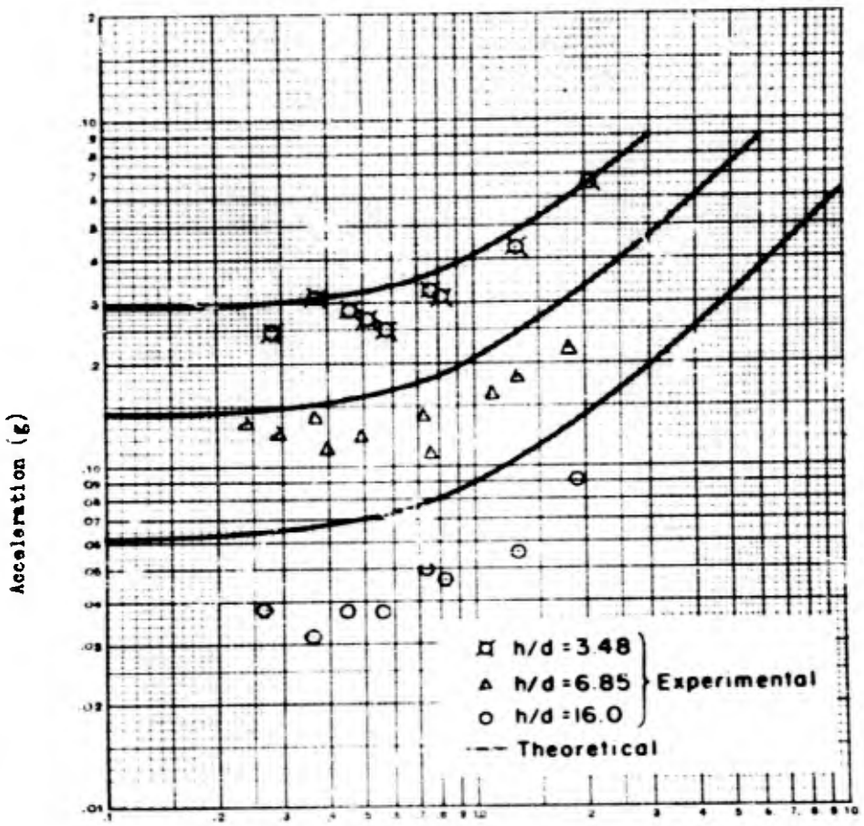

Fig. 2.12 Comparison of Theoretical and Experimental Relationships between Acceleration and Ω (Circular Frequency/ Stability Constant) for Several h/d Values

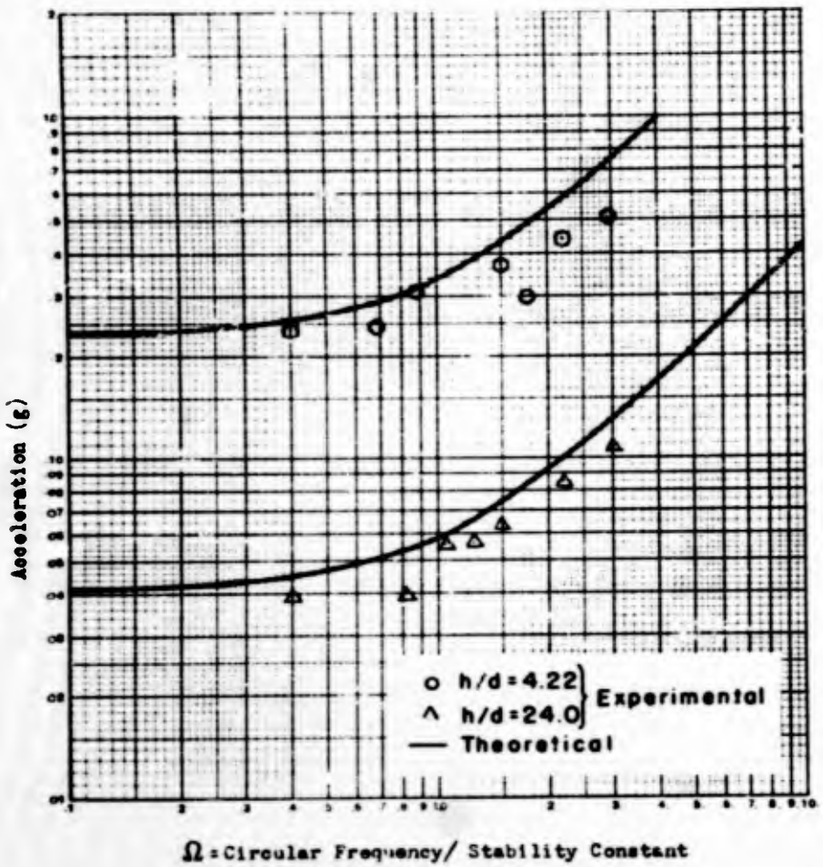

Fig. 2.13 Comparison of Theoretical and Experimental Relationships Between Acceleration and Ω (Circular Frequency/ Stability Constant) for Several h/d Values

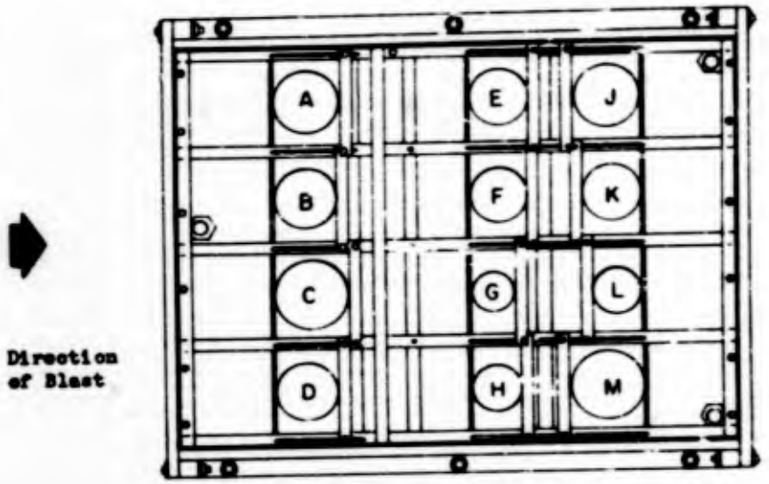

Note: Pins A through H fall in Positive Phase
Pins J through M fall in Negative Phase

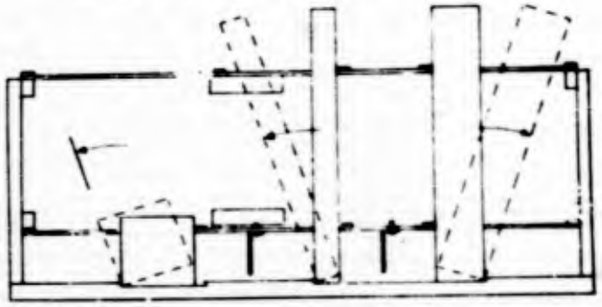

Fig. 2.14 Sketch of Pin Installation

TABLE 2.1

Chart of Pin Locations, Surface Shot - South Blast Line

Pin	Sta 5 + 62.5	Sta 7 + 50	Sta 8 + 75	Sta 10 + 00	Sta 12 + 50	Sta 15 + 00	Sta 18 + 75
A	3 x 5/8 •	3 x 3/8 •	3 x 1/4 •	3 x 1/4 •	3 x 1/4 •	3 x 3/16 •	3 x 3/16 •
B	3 x 3/4 •	3 x 1/2 •	3 x 3/8 •	3 x 5/16 •	3 x 5/16 •	3 x 1/4 •	3 x 1/4 •
C	3 x 7/8 •	3 x 5/8 •	3 x 7/16 •	3 x 3/8 •	3 x 3/8 •	3 x 5/16 •	3 x 5/16 •
D	3 x 1 •	3 x 3/4	3 x 1/2 •	3 x 7/16 •	3 x 7/16 •	3 x 3/8 •	3 x 3/8
E	3 x 1 1/2	12 x 1 3/8 •	12 x 1 •	12 x 7/8 •	12 x 3/4 •	12 x 1/2 •	12 x 1/2
F	12 x 2	12 x 1 1/2 •	12 x 1 1/4 •	12 x 1 •	12 x 7/8 •	12 x 5/8 •	12 x 5/8
G	12 x 2 1/2	12 x 1 3/4 •	12 x 1 3/8 •	12 x 1 1/4 •	12 x 1 •	12 x 3/4 •	12 x 3/4
H	12 x 3	12 x 2	12 x 1 1/2 •	12 x 1 1/2 •	12 x 1 1/8 •	12 x 7/8 •	12 x 7/8
J	3 x 5/8	3 x 5/8 •	3 x 1/4 •	3 x 1/4 •	3 x 3/8 •	3 x 3/16 •	3 x 3/16 •
K	3 x 7/8	3 x 3/4	3 x 1/2	3 x 7/16 •	3 x 3/16 •	3 x 3/8 •	3 x 3/8 •
L	12 x 1 1/2	12 x 1 3/8 •	12 x 1	12 x 7/8 •	12 x 7/8 •	12 x 1/2 •	12 x 7/8
M	12 x 3	12 x 2	12 x 1 1/2	12 x 1 1/4 •	12 x 5/8 •	12 x 7/8 •	12 x 1/2 •

• Pin overturned during test

See Figure 2.17 for pin locations

TABLE 2.2

Chart of Pin Locations, Surface Shot - East Blast Line

Station / Pin	6 + 25	7 + 50	10 + 00	12 + 50
A	3 x 5/8 *	3 x 3/8 *	3 x 1/4 *	3 x 3/16 *
B	3 x 3/4 *	3 x 1/2	3 x 5/16 *	3 x 1/4 *
C	3 x 7/8 *	3 x 5/8	3 x 3/8 *	3 x 5/16 *
D	3 x 1	3 x 3/4	3 x 7/16 *	3 x 3/8 *
E	12 x 1 3/4	12 x 1 3/8	12 x 7/8	12 x 1/2 *
F	12 x 2 1/4	12 x 1 1/2	12 x 1	12 x 5/8 *
G	12 x 2 3/4	12 x 1 3/4	12 x 1 1/8	12 x 3/4
H	12 x 3	12 x 2	12 x 1 1/4	12 x 7/8
J	3 x 5/8	3 x 3/8 *	3 x 1/4 *	3 x 3/16 *
K	3 x 1	3 x 3/4	3 x 7/16 *	3 x 3/8 *
L	12 x 1 3/4	12 x 1 3/8	12 x 1 1/4	12 x 1/2 *
M	12 x 3	12 x 2	12 x 7/8 *	12 x 7/8

* Pin overturned during test

See Figure 2.14 for pin locations

TABLE 2.3

Chart of Pin Locations, Surface Shot - West Blast Line

Pin \ Station	6 + 25	7 + 50	10 + 00	12 + 50
A	3 x 5/8	3 x 3/8 *	3 x 1/4 *	3 x 5/16 *
B	3 x 3/4	3 x 1/2 *	3 x 5/16	3 x 1/4
C	3 x 7/8	3 x 5/8 *	3 x 3/8 *	3 x 5/16 *
D	3 x 1	3 x 3/4	3 x 7/16 *	3 x 3/8 *
E	12 x 1 3/4	12 x 1 3/8	12 x 7/8	12 x 1/2 *
F	12 x 2 1/4	12 x 1 1/2 *	12 x 1	12 x 5/8 *
G	12 x 2 3/4	12 x 1 3/4	12 x 1 1/8	12 x 3/4 *
H	12 x 3	12 x 2	12 x 1 1/4	12 x 7/8 *
J	3 x 5/8	3 x 3/8 *	3 x 1/4 *	3 x 3/16 *
K	3 x 1	3 x 3/4	3 x 7/16 *	3 x 3/8 *
L	12 x 1 3/4	12 x 2	12 x 1 1/4	12 x 5/8 *
M	12 x 3	12 x 1 3/8 *	12 x 7/8 *	12 x 7/8 *

* Pin overturned during test

See Figure 2.14 for pin locations

TABLE 2.4

Chart of Pin Locations, Underground Shot - South Blast Line

Pin	Sta 5 + 62.5	Sta 7 + 50	Sta 8 + 75	Sta 10 + 00	Sta 12 + 50	Sta 15 + 00	Sta 18 + 75
A	3 x 1 *	3 x 5/8 *	3 x 7/16 *	3 x 7/16 *	3 x 5/16 *	3 x 1/4 *	3 x 3/16 *
B	3 x 1 1/2 *	3 x 3/4 *	3 x 1/2 *	3 x 1/2 *	3 x 3/8 *	3 x 3/8 *	3 x 1/4 *
C	3 x 2	3 x 7/8 *	3 x 5/8 *	3 x 5/8 *	3 x 5/8	3 x 7/16 *	3 x 5/16 *
D	3 x 2 1/2	3 x 1 *	3 x 3/4 *	3 x 3/4 *	12 x 11/16 *	3 x 1/2 *	3 x 3/8 *
E	3 x 3	12 x 1 3/4 *	12 x 1 1/4 *	12 x 1 *	12 x 1 *	12 x 5/8 *	12 x 5/8 *
F	12 x 2 *	12 x 2 *	12 x 1 1/2 *	12 x 1 1/4 *	12 x 1 1/4 *	12 x 1	12 x 11/16 *
G	12 x 2 1/2	12 x 2 1/2	12 x 1 3/4 *	12 x 1 3/8 *	12 x 1 3/8 *	12 x 1 1/4 *	12 x 1
H	12 x 3	12 x 3	12 x 2 *	12 x 1 1/2 *	12 x 1 1/2	12 x 1 1/2	12 x 1 1/4
J	3 x 1 *	3 x 5/8	3 x 5/8 *	3 x 3/8 *	3 x 1/4 *	3 x 1/4 *	3 x 1/4 *
K	3 x 2	3 x 1 *	3 x 3/4 *	3 x 5/8 *	3 x 7/16 *	3 x 1/2 *	3 x 3/8 *
L	3 x 3	12 x 1 3/4	12 x 1 1/4 *	12 x 1 *	12 x 1	12 x 1 1/2	12 x 1 *
M	12 x 3	12 x 3	12 x 2 *	12 x 1 1/2	12 x 1 1/4	12 x 1	12 x 1 1/4

* Pin overturned during test

See Figure 2.14 for pin locations

TABLE 2.5

Chart of Pin Locations, Underground Shot - East Blast Line

Station / Pin	6 + 25	7 + 50	10 + 00	12 + 50
A	3 x 3/4	3 x 5/8	3 x 5/16 *	3 x 3/8 *
B	3 x 1 1/2	3 x 3/4	3 x 3/8 *	3 x 7/16 *
C	3 x 1	3 x 7/8	3 x 7/16 *	3 x 1/2 *
D	3 x 2	3 x 1	3 x 1/2	3 x 5/8
E	3 x 2 1/2	12 x 1 3/4	12 x 1 *	12 x 11/16 *
F	12 x 2 1/2	12 x 2 1/2	12 x 1 1/4	12 x 3/4 *
G	12 x 2 3/4	12 x 2	12 x 1 3/8	12 x 7/8 *
H	12 x 3	12 x 3	12 x 1 1/2	12 x 1 1/8 *
J	3 x 3/4	3 x 5/8	3 x 1/4 *	3 x 1/4 *
K	3 x 2 1/2	3 x 1	3 x 1/2 *	3 x 1/2 *
L	12 x 2 1/2	12 x 1 3/4	12 x 1 1/2	12 x 5/8 *
M	12 x 3	12 x 3	12 x 1	12 x 1 *

* Pin overturned during test

See Figure 2.14 for pin locations

TABLE 2.6

Chart of Pin Locations, Underground Shot - West Blast Line

Station / Pin	6 + 25	7 + 50	10 + 00	12 + 50
A	3 x 3/4 *	3 x 5/8 *	3 x 3/8 *	3 x 3/8 *
B	3 x 1 *	3 x 3/4 *	3 x 7/16 *	3 x 7/16 *
C	3 x 1 1/2 *	3 x 7/8 *	3 x 1/2 *	3 x 5/8 *
D	3 x 2	3 x 1 *	3 x 3/4 *	12 x 5/8 *
E	3 x 2 1/2	12 x 1 3/4 *	12 x 1 *	12 x 11/16 *
F	12 x 2 1/2	12 x 2 *	12 x 1 1/4 *	12 x 3/4 *
G	12 x 2 3/4	12 x 2 1/2 *	12 x 1 3/8 *	12 x 1 *
H	12 x 3	12 x 2 5/8	12 x 1 1/2 *	12 x 1 1/4 *
J	3 x 3/4 *	3 x 5/8 *	3 x 1/4 *	3 x 1/4 *
K	3 x 2 1/2	3 x 1	3 x 5/16 *	3 x 1/2 *
L	12 x 2 1/2	12 x 1 3/4 *	12 x 1 *	12 x 1 1/4 *
M	12 x 3	12 x 3	12 x 1 1/2 *	12 x 1 *

* Pin overturned during test

See Figure 2.14 for pin locations

CHAPTER 3

OPERATIONS

3.1 SITE CONDITIONS

The geology of the general area has been described in the United States Geological Survey report on Project 1 (8)a entitled "Operations WINDSTORM and JANGLE, Geologic, Hydrologic and Thermal Features of the Site", dated Feb. 1952. Data on a seismic refraction survey of Nye County, Nevada, dated 27 July 1951 by the United States Geophysical Company, Inc. is available in the JANGLE Report Series as Project 1 (8)a-1. In general, the valley fill at the surface and underground test areas can be described as an incoherent alluvium which originated in the siliceous volcanic formations forming the adjacent highlands. It is composed of fine to coarse sand and gravel with numerous, discontinuous layers of caliche of random depth.

None of the information on the detailed properties of the soil at each installation and along each blast line, has been received to date. Consequently, since very little is known on the engineering properties of the ground, it is impractical to attempt correlations with the very extensive data available from numerous high explosives tests in other types of media. Similarly, no attempt is made to predict effects due to other depths of detonation or to scale the available data to other sizes and types of weapons.

3.2 FIELD LAYOUT

The locations of shock pin installations relative to Ground Zero were identical for the surface and underground sites. The detailed layout plan is shown in Fig. 3.1 and a typical installation is illustrated by Fig. 3.2. The base plate of each installation was approximately two feet below the ground surface, and was grouted and bolted to a concrete pad which in turn was firmly anchored into the ground by means of anchor rods and by providing good contact with the soil on all sides of the pad.

3.3 CONSTRUCTION AND INSTALLATION

The corrugated metal pipe and the dome-shaped lids used as shelters for the shock pin installations were originally procured by the Bureau of Yards and Docks of the Navy Department for use at the Amchitka site. All construction at the Nevada site was performed by

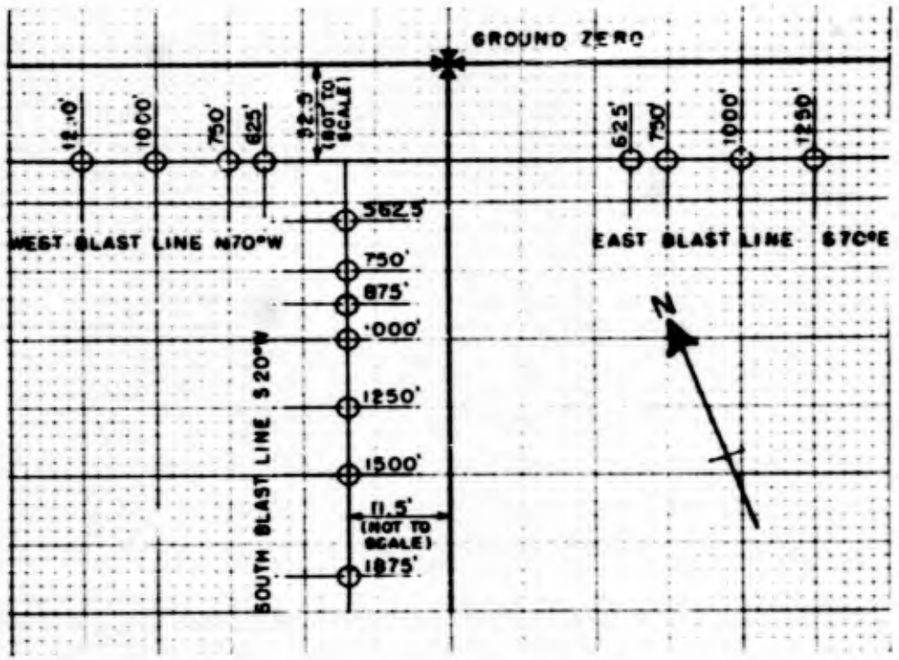

Fig. 3.1 Operation JANGLE, Underground and Surface Sites, Project 1.7, Location Plan

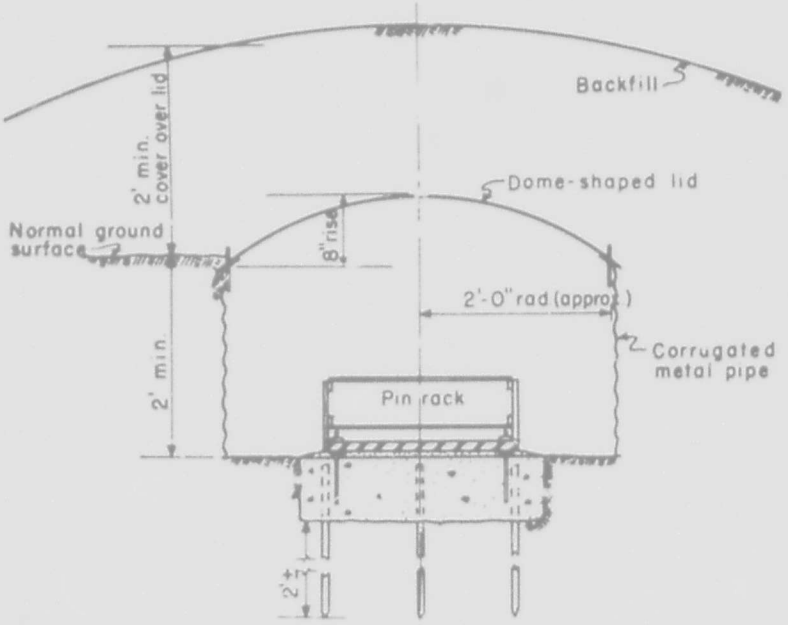

Fig. 3.2 Approximate Cross Section of Typical Shock Pin Installation

Fig. 3.3 Installation Prior to Grouting Pin Plate and Placing Corrugated Liner

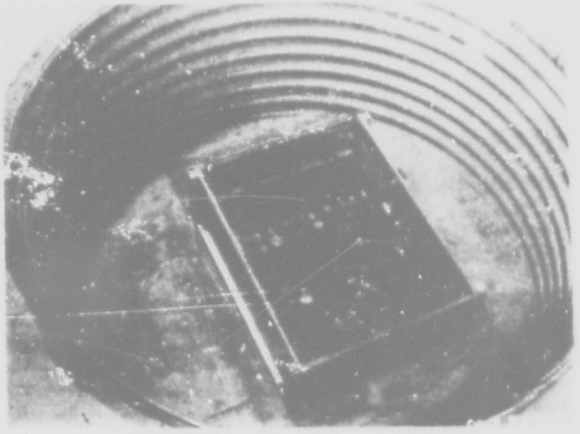

Fig. 3.4 A Completed Installation with Pins in Position

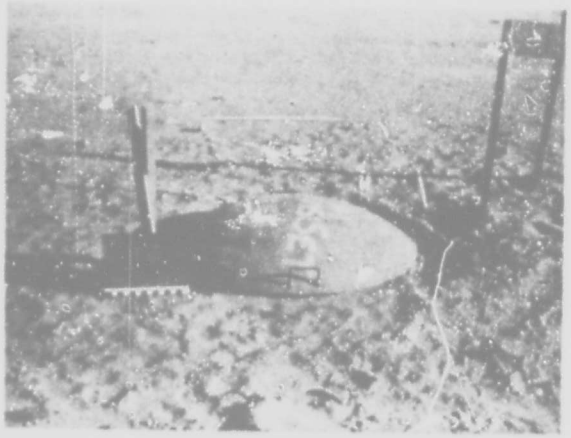

Fig. 3.5 Installation with Lid in Place, Prior to Placing Protective Earth Fill

Fig. 3.6 Completed Installation Prior to Test

the AEC's general contractor. The pin plates were set and grouted by project personnel who also installed the racks and pins and made the pre-test and post-test examinations. Figs. 3.3 through 3.6 illustrate various steps in the construction and installation sequence.

3.4 COLLECTION OF DATA

As soon as each area could be safely entered after the tests, a careful examination was made of the exterior of each installation in order to record any visual damage or changed conditions. This included checks for fissuring and erosion of the earth cover over the shelter, as well as any cracking or settling which might indicate that the shelter had moved in a different manner than the surrounding earth.

Excavating equipment and laborers were then used to uncover the shelters sufficiently to permit removal of the lids and allow entry into the shelters. The positions of all disturbed pins were then sketched and photographs obtained, and a careful check was made within the shelter for general evidence of damage or of separation between the concrete anchor pad and the surrounding earth. Typical views of the post-shot conditions of the shelters and the pin installations are shown by Figs. 3.7 and 3.8.

3.5 PRE-TEST AND POST-TEST SURVEYS

Numerous tests were made, prior to the shot, to determine whether any pins could be accidentally upset during the process of sealing and covering the shelters, or by the operation of heavy construction equipment adjacent to the shelter before the shot and during the excavation work following the shot. It was found that with the pins located completely clear of the supporting grid and spacer bars, the pins could not be upset by bumping the rack or shelter, or by vibrations of the heavy equipment to be used in the areas. In one instance evidence was found where a steel-track vehicle, probably a tractor, had traveled across an uncovered shelter without upsetting any pins or collapsing the thin, metal-dome lid.

In order to determine whether the surface shot could upset pins in the underground shot area, and vice versa, the lightest sets of pins were set at several of the underground installations nearest the surface area, and then rechecked after the surface shot. Similar checks were made in the surface area for the underground shot. No pins were upset in either of the above check series. However, a similar check at the surface shot area during the last shot of the BUSTER series gave a very uniform relation between the slenderness ratio of the largest pins upset and the distance from the shot to

Fig. 3.7 Surface Shot - Condition of Protective Cover as a Result of Test

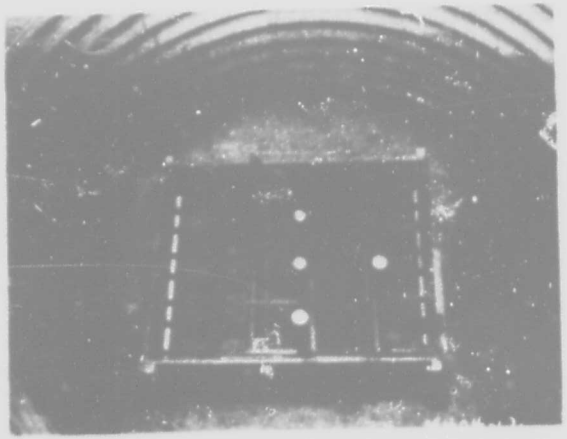

Fig. 3.8 Typical Condition of Shock Pin Installation During Post-Test Survey

the pin sets. It should be noted that the BUSTER air burst, while larger than the JANGLE underground shot, upset numerous pins at distances greater than the corresponding distance between the surface and underground shots.

When project personnel arrived on the site prior to the test, it was found that the installations of Projects 1.6 and 1.7 had not been included in the plans for survey. Consequently project personnel eventually were required to perform considerable survey work in order to establish possible displacements. Since only relatively rough surveys were made by project personnel, information on precise surveys will not be available until later in the year when the United States Coast and Geodetic Survey submits its data.

3.6 SALVAGE

None of the shelters, racks, pins, or any other components were damaged by the atomic explosion. The main damage to the installations consists of extensive rusting of the milled surfaces of the pins and pin plates which occurred as a result of the long period during which the shelters were open to the weather waiting for the surveys on these installations to be completed by the United States Coast and Geodetic survey.

No salvage is contemplated since the Office, Chief of Engineers has no further tests scheduled which require shock pin installation. The low cost of the installations, the very high cost of salvage work, if done by the contractor on the site, and the lack of suitable safe, dry storage in the test area, does not justify any recovery work at this time. Some salvage by other groups may be practical if they can use the shelters or other parts for future projects in the area.

CHAPTER 4

TEST RESULTS

4.1 GENERAL SUMMARY OF DATA ON SHOCK PINS

As we well know at the present time, the general order of magnitudes of accelerations resulting from the JANGLE tests was in fair agreement with the predictions of the Stanford Research Institute and Naval Ordnance Laboratory. The frequencies of the ground motions, however, were far greater than any of the predictions. This latter factor exerted a profound influence upon the use of shock pins for measurement of ground accelerations.

Let us refer again to the plot of acceleration vs circular frequency for the 3 inch and 12 inch pins shown in Fig. 2.2. It can be readily seen that for high frequency values, the plots for the two heights of pins used in the tests are essentially parallel. It was hoped that by determining the limiting h/d values of both heights of pins which had overturned during the tests, the acceleration and corresponding frequency occurring at each test point could be ascertained. However, the poorly defined intersection of curves occurring at the test frequencies, almost completely invalidated this concept.

In lieu of this method, it was decided to obtain values of the characteristic frequencies of ground accelerations occurring at the various installations from the electronic records of the Naval Ordnance Laboratory. Plots of the characteristic periods of initial acceleration cycle vs λ for both the surface and underground tests are shown in Fig. 4.1. Using the periods corresponding to the various λ values at which the shock pin installations were located, we were able to determine the values of Ω for each of the pin heights. With these values and the appropriate h/d ratios of the pins in question, the corresponding magnitudes of acceleration were obtained from Fig. 2.1.

The results for both the surface and underground tests are graphically represented in Figs. 4.2 through 4.10. These plots show the acceleration occurring at the various λ values of the shock pin installations. It will be noted that whenever the test data permitted, bracketing values of the acceleration were indicated. That is to say: if a given pin had overturned, it did not necessarily mean that the acceleration corresponding to that pin was definitely

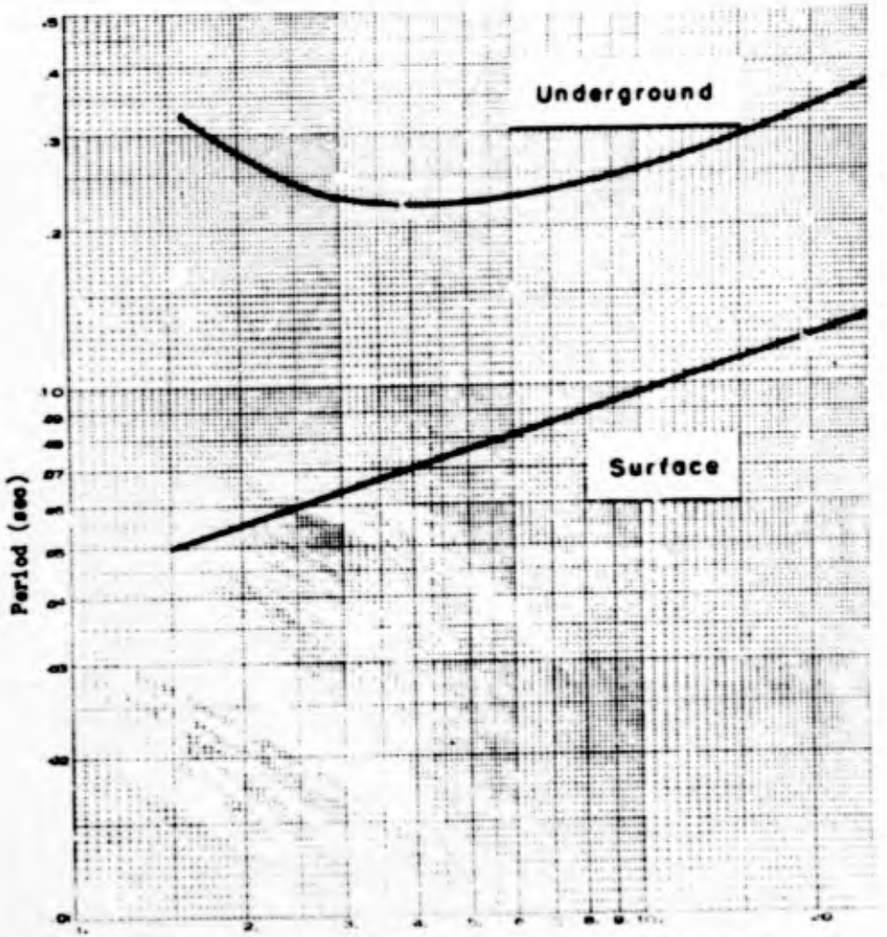

Fig. 4.1 JANGLE Characteristic Period of Initial Acceleration Cycle vs Lambda (from Naval Ordnance Laboratory Accelerograms)

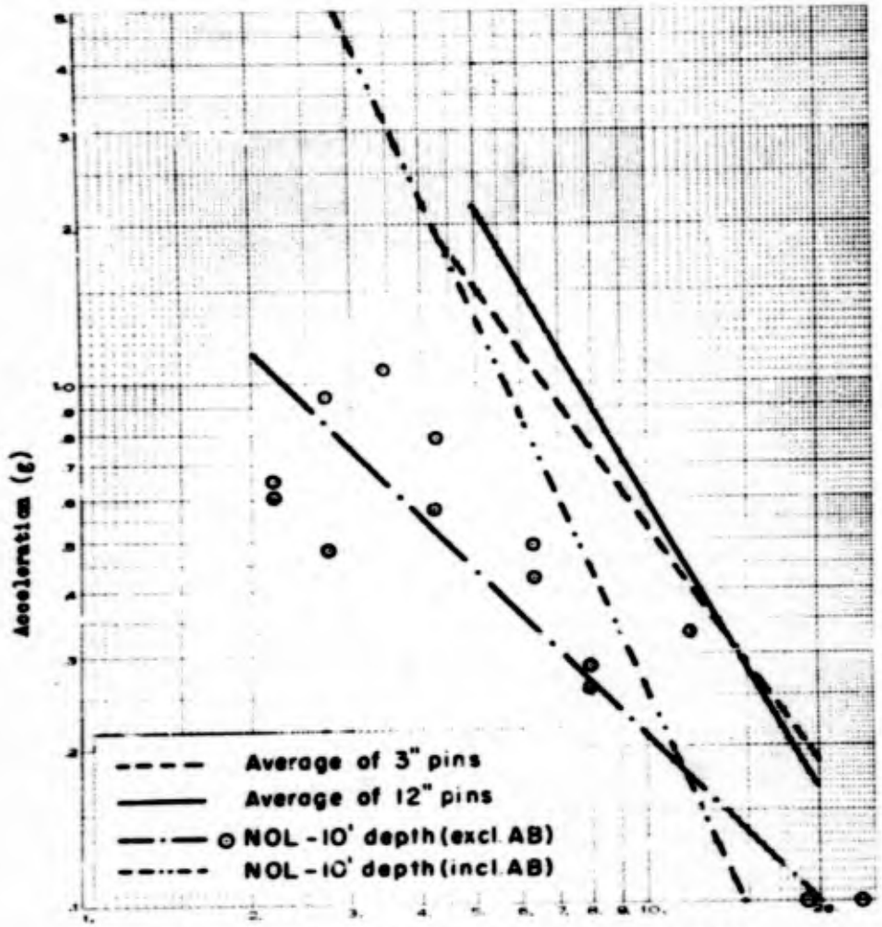

Fig. 4.2 Surface Shot - Positive Phase; Peak Horizontal Acceleration vs Lambda - South Blast Line

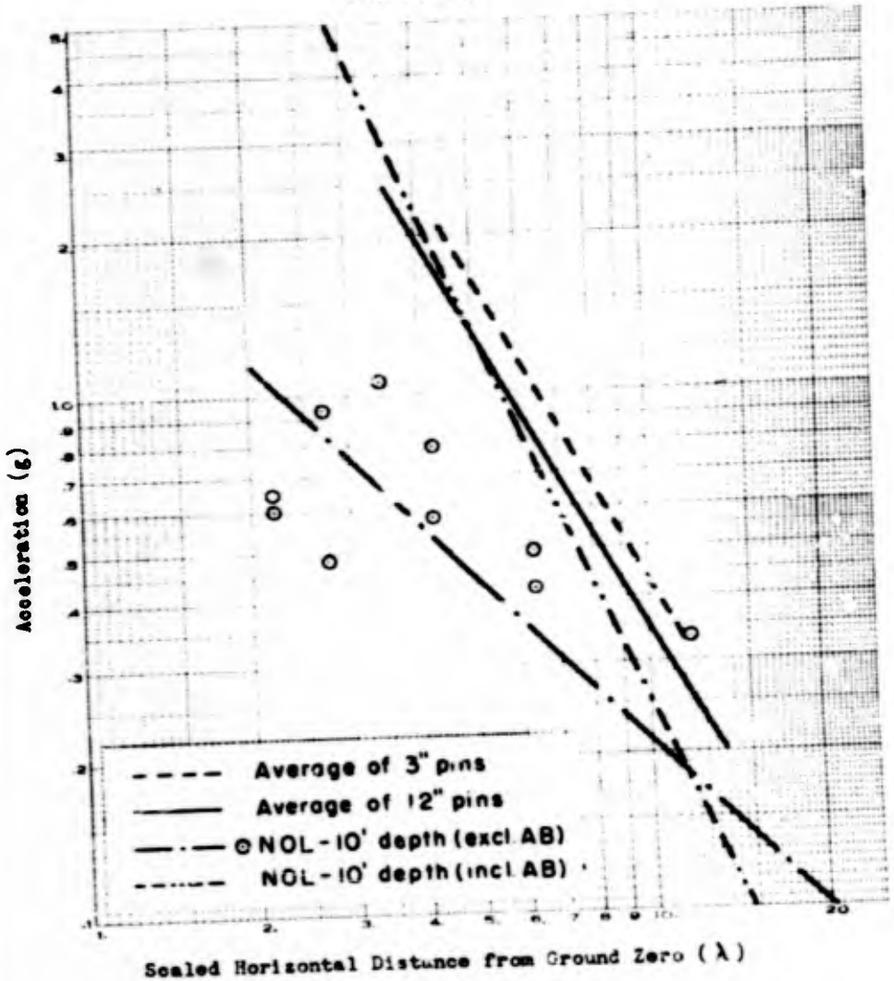

Fig. 4.3 Surface Shot - Positive Phase; Peak Horizontal Acceleration vs Lambda - East and West Blast Lines

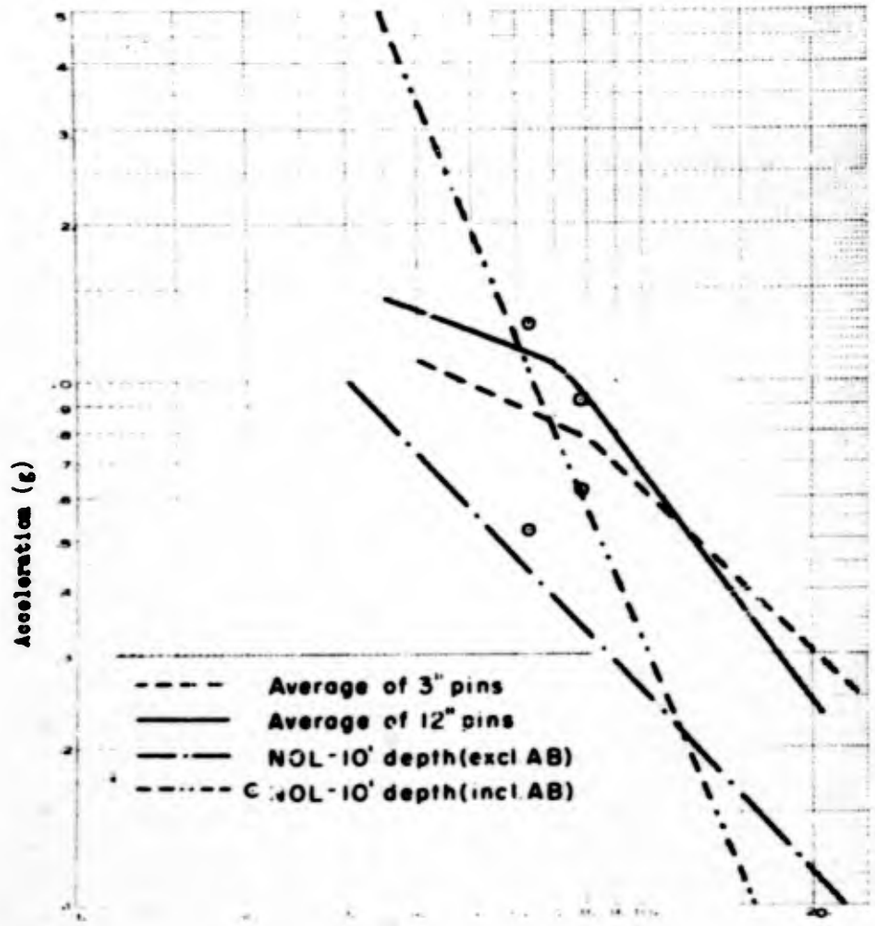

Fig. 4.4 Surface Shot - Negative Phase; Peak Horizontal Acceleration vs Lambda - South Blast Line

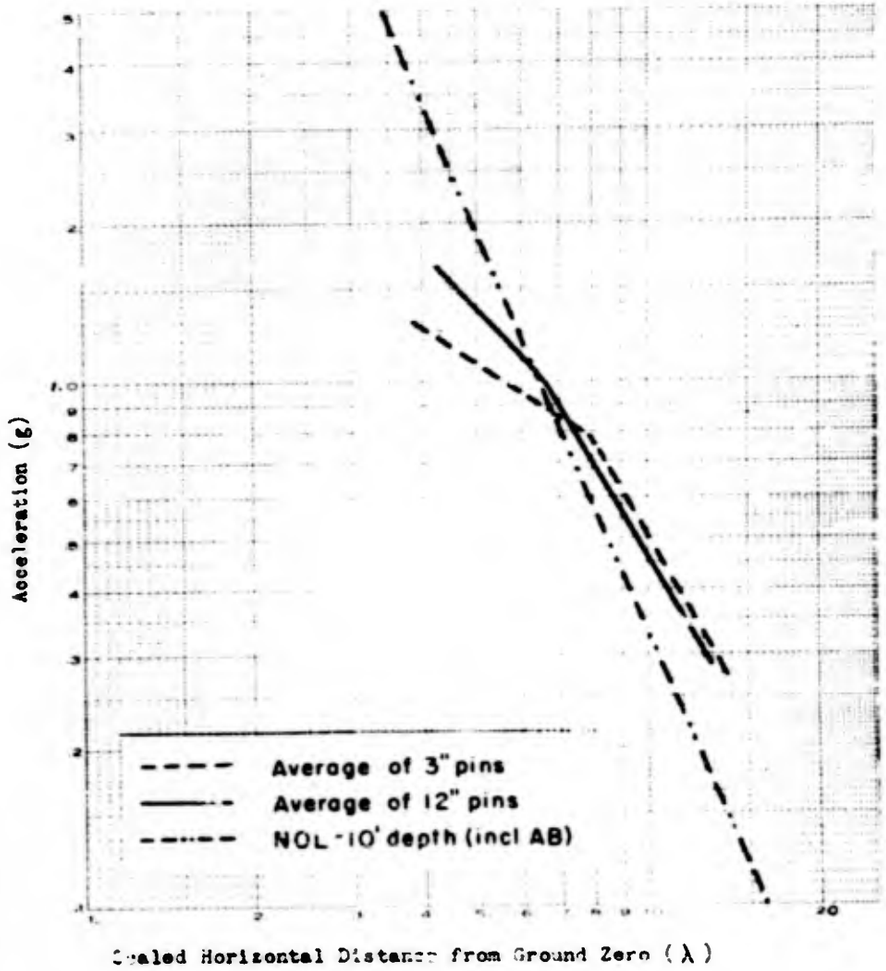

Fig. 4.5 Surface Shot - Negative Phase; Peak Horizontal Acceleration vs Lambda - East and West Blast Lines

PROJECT 1.7

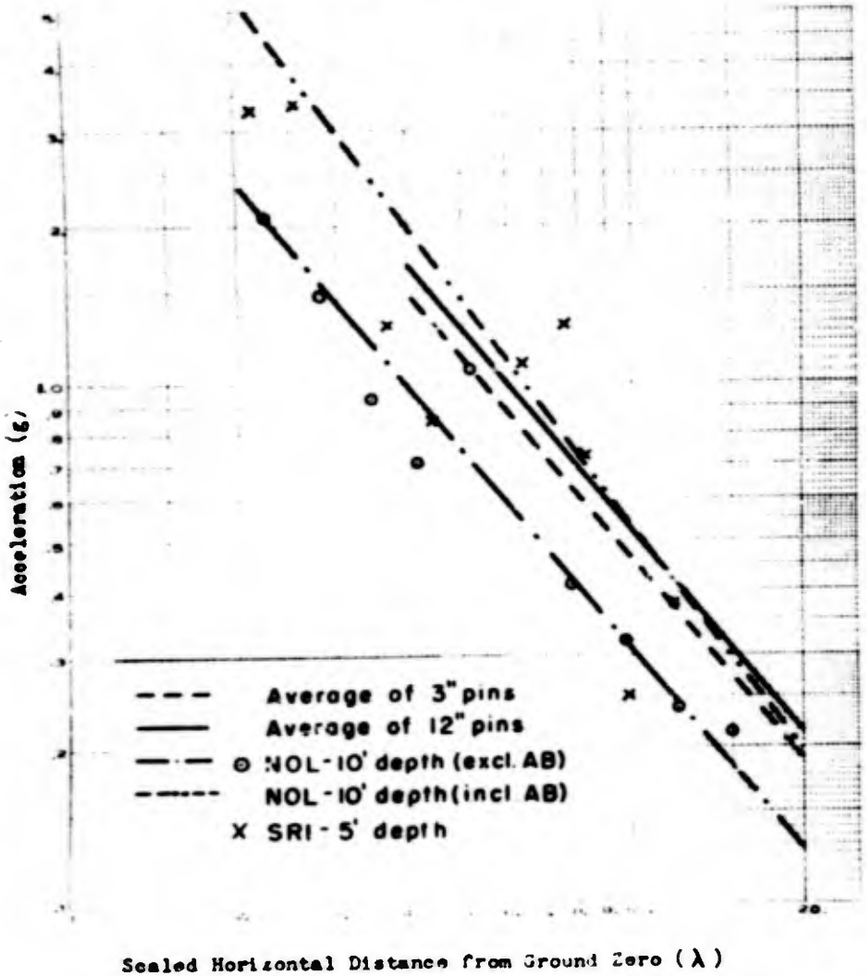

Fig. 4.6 Underground Shot - Positive Phase; Peak Horizontal Acceleration vs Lambda - South Blast Line

PROJECT 1.7

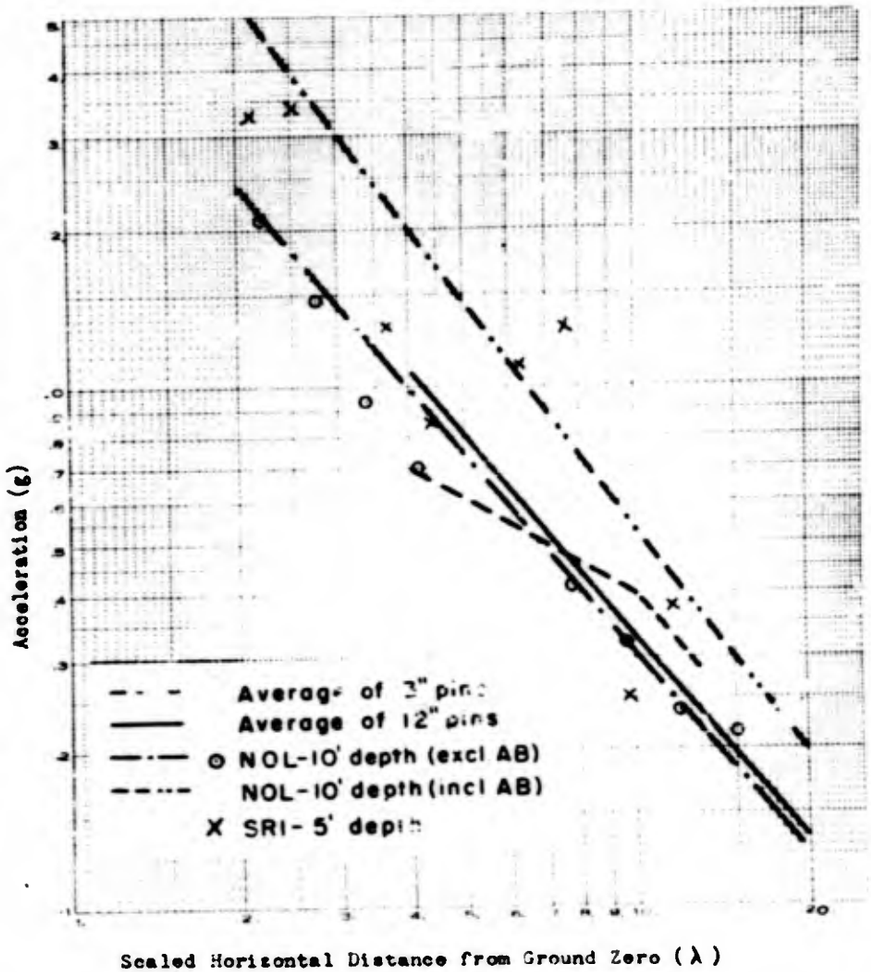

Fig. 4.7 Underground Shot - Positive Phase; Peak Horizontal Acceleration vs Lambda - East Blast Line

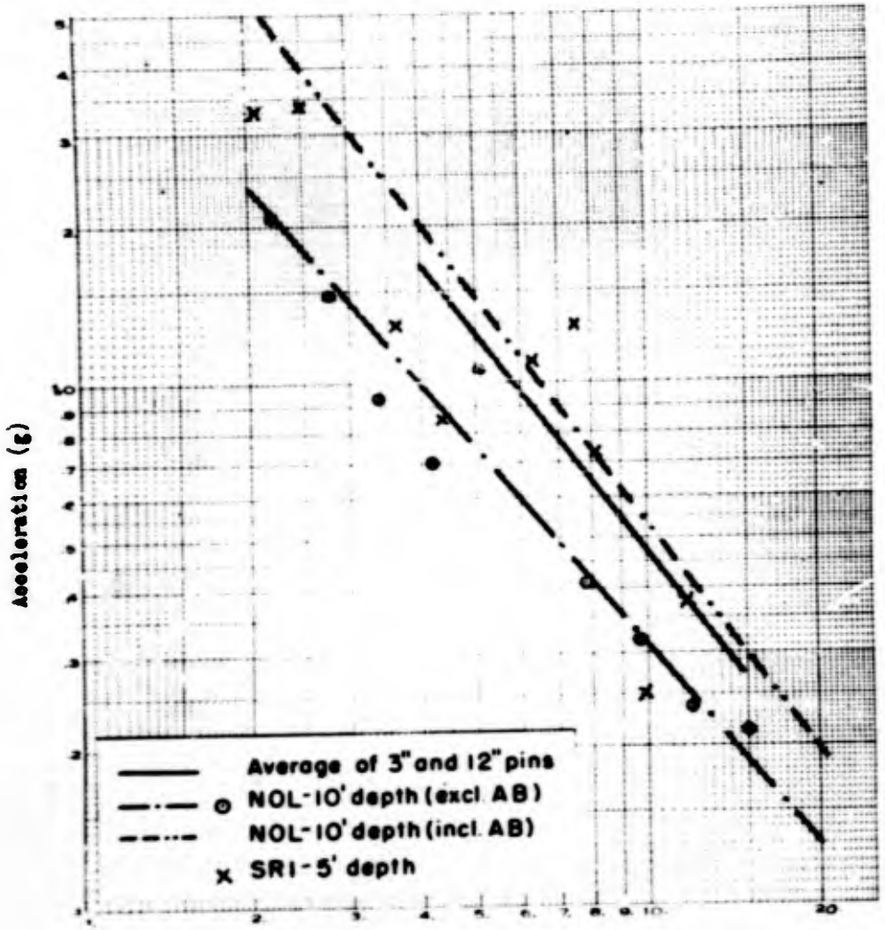

Fig. 4.8 Underground Shot - Positive Phase; Peak Horizontal Acceleration vs Lambda - West Blast Line

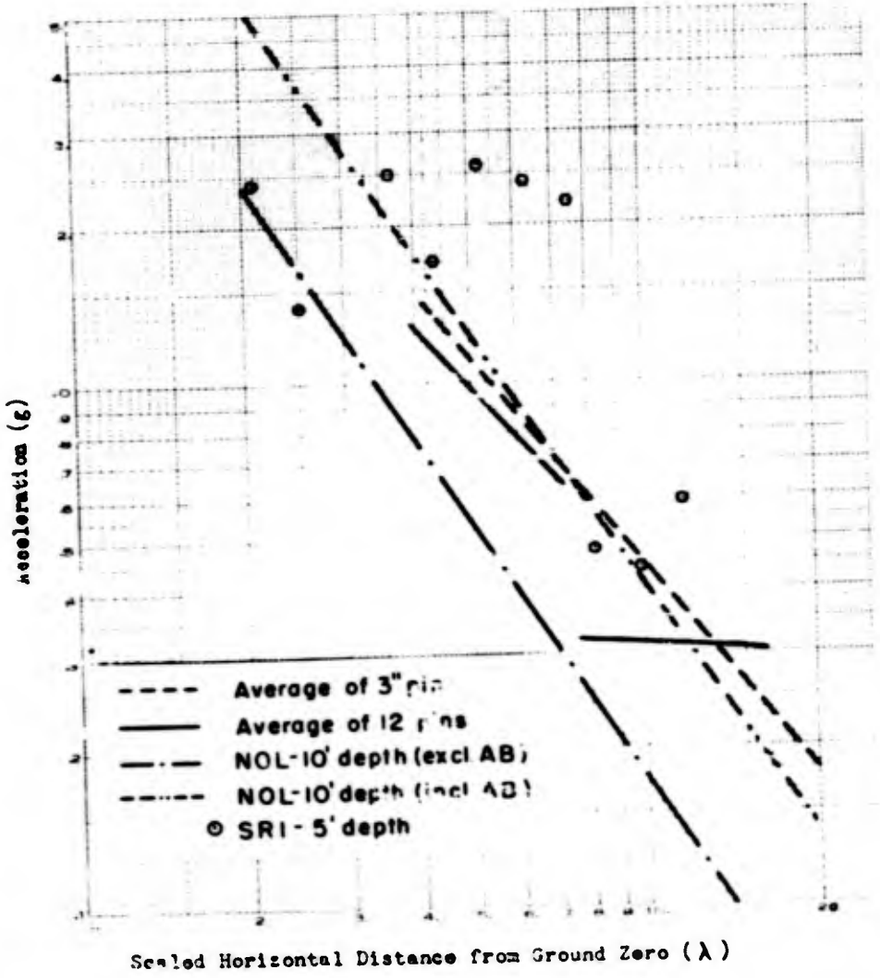

Fig. 4.9 Underground Shot - Negative Phase; Peak Horizontal Acceleration vs Lambda - South Blast Line

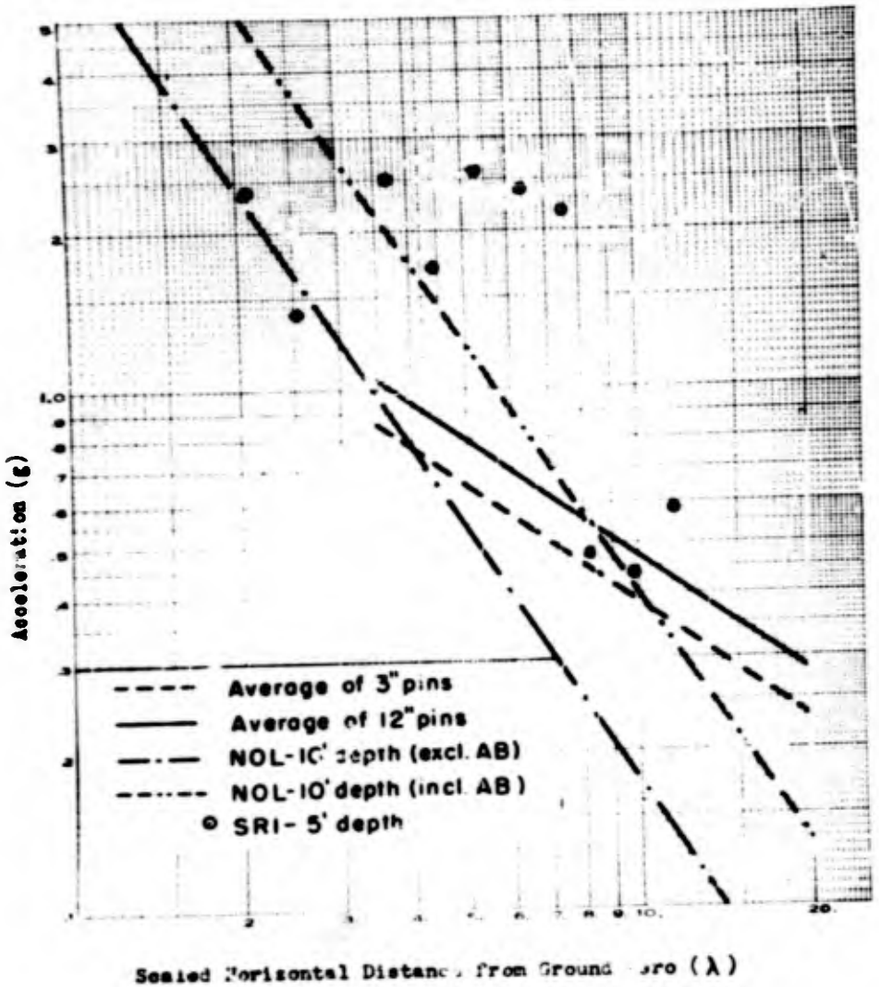

Fig. 4.10 Underground Shot - Negative Phase; Peak Horizontal Acceleration vs Lambda - East and West Blast Lines

the acceleration that had occurred, but rather that the acceleration was greater than that value. Whenever possible then, we computed the acceleration necessary to overturn the next larger sized pin which had not overturned during the test. In this manner we could then conclude that the acceleration that had taken place was between the values necessary to overturn these two pins. Unfortunately, in many cases the upper or lower ranges were completely lacking due to either all the pins overturning, or else all remaining standing. This fact in itself is not valueless, however, as it at least supplied us with either an upper or lower limit of acceleration occurring at the point.

In addition to the acceleration values obtained through the use of shock pins, Figs. 4.2 through 4.10 also show the values of acceleration obtained by the Naval Ordnance Laboratory and in some cases the Stanford Research Institute, through their electronic accelerographs. In this manner, we were provided with some method of comparing the values obtained by using shock pins with those of more exact measuring instruments.

4.2 CONDITION OF SHELTERS

None of the shelters at either the surface or underground test areas suffered damage, displacement, or permanent distortion due to the atomic tests. Some erosion and fissuring occurred in the earth fill over the domes but, with the exception of a very minor amount of cracking in the earth adjacent to the concrete pad in one shelter, there was no evidence that the shelters, concrete pads, and the foundation strata failed to move as a unit. No survey data have been received from the United States Coast and Geodetic Survey to date, but it is suspected that the pin plates suffered no permanent displacement.

4.3 EFFECTS OF EARTH COVER

It was originally planned to place an earth cover of two foot minimum thickness over each shelter as shown in Fig. 3.2 in order to reduce air blast effect and to prevent collapse or displacement of the thin metal dome which sheltered the pin sets. As finally built, the minimum depth of earth for the various shelters varied between one-half and two feet. For the locations and weapon sizes used in Operation JANGLE, one-half foot of earth cover would probably have been adequate for all the installations.

CHAPTER 5

DISCUSSION

5.1 COMPARISON OF PREDICTED AND OBSERVED VALUES

Within the limit of accuracy of shock pins as a means of determining ground accelerations, the general order of magnitude of the predicted and observed values of horizontal acceleration appeared to be essentially the same.

5.2 ACTUAL VARIATIONS FROM BASIC ASSUMPTIONS AND THEIR EFFECTS ON RESULTS

In the development of the theoretical shock pin equation, (Eq. 2.2), only the effect of horizontal acceleration was considered. This was adopted for reasons stated in sub-paragraph 2.2.2. Likewise, the calibration procedure carried out in the laboratory delivered only horizontal acceleration to the shock pins.

In actual field tests such as the surface and underground shots of Operation JANGLE, it was well known that the motion was not as simple as was assumed in the analysis. It was recognized that vertical and transverse components of the acceleration existed, but that the effect of these components was of secondary importance as compared with the horizontal motion. The effect of neglecting the vertical acceleration that does exist, and computing horizontal accelerations from the theoretical shock pin equation (Eq. 2.2), would be as follows:

1. We would obtain horizontal accelerations of a higher value than actually existed. This is to say: a pin with a given h/d ratio and theoretically requiring a given value of horizontal acceleration to cause overturning, would possibly be overturned at a lesser value of horizontal acceleration than computed.

2. The 12 inch pins, being more slender than the 3 inch pins, would be more sensitive to the effects of vertical acceleration. They would thus be more easily overturned due to the effects of the vertical acceleration, and consequently would indicate higher horizontal accelerations than the 3 inch pins when using the theoretical equation. In several cases, this appears to be true.

5.3 COMPARISON WITH DATA OF [illegible] PROJECTS

As can be seen in Figs. 4.3 through 4.10 inclusive, the values of horizontal acceleration obtained using shock pins appear to be in reasonable agreement with the more exact data obtained by the Naval Ordnance Laboratory, and by the Stanford Research Institute. Considerable spread of the test data exists, but it is not considered excessive in view of the complex nature of the ground motion that occurred during the tests.

In many cases, the values of horizontal acceleration obtained using shock pins appear to show a less rapid attenuation with increasing λ values, than the more precise records indicate. This would be expected due to the fact that the more slender pins were utilized at the larger λ values, these more slender pins being more susceptible to the effects of vertical acceleration than the stubbier pins. As was explained in 5.2, this fact tended to give higher indicated values of horizontal acceleration than actually existed during the tests.

CHAPTER 6

CONCLUSIONS

6.1 CONCLUSIONS

This report is considered final, insofar as project personnel are concerned, and no further action is contemplated to analyze and report any related data which may later become available from other organizations. All statements apply only to test conditions similar to those of Operation JANGLE and the Nevada Test Site unless specifically stated otherwise. The following conclusions are based on the experience and data obtained to date from Operation JANGLE.

1. Shock pins may be used to provide a very rough value of the horizontal acceleration occurring at various distances from a shot point. This may only be done, however, when some approximate indications as to the magnitude and frequency of the acceleration and the distances to the various shock pin installations are known. This information is necessary so that shock pin sizes may be selected accordingly.

2. In the post-test calculations, to determine the magnitude of acceleration that was required to overturn a given size shock pin, we must have some indication as to the frequency of the acceleration before any definite numerical values can be determined.

In some instances, it may be possible to utilize two sets of pins with different pin heights. In such a case, we might be able to obtain the horizontal acceleration that occurred without being directly concerned with a frequency determination, or a correlation with other instrumentation methods. This could theoretically be accomplished by the simultaneous solution of Eq. 2.2 with the appropriate constants for the pin heights substituted therein. As was described in sub-paragraph 2.3, such an approach is practicable only if reasonably sharp intersections of the curves representing the equations for the pin heights are attainable. For the accelerations and frequencies associated with large explosions, however, wide variations in pin heights are required in order to obtain these sharp intersections. This method has the disadvantages of requiring extremely cumbersome and heavy pins in the one case, and very small pins on the other. With the larger pins, the cost of materials, fabrication, shipment, and installation would be high.

3. The pin shelters used in the tests were very satisfactory, no damage to any installations having occurred during the test.

4. There appears to be some lack of symmetry with respect to the magnitude of accelerations along the various blast lines. This may possibly be partly due to the approximate nature of shock pin instrumentation. However, the heterogeneous nature of the soil medium is probably the main contributing factor.

5. The accelerations obtained using shock pins at both the surface and underground tests, seem to be of the same general order of magnitude.

6. It is believed that the shock pins used in the field tests measured peak horizontal acceleration with air blast included. This is borne out in Figs. 4.2 through 4.10. The average values of acceleration obtained using shock pins consistently appear to be in fair agreement with the Naval Ordnance Laboratory values of acceleration (air blast included).

CHAPTER 7

RECOMMENDATIONS

7.1 RECOMMENDATIONS

If the future use of shock pins as a rough means of measuring magnitudes of acceleration is contemplated, the following recommendations are made:

1. Utilize a well machined pin plate surface, and insure that all shock pins are satisfactorily squared and faced.

2. To eliminate small irregularities between pin ends and pin plate surface, it is suggested that a concave surface be machined on the bottom ends of all shock pins.

3. Rather than employ the method of utilizing widely varying pin heights as a means of determining horizontal acceleration, without being dependent upon a determination of the frequency of ground motion obtained from other sources, it is suggested that small convenient pin heights be used. Using these smaller pins, of say from 3 to 6 inches in height, considerable saving in shipping, fabrication, material and installation will be realized.

4. If we follow recommendation number 3, we will be dependent upon a correlation with the more precise instrumentation methods. For purposes of planning for future tests, this means that some predictions as to the anticipated frequency of acceleration must be made. For such planning, it is believed that a reasonably reliable prediction of the anticipated frequency may be obtained from the expression:

$$f = \frac{\sqrt{2}}{3\pi} \cdot \frac{v}{r} \qquad (7.1)^1$$

where: v = Seismic velocity (ft/sec)

r = Crater radius (ft) (from Lamerson's Crater Formula)

[illegible] and C. J. Cheney, Generation and Propagation of Ultrasonic Waves in [illegible], U. S. Bureau of Mines Report of Investigations [illegible], Department of the Interior, 1950.

f = Frequency (cps)

5. In providing earth cover for shock pin installations, it is believed that approximately 6 inches of fill over each installation is sufficient. This will considerably reduce the amount of radiation absorbed by personnel in the uncovering operation after a test.

6. Due to the comparatively inexpensive nature of shock pin instrumentation, it is suggested that a greater number of installations per blast line, covering a wider range of λ values, should be used in future tests.

APPENDIX A

THEORETICAL ANALYSIS

The following analysis is a derivation of Eq. 2.2 used in the text of this report. All symbols used in this analysis are defined in the NOTATION, pages x and xi.

A.1 DEVELOPMENT OF DIFFERENTIAL EQUATION

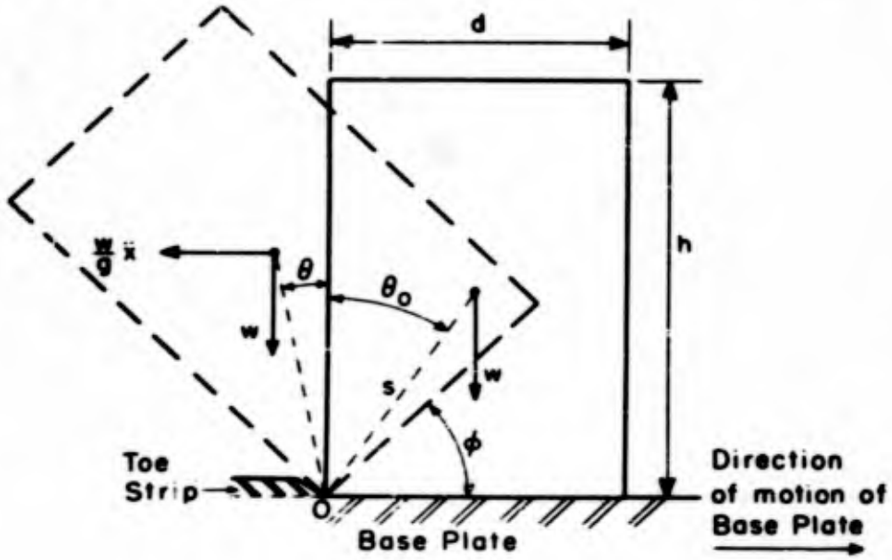

Fig. A.1

Let us consider the cylindrical shock pin shown in Fig. A.1. If the base upon which the pin is resting is suddenly displaced to the right, and sliding between the shock pin and the base is prevented by a toe strip, the pin will tend to overturn as shown in Fig. A.1. Then, the differential equation of motion is:

$$I\ddot{\theta} = W s \sin\theta + \frac{W}{g} s \cos\theta \, A_m \sin\omega(t + t_o) \qquad (A.1)$$

where: $\phi = \theta + \theta_o$ and

t_o = Correction applied to make $\dot{\theta} = 0$ at $t = 0$

Substituting $\phi - \theta_o$ for θ in Eq. A.1, we obtain:

$$\ddot{\phi} = \frac{Ws}{I} \sin(\phi - \theta_c) + \frac{Ws}{I} \cos(\phi - \theta_o) \, a \sin\omega (t + t_o) \qquad (A.2)$$

where $\frac{A_m}{g}$ = a in gravity units.

$\tau = \alpha t$ where $\alpha^2 = \frac{Ws}{I}$

Multiplying both sides by ω and solving for ωt we get

$$\omega t = \frac{\omega}{\alpha} \cdot \tau .$$

We may write

$$\frac{d\phi}{dt} = \frac{d\phi}{d\tau} \frac{d\tau}{dt} = \alpha \frac{d\phi}{d\tau},$$

Differentiating we get

$$\frac{d^2\phi}{dt^2} = \alpha^2 \frac{d^2\phi}{d\tau^2} \; ; \; \ddot{\phi} = \alpha^2 \phi''$$

and substituting into (A.2) we obtain:

$$\phi'' - \sin(\phi - \theta_o) = \cos(\phi - \theta_o) \, a \sin\frac{\omega}{\alpha}(\tau + \tau_o).$$

Now assuming:

$$\sin(\phi - \theta_o) \approx \phi - \theta_o, \text{ and } \cos(\phi - \theta_o) \approx 1,$$

we obtain

$$\phi'' - \phi = a \sin\frac{\omega}{\alpha}(\tau + \tau_o) - \theta_o . \qquad (A.3)$$

A.2 SOLUTION OF DIFFERENTIAL EQUATION

A.2.1 Determination of General Solution

The homogeneous solution is

$$\phi = C_1 \cosh \tau + C_2 \sinh \tau .$$

For a particular solution, assume:

$$\phi = M \sin \frac{\omega}{\alpha} (\tau + \tau_o) + N ,$$

$$\phi' = M \frac{\omega}{\alpha} \cos \frac{\omega}{\alpha} (\tau + \tau_o) ,$$

$$\phi'' = - M (\frac{\omega}{\alpha})^2 \sin \frac{\omega}{\alpha} (\tau + \tau_o) .$$

Substituting into (A.3), grouping the terms, and substituting:

$$M = - \frac{a}{1 + (\frac{\omega}{\alpha})^2} ,$$

$$N = \theta_o ,$$

we find the general solution:

$$\phi = C_1 \cosh \tau + C_2 \sinh \tau -$$

$$\frac{a}{1 + (\frac{\omega}{\alpha})^2} \sin \frac{\omega}{\alpha} (\tau - \tau_o) + \theta_o \qquad \text{(A.4)}$$

A.2.2 Evaluation of Constants

We may now evaluate the constants from the initial conditions.

Since at $t = 0$; $\tau = 0$ and $\phi = 0$

$$C_1 - \frac{a}{1 + (\frac{\omega}{\alpha})^2} \sin \frac{\omega}{\alpha} \tau_o + \theta_o = 0$$

or $$C_1 = \frac{a}{1 + (\frac{\omega}{\alpha})^2} \sin \frac{\omega}{\alpha} \tau_o - \theta_o . \qquad \text{(A.5)}$$

Differentiating (A.4)

$$\phi' = C_1 \sinh \tau + C_2 \cosh \tau - \frac{a (\frac{\omega}{\alpha})}{1 + (\frac{\omega}{\alpha})^2} \cos \frac{\omega}{\alpha}$$

$$(\tau + \tau_o) .$$

In addition, at $t = 0$; $\tau = 0$ and $\phi' = 0$.

Solving for C_2 we get

$$C_2 = \frac{(\frac{\omega}{\alpha})}{1 + (\frac{\omega}{\alpha})^2} . a \cos \frac{\omega}{\alpha} . \tau_o . \qquad \text{(A.6)}$$

Therefore substituting (A.5) and (A.6) into (A.4) we obtain:

$$\phi \left[\frac{a \sin \frac{\omega}{\alpha} . \tau_o}{1 + (\frac{\omega}{\alpha})^2} - \theta_o \right] \cosh \tau +$$

$$\left\{ \left[\frac{\omega}{\alpha} \Big/ 1 + (\frac{\omega}{\alpha})^2 \right] a \cos \frac{\omega}{\alpha} \tau_o \right\} \sinh \tau -$$

$$\frac{a}{1 + (\frac{\omega}{\alpha})^2} \sin \frac{\omega}{\alpha} (\tau + \tau_o) + \theta_o . \qquad \text{(A.7)}$$

τ_o is evaluated in the following manner:

At $t = 0$; $\phi'' = 0$, $\phi = 0$, and $\tau = 0$.

Then from Equation (A.3)

$$\sin \frac{\omega}{\alpha} \tau_o = \frac{\theta_o}{a} .$$

From the properties of the right triangle (See Fig. A.2.)

$$\cos \frac{\omega}{\alpha} . \tau_o = \frac{\sqrt{a^2 - \theta_o^2}}{a} .$$

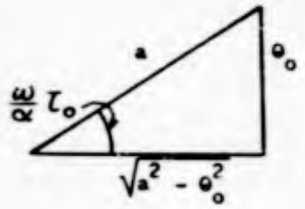

Fig. A 2

Then, $\sin\left(\frac{\omega}{\alpha}\tau + \frac{\omega}{\alpha}\tau_o\right) = \sin\frac{\omega}{\alpha}\tau\cos\frac{\omega}{\alpha}\tau_o + \cos\frac{\omega}{\alpha}\tau\sin\frac{\omega}{\alpha}\tau_o$

Substituting into (A.7)

$$\phi = \theta_o\left[-\frac{\left(\frac{\omega}{\alpha}\right)^2\cosh\tau}{1+\left(\frac{\omega}{\alpha}\right)^2} - \frac{\cos\frac{\omega}{\alpha}\tau}{1+\left(\frac{\omega}{\alpha}\right)^2}\right] +$$

$$\frac{\sqrt{a^2-\theta_o^2}}{1+\left(\frac{\omega}{\alpha}\right)^2}\left[\frac{\omega}{\alpha}\sinh\tau - \sin\frac{\omega}{\alpha}\tau\right] + \theta_o \quad \text{(A.8)}$$

When $\phi = \theta_o$, pin is in unstable equilibrium.

Then

$$\frac{\sqrt{a^2-\theta_o^2}}{\theta_o} = \frac{\left(\frac{\omega}{\alpha}\right)^2\cosh\tau + \cos\frac{\omega}{\alpha}\tau}{\frac{\omega}{\alpha}\sinh\tau - \sin\frac{\omega}{\alpha}\tau} \quad \text{(A.9)}$$

A.3 APPROXIMATE SOLUTION

An approximate solution of the above equation for slender pins is:

$$\sqrt{\left(\frac{a}{\theta_o}\right)^2 + 1} \approx \Omega \text{ or } \frac{a}{\theta_o} \approx \sqrt{1+\Omega^2} \quad \text{(A.10)}$$

Where: $\Omega = \omega/\alpha$

θ_o = ratio diameter/height for small angles

a = acceleration in g's

In the text this relationship is referred to as follows:

$$a = \frac{d}{n}\sqrt{1+\Omega^2} \quad \text{(2.2)}$$

BIBLIOGRAPHY

Akima, Tetsuo. Experiments on the Overturning of Circular Columns by the Aid of a Shaking Table. Bulletin of the Earthquake Research Institute, Tokyo University, 1950.

Leet, Don L. Vibrations from Blasting. Wilmington, Delaware: Hercules Powder Co., 1940.

Rockwell, Edward H. Vibrations Caused by Quarry Blasting and Their Effect on Structures. The Explosives Engineer, March and April, 1927.

Lampson, C. W. Final Report on Effects of Underground Explosions. OSRD Report No. 6645. 1946

Campbell, D. C., LCDR, USN, Program One, Report Three, with supplements. Technical Operations Squadron (Prov) August 1951.

AFSWP. Capabilities of Atomic Weapons. July, 1951.

AFSWP. Windstorm Handbook. November 1950.

Spilhaus, A. F., Operation JANGLE, Weapons Effects Tests, Preliminary Report. January 1952.

Doll, E. B. and D. C. Sachs. HE Tests - Operation JANGLE, Interim Report, Stanford, California. Stanford Research Institute, October 1951.

Doll, E. B. HE Tests - Operation JANGLE, Interim Report - Part II. Stanford, California, Stanford Research Institute, October 1951.

Doll, E. B. Underground Explosion Tests at Dugway, Interim Report, Stanford, California, Stanford Research Institute, July 1951.

ERA, Inc., Instrumentation for Underground Explosion Test Program, Interim Technical Report No. 1, Dry Clay, Dugway. St. Paul, Minn. Engineering Research Associates, Inc., 1 August 1951.

ERA, Inc., Instrumentation for Underground Explosion Test Program, Interim Technical Report No. 2, Dry Sand, Dugway. St. Paul, Minn. Engineering Research Associates, Inc. 1 October 1951

ERA, Inc., Instrumentation for Underground Explosion Test Program, Interim Technical Report No. 4, Dry Clay, Dugway. St. Paul, Minn.

Engineering Research Associates, Inc. 1 November 1951.

Shepard, E. R. Subsurface Explorations by Geophysical Methods. Philadelphia, Pa. American Society for Testing Materials, 1949.

Crandell, F. J. Ground Vibration Due to Blasting and its Effect Upon Structures. Journal of the Boston Society of Civil Engineers, April 1949.

Rugg, A. M. Seismic Refraction Survey for Navy Contract NOY 26616, Nye County, Nevada. United Geophysical Company, Inc. 27 July 1951.

Walley. F. A Second Survey of Earth Effects, British Ministry of Home Security, Research and Experiments Department. (Great Britain).

Isthmian Canal Studies - 1947, Appendix 6 of the Report of the Governor of the Panama Canal.

Morris, G. Vibrations Due to Blasting and their Effects on Building Structures. Imperial Chemical Industries, Ltd. Nobel Division. Great Britain.

Obert, L and Duvall, W. I. Generation and Propagation of Strain Waves in Rock - Part I U. S. Bureau of Mines, Report of Investigation No. 4683, U. S. Department of Interior, 1950.

Matsuda, F. and Saxe H. C. Pre-Test Report, Program One, Project 1.7 "Shock Pins", Cambridge, Mass., Massachusetts Institute of Technology, Dept. of Civil and Sanitary Engineering, August 1951.

SECRET

OPERATION JANGLE

PROJECT 1(9)a

GROUND ACCELERATION, GROUND AND AIR PRESSURES FOR UNDERGROUND TEST

By

E. B. Doll and V. Salmon

April 1952

STANFORD RESEARCH INSTITUTE
STANFORD, CALIFORNIA

SECRET

RESTRICTED DATA
ATOMIC ENERGY ACT 1946

CONTENTS

ILLUSTRATIONS

TABLES

ABSTRACT

The earth accelerations, earth pressures, and air-blast pressures measured in Project 1(9)a of the underground nuclear explosion are reported. These measurements were taken on a blast line which was 90° removed from the major blast line and gages of the variable-reluctance type were used. Reproductions of representative oscillograph gage records are presented.

Comparisons are made between the Project 1(9)a results and the predictions made in the report on Project 1(9)-1. These predictions were made on the basis of direct scaling of the Operation JANGLE scaled HE tests up to an assumed 1.0 KT equivalent TNT charge. For air pressure, the nuclear charge is found to be equivalent to about a 0.85 KT charge of TNT. However, it is not possible to assign a unique charge equivalence with respect to earth acceleration or earth pressure. In almost every case the earth phenomena results indicate an energy equivalence somewhat less than 1.0 KT of TNT.

The earth phenomena are found to be a combination of air-induced and direct-earth effects. Attempts are made to separate these air-blast induced effects from the direct earth phenomena. Some rough integrations of the horizontal earth accelerations, yielding particle velocities, are presented and discussed. A brief discussion of damage criteria in relation to surface structures is included.

The results of the underground nuclear explosion are compared with the HE-1 and HE-2 tests of Operation JANGLE and with the Dugway dry clay tests of 1951.

CHAPTER 1

INTRODUCTION

1.1 OBJECTIVE

The program covered by Project 1(9)a of the underground nuclear test at the Nevada Test Site during November 1951 had as its principal objectives the following:

1. To use techniques and instrumentation as similar as possible to those used on the scaled HE tests (Project 1(9)-1), and on similar tests at the Dugway Proving Ground, so as to obtain correlation between these tests and underground nuclear explosions.

2. To obtain information so that general phenomena resulting from nuclear explosions can be compared with those resulting from TNT explosions.

3. To obtain specific information bearing on certain of the useful military effects of a shallow underground 1 KT nuclear explosion, and to obtain data to assist in the extrapolation of these effects to those of a 20 KT weapon.

4. To supply back-up measurements for the Naval Ordnance Laboratory (earth acceleration, Project 1.1), Ballistic Research Laboratories (earth pressure, Project 1.2a-2), and Sandia Corporation (air-blast pressure, Project 1.4).

5. To make measurements of underground explosion phenomena on a gage line 90 degrees removed from the main blast line in order to estimate the asymmetry of the phenomena.

6. To make measurements for indicating approximately the effect of gage burial depth upon measurements of underground phenomena.

7. To obtain additional information in the general field of underground explosion phenomena with respect to such items as attenuation characteristics, wave form, and scale and model laws.

1.2 HISTORICAL

For the detailed historical background leading up to Project 1(9)a of the nuclear test the reader is referred to Section 2.1 of the Stanford Research Institute report on scaled HE tests (Project 1(9)-1).[1] As stated in this reference, it must be emphasized that as larger test charges are investigated the departure of the earth from a homogeneous isotropic medium plays an increasingly important role in influencing the resulting phenomena.

1.3 THEORETICAL

Reference is made to Section 1.3 of the scaled HE tests report (Project 1(9)-1),[1] in which a discussion of the model law as normally applied to explosion phenomena is presented. As in that report, the symbol λ is here used in describing the reduced or scaled dimensions of an experiment, where λ is defined by the relation,

$$\lambda = R/W^{1/3} \qquad (1.1)$$

In this equation, following the established convention, R is the horizontal radius in feet as measured from ground zero and W is the weight of the charge in pounds of TNT of equivalent energy release. In this report, λ refers specifically to scaled horizontal distances measured from ground zero. The term λ_c describes the charge depth and the term λ_g describes the gage depth.

In relation to scale or model law conditions, the underground test presented two main disturbing problems on the basis of past experience. Primarily, the equivalent charge weight was considerably greater than those that had been used at Dugway[2,3,4] and in the JANGLE scaled HE tests.[1,5,6,7] Secondly, the charge was assumed to give rise to an energy release of 1 KT of TNT explosive and therefore the charge burial depth, λ_c, was determined with this assumption in mind.

The first of these considerations, the magnitude of the nuclear charge, would be expected to give rise to deviations from the model law because the properties of the medium do not in practice follow this law. For example, while in a theoretical sense the properties

---

* Superscript numbers refer to references listed in the Bibliography at the end of this report.

of the medium may change if they satisfy the condition that they be identical at scaled distances, nevertheless in practical applications to underground explosion phenomena this kind of permitted variation is unrealistic, and homogeneity and isotropy of the medium are required. As was stated previously, inhomogeneities in the medium become more important as the size of the charge is increased. The reasoning here is tied up with Equation 1.1, from which it is noted that for a constant reduced distance, λ, the reference distance in feet must increase as the cube root of the weight of the charge increases. When this reference distance approaches the dimensions of variations from homogeneity in the medium, these variations can significantly alter the model law behavior of the explosion phenomena.

The second of the factors described above, the assumption that the energy release of the underground nuclear charge is equivalent to 1 KT of TNT detonated at the same scaled depth, must also be considered. It is at once obvious that the explosive source characteristics of a nuclear charge are not equivalent to those of a TNT charge; for instance, the equivalent yield for thermal and radiation effects will obviously be different from the equivalent yield for such mechanical effects as pressure and acceleration. Moreover, the hydrodynamics and thermodynamics of the expanding gas bubble are different for the two types of explosions. For relatively shallow charge depths it is believed that the effect of these differences would be even more pronounced, since the energy partition in the venting processes can be critically affected by the thermodynamics of the gas bubbles. These facts were known when the predictions were made concerning phenomena to be produced by the underground nuclear explosion.[6,7] However, there were not sufficient data available prior to the underground test to ascertain the details of how a nominal 1 KT nuclear explosion might differ from the explosion of 1 KT of TNT. For this reason, predictions made using the model law assumed a charge of 1 KT of TNT.

The experiment described in this report was intended to investigate ground motions, ground pressures, and air pressures produced by a buried (shallow) nuclear explosive. All of these physical quantities are functions of at least two independent variables, the horizontal distance from ground zero (R) and the time (t). When scaling or model laws are applied to a phenomenon, it would be misleading and incomplete to omit either of these independent variables from consideration. If a particular quantity considered in its entirety (throughout the region of interest for variations of both R and t) does not meet model law requirements from one test to another, then at best the scale laws produce only an estimate of an upper or a lower limit.

If model law conditions are met, the scale factor, S, between two explosion tests can be defined by

$$S = (W_2/W_1)^{1/3} \qquad (1.2)$$

where W_1 and W_2 are the charge weights in pounds of TNT of equivalent energy release. In the HE tests[1,5] the scaled experiments (HE-1 and HE-2) were compared using many different criteria such as peak air-blast pressure, positive duration of air pressure, and first positive peak earth acceleration. Using these criteria, it was shown that the cube root of the calculated energy release ratio for the air and earth effects due to the two explosions was close to the scale factor, S, for the tests.

In a similar manner, the equivalent energy release associated with each of the various phenomena measured in the underground test may be computed by comparisons to the HE tests results.[1,5] The principal question then remaining is that of energy partition, which is probably different for HE and nuclear explosions. For example, the calculation of the air-blast equivalent TNT tonnage can be made with the understanding that this need not apply to other phenomena.

These considerations will be discussed in more detail and examples will be presented in Chapter 5 (Discussion) of this report.

CHAPTER 2

TEST DESCRIPTION

2.1 SITE

The test site for the Project 1(9)a underground nuclear explosion was located at Yucca Flat, a portion of the Nevada Test Site, Mercury, Nevada. The reader is referred to the Project 1(9)-1 report[1] for a description of the test site.

2.2 EXPLOSIVE CHARGE

The nuclear charge was buried at a depth of 17 feet. On a scaled basis this depth would correspond to λ_c equal to 0.135 for a charge of 1.0 KT of TNT equivalent energy release. This λ_c value is approximately equal to that used in the HE-1 and HE-2 scaled tests conducted under Project 1(9)-1.[1]

For this report it will be assumed for the most part that the charge had a nominal energy release of 1.0 KT of TNT. Unless otherwise stated, values of λ are based on this figure, with $W^{1/3} = 126$ (i.e. $\lambda = 1$ corresponds to R = 126 feet).

2.3 GAGE LINE

The gage line used for Project 1(9)a measurements was 90 degrees removed from the major blast line. The major blast line was parallel to the line used for the HE-2 test of Project 1(9)-1. Figure 2.. illustrates the gage station layout used in the underground test.

The principal earth acceleration measurements were made at a gage depth of five feet. Two components of acceleration were measured, the horizontal radial component and the vertical component. Earth accelerations were obtained at ranges varying in λ from 2.38 to 24.4 (262 to 3080 feet), with the principal concentration of instruments in the region λ less than 10 (1260 feet). In addition, two-component earth accelerations were measured at gage depths of 17, 34, and 68 feet at nominal values of λ of 3.0 and 8.15. For correlation with data taken by the Naval Ordnance Laboratory, some horizontal earth acceleration measurements were made at gage depths of 10 feet. These gages were placed in λ range from 2.70 to 15.

MINOR BLAST LINE
PROJECT 1(9)a

Fig. 2.1 Blast Line Layout for the Underground Test

PROJECT 1.1a

Earth pressure measurements were made at a gage depth of 10 feet for λ ranging from 1.72 to 24.4, with the principal concentration in the region of λ less than 10. In addition, earth pressure gages at depths of 17 and 34 feet were included at λ = 1.72 and at depths of 17 feet, 34 feet, and 68 feet for λ values of 3.0 and 8.15.

Air-blast pressures were obtained at a height of 40 inches above the ground surface at distances ranging from λ = 2.5 to 24.4. Previous measurements at Dugway indicated no significant difference in pressure as a function of height above the ground up to a scaled gage height of λ_g = - 0.3 (34 feet for 1 KT).

The five-foot deep accelerometers were placed on a radial line and the remaining gages were located as close as possible to this same line.

CHAPTER 3

INSTRUMENTATION

With a few minor exceptions, the instrumentation on Project 1(9)a (underground nuclear test) was the same as that used on Project 1(9)-1 (scaled HE tests). For a complete description of the apparatus and general experimental procedures the reader is referred to Chapter 4 of the report on Project 1(9)-1.[1]

3.1 RECORDING STATION

A buried recording shelter located 2000 feet from ground zero housed the recorders and the associated control equipment. This shelter was a concrete structure 8 feet by 11 feet and 7 feet high, having walls 2 feet thick and covered with 2 feet of earth. Access to the shelter interior was through a small hatch on the top. Adequate protection from radiation was obtained without further aids. No trace of background fogging on the photosensitive oscillograph paper was detected.

The shelter was designed for unattended remote operation of the recording equipment. The remote operation was controlled by the central automatic sequence-timer system provided for all participants in the test program. Unlike the scaled HE test operation,[1] there were no monitoring circuits to the distant control point. The timer operated as follows: AC power to the carrier oscillators on at zero time minus 30 minutes, recorder warm-up battery circuits on at minus 5 minutes, and recorder paper transport on at minus 15 seconds. It was further arranged that the minus 15 seconds signal initiated a time delay relay designed to shut off all equipment at plus 2 minutes.

3.2 POWER

The AC power was supplied from the central distribution system established at the test site. In addition a gasoline-driven generator was connected to a dummy load and was kept on a stand-by basis near the recording shelter. An automatic transfer circuit was provided to transfer this generator to the recording equipment in the event of central power failure. The generator was started three hours prior to zero time; however, its use was not required.

The power for the recorders was supplied from batteries installed in the underground shelter.

3.3 CABLE

Most of the cables used in the scaled HE tests did not exceed 1000 feet in length. However, since some gage cables up to 2000 feet in length were used in the underground nuclear test, it became necessary to modify the circuits associated with these long cables. This involved changing the input networks to achieve proper phase relations at the ring demodulator element of the recording circuit.

3.4 FIELD CALIBRATION

The methods of field calibration were essentially those used in the scaled HE tests. Some refinements were introduced in the form of more precise instruments and techniques. A dead-weight tester was used to calibrate the earth pressure gages and the air pressure gages after they were connected to their respective cables and associated operating circuits.

3.5 EARTH COUPLING

The earth acceleration canisters (each containing two accelerometers), which were buried in 5- and 10-foot holes, were cemented in with Calseal, a quick-setting gypsum cement. The holes were then filled with tamped earth. The 17-, 34-, and 68-foot canisters were cemented similarly, but only about five feet of earth was placed on top of them.

In the case of the earth pressure gage coupling, each of the 10-foot gage holes was filled to the top with a thin solution of Aquagel. This filling process was duplicated for the deeper gage holes. Precautions were taken to see that all holes were filled to the top at the time of the test.

CHAPTER 4

RESULTS

4.1 INSTRUMENT PERFORMANCE

Table 4.1 presents the over-all gage plan for the Project 1(9)a underground nuclear explosion test. A total of 72 gage channels were used. Of these gage channels, 60 included the dual recording feature for increased dynamic range and 12 used single galvanometers, giving a total of 132 gage traces.

All instrumentation performed satisfactorily, with one exception. The paper feed mechanism jammed on one recorder, and records were obtained on only 57 of the 72 gage channels connected. It was fortuitous that the lost recorder included the channels of least importance. The defective recorder ultimately functioned in time to obtain most of the record from the outermost air-pressure gage. These late traces indicated that all gage channels functioned properly. In Table 4.1, parentheses designate the gages from which the incomplete records were obtained.

4.2 TRANSIENT RECORDS

This report includes all the data obtained at the test site in connection with Project 1(9)a, with the exception of the 10-foot earth acceleration measurements taken for correlation with those of the Naval Ordnance Laboratory. Copies of these latter data have been forwarded directly to NOL.

Figure 4.1 shows a portion of an oscillograph camera record obtained in this test, reduced in size from the original height of 12 inches. The polarity is such that positive record deflections correspond to positive pressures, radially outward horizontal accelerations, and upward vertical accelerations. In order to reduce the data further and form conclusions about relative wave forms and amplitudes, it is necessary to trace each individual gage record onto a separate sheet of paper. No smoothing or editing of these records is done when they are traced. Figures 4.2 to 4.12 inclusive show some representative gage records obtained on this underground nuclear test.

TABLE 4.1

General Gage Plan*

Sta. No.	Horisontal Radius (ft)	Horisontal Radius λ	Accelerometers H,V 5 ft	Accelerometers H 10 ft	Accelerometers H,V 17 ft	Accelerometers H,V 34 ft	Accelerometers H,V 68 ft	Earth Pressure P 10 ft	Earth Pressure P 17 ft	Earth Pressure P 34 ft	Earth Pressure P 68 ft	Air-Blast AB
1	217	1.72						2	2	2		
2	262	2.08	2,2					2				
3	314	2.49	2,2					(2)				1
4	340	2.70		1								
5	378	3.0	(2,2)		(2,2)	(2,2)	(2,2)	2	2	2	2	
6	456	3.62	2,2					2				
7	520	4.13		1								
8	542	4.30	2,2					2				1
9	642	5.1		1								
10	655	5.2	2,2					2				
11	788	6.25	2,2					2				
12	934	6.3		1								
13	945	7.5	2,2					2				1
14	1025	8.15	2,2		2,2	2,2	2,2	(2)	(2)	(2)	(2)	
15	1213	9.63		(1)								
16	1230	9.75	2,2					2				
17	1480	11.7	2,2					2				1
18	1890	15.0		1								
19	2130	16.9	2,2					2				1
20	3080	24.4	2,2					2				(1)

*The letters H and V in the headings refer to horisontal and vertical accelerometers respectively. The gage burial depths are also given in the headings. The fifth column presents the gages used for correlation with measurements by the Naval Ordnance Laboratory. The numbers refer to the number of galvanometers connected to each gage channel. The number 1 designates a so-called single channel and the 2 refers to a duo-channel.

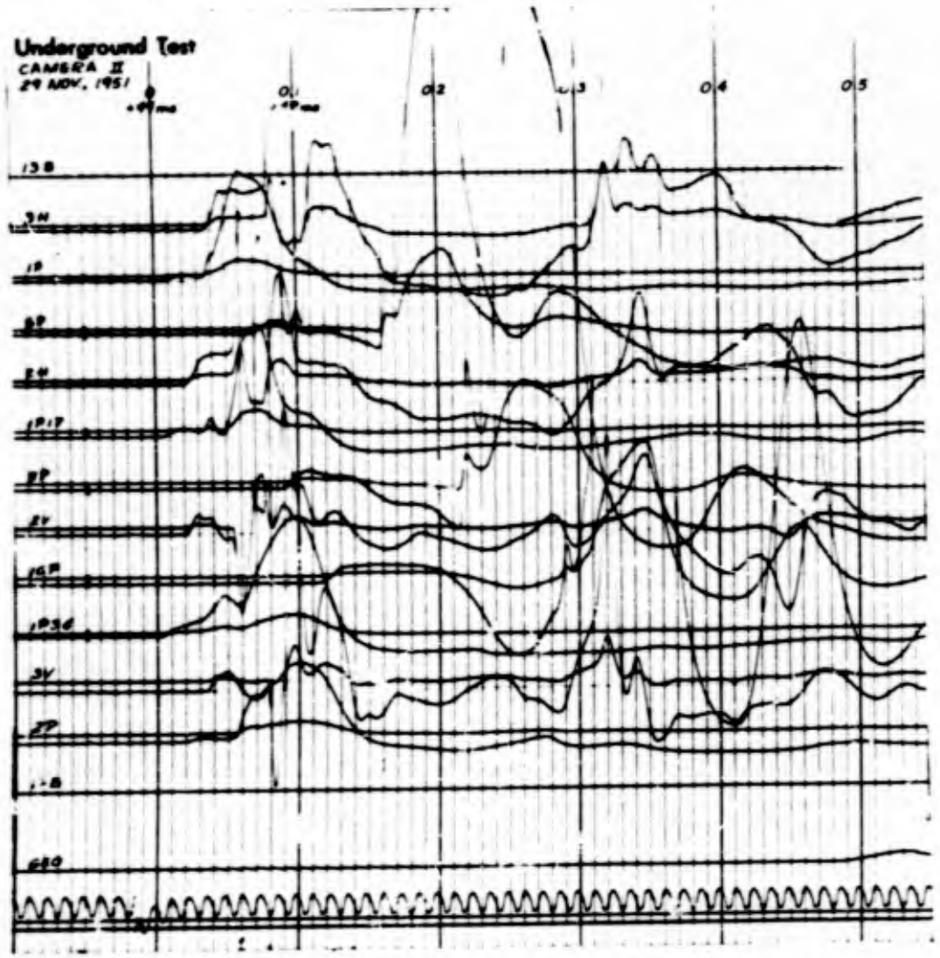

Fig. 4.1 Reduction of Typical Oscillograph Record. Height of original record 12 inches

The air-blast pressures as a function of time are presented in Figure 4.2 (note that the two bottom curves have interrupted time axes). The air-blast pressures were not reduced to sea-level equivalent pressures, since the scaled HE tests and the underground nuclear test were performed at the same site. Figures 4.3 and 4.4 show horizontal earth accelerations as they appeared on the oscillograph records, while the vertical earth accelerations are displayed in Figures 4.5 and 4.6.

It was possible, using a graphical method, to obtain a rough preliminary determination of the first integral of the horizontal earth acceleration records. This integration yields the horizontal particle velocity, a few representative curves of which are shown in Figure 4.7.

Figures 4.8 and 4.9 display the results of the deep acceleration measurements made with gages placed at four different depths. The earth pressure records from the gages closest to the charge are shown in Figure 4.10. And finally, the deep earth pressure transient records are presented in Figures 4.11 and 4.12.

4.3 Tables

As an introduction to the data in tabular form, Figure 4.13 presents a series of idealized transient records which are labeled to correspond to the table headings of Tables 4.2, 4.3, 4.4, and 4.5. Each curve in Figure 4.13 is marked for proper table reference.

The gage code numbers describe the type of gage used and its relative position on the blast line. The first number refers to the gage station number and locates the gage on the blast line (see Figure 2.1 and Table 4.1). The letter following the station number indicates the type of gage. The letters H and V designate the horizontal and vertical earth accelerometers respectively. The letter P refers to earth pressure and B to air-blast pressure. The numbers after the letter designate the depth of burial (in feet) of the gage. The absence of numbers after H or V indicates a five-foot burial depth, whereas the P gages were 10 feet deep unless otherwise indicated.

The λ values given in the tables were computed on the basis of the underground nuclear charge as a nominal equivalent of 1.0 kT of TNT, $W^{1/3}$ = 126 feet. The data contained in these tables are presented in graphical form in Chapter 5 of this report.

4.4 FUTURE WORK

A more complete analysis of the data from this explosion test can be made when the earth acceleration records are integrated to yield earth velocity and, finally, earth displacement. A rough integration of only the horizontal acceleration was done; however, more precise methods are needed before firm conclusions can be drawn. These more accurate integrations will be made at a later date, in time to be included in the final contract report of Project 1(9)a.[8] Although the permanent displacement survey results on Project 1(9)a are not yet available, it is hoped that these results can be used for checking the displacements found from double integration of the acceleration records.

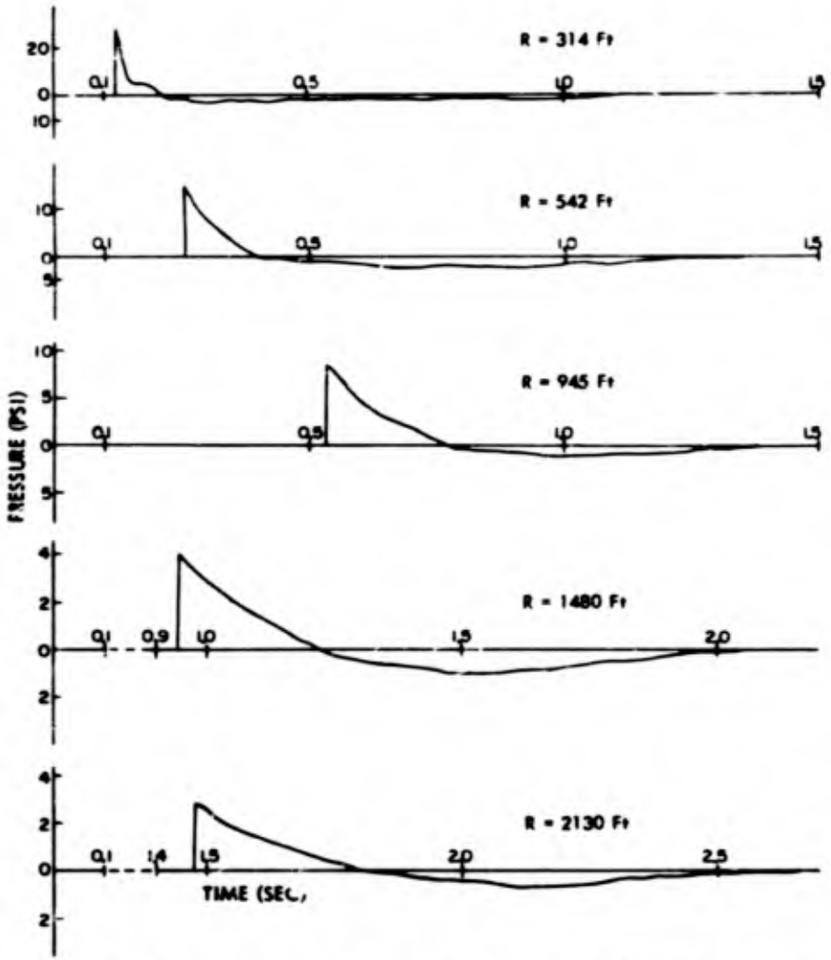

Fig. 4.2 Air Blast Pressure vs. Time for the Underground Test. Note interrupted time scales on bottom two curves

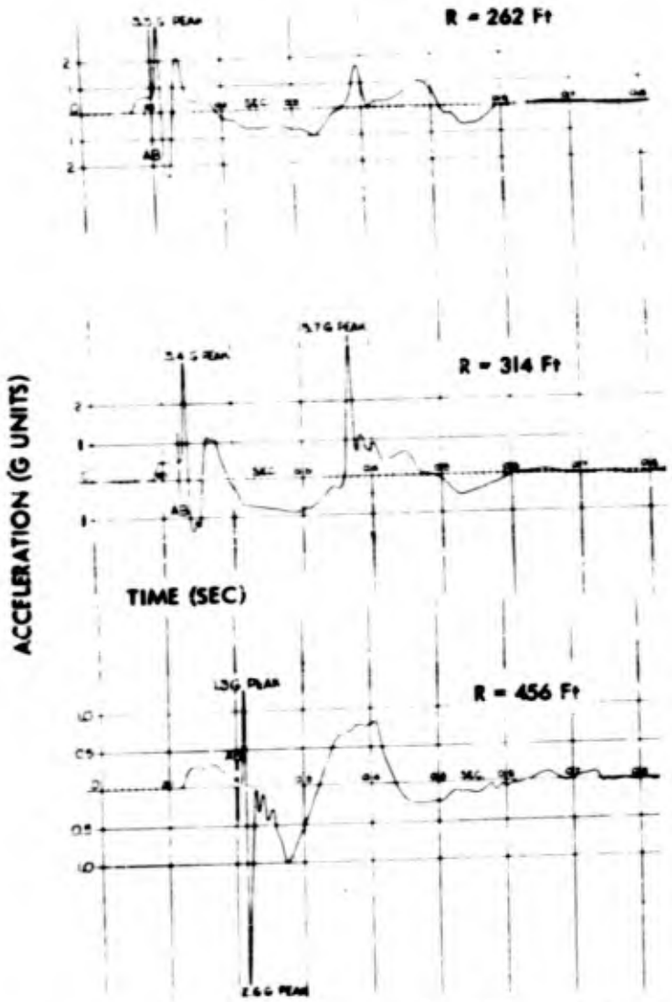

Fig. 4.3 Horizontal Earth Acceleration vs. Time for the Underground Test. Gage depth, 5 feet

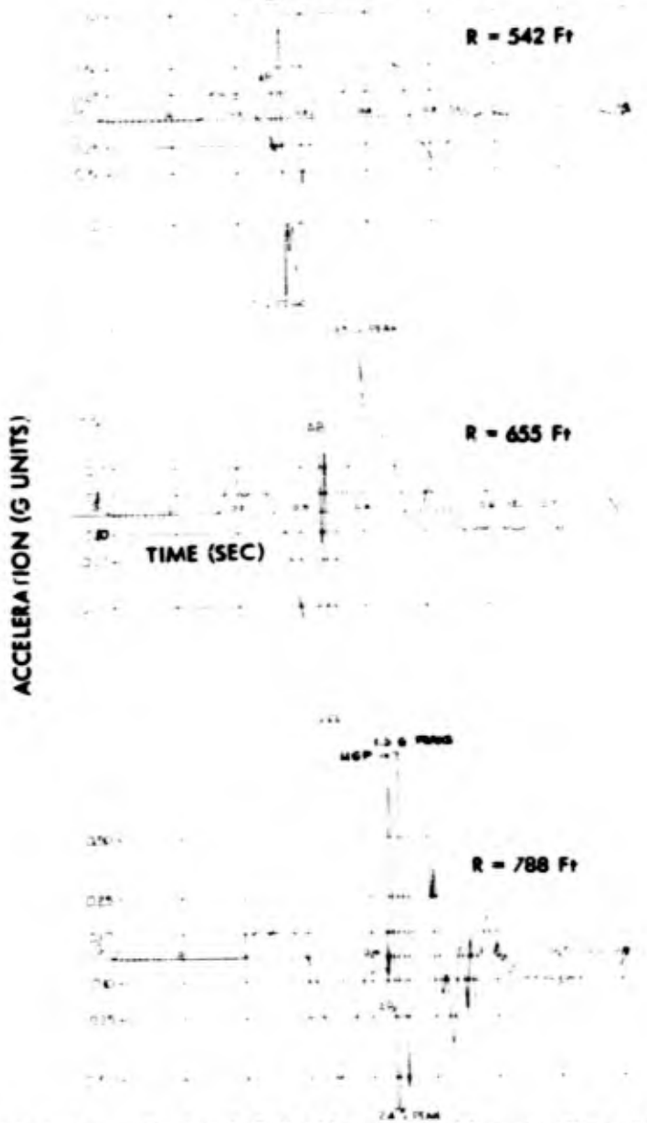

Fig. 4.4 Horizontal Earth Acceleration vs. Time for the Underground Test. Gage depth, 5 feet

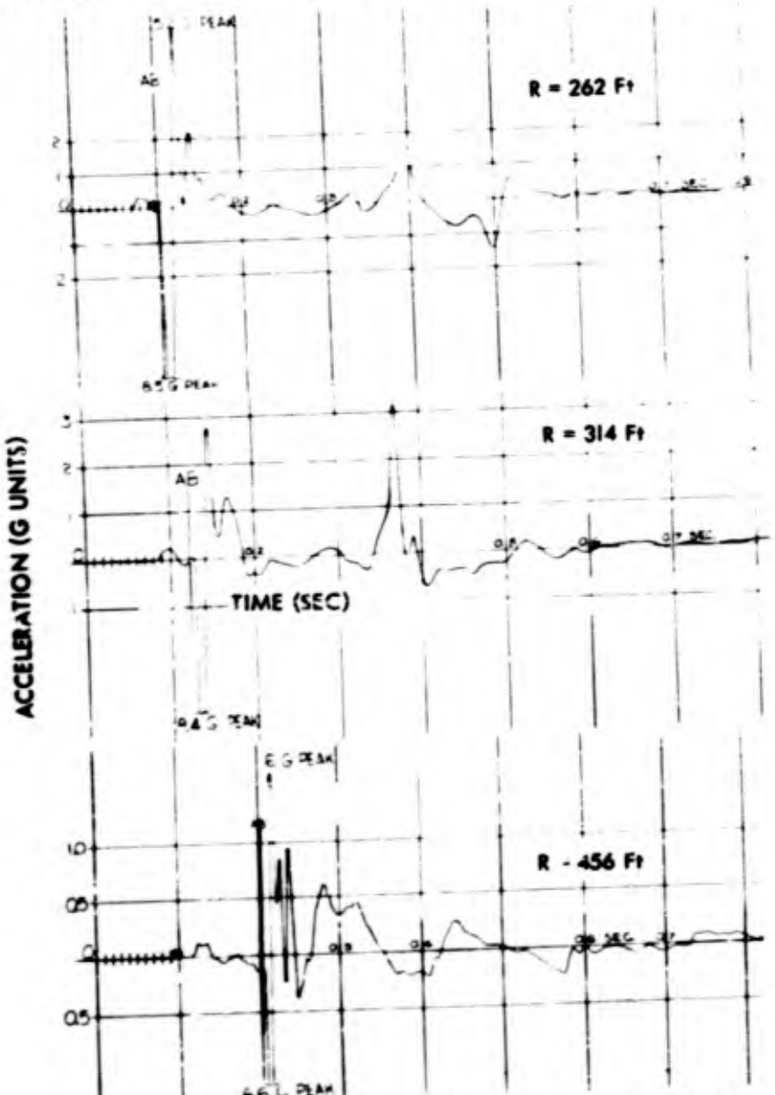

Fig. 4.5 Vertical Earth Acceleration vs. Time for the Underground Test. Gage depth, 5 feet

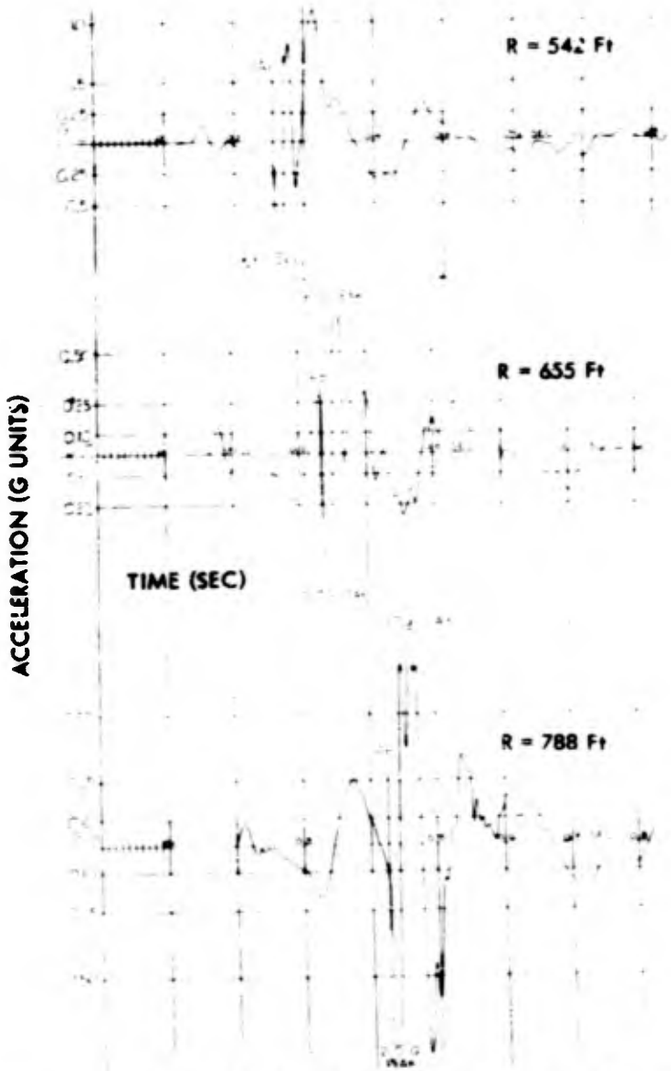

Fig. 4.6 Vertical Earth Acceleration vs. Time for the Underground Test. Gage depth, 5 feet

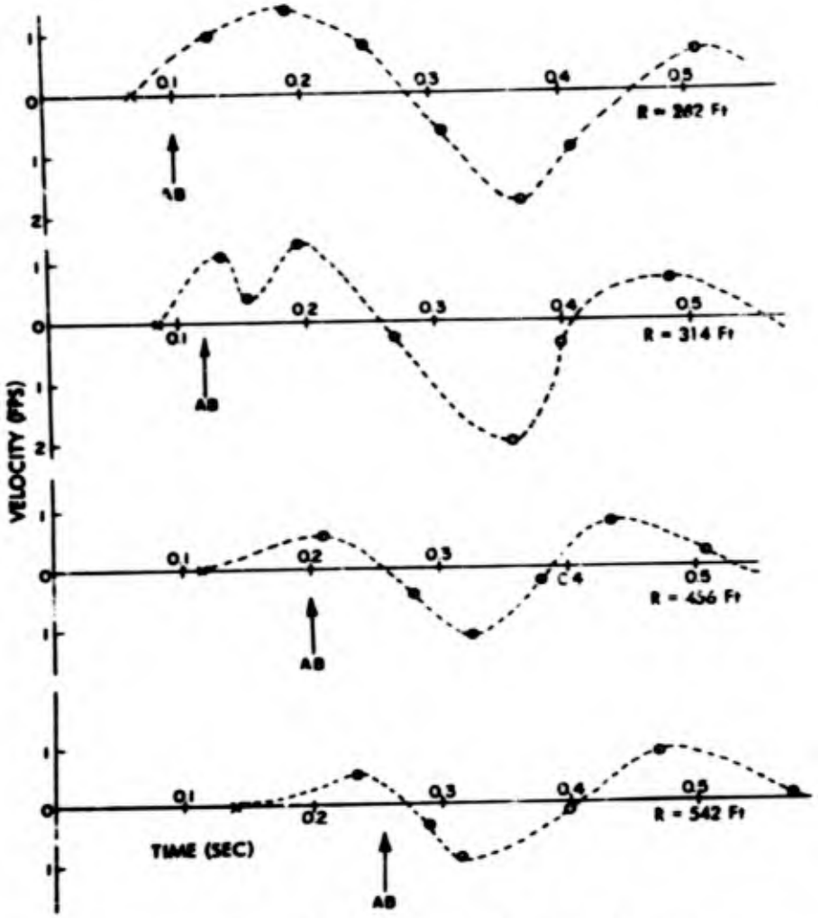

Fig. 4.7 Horizontal Earth Velocity vs. Time for the Underground Test. These curves are the results of rough integrations of the horizontal acceleration records.

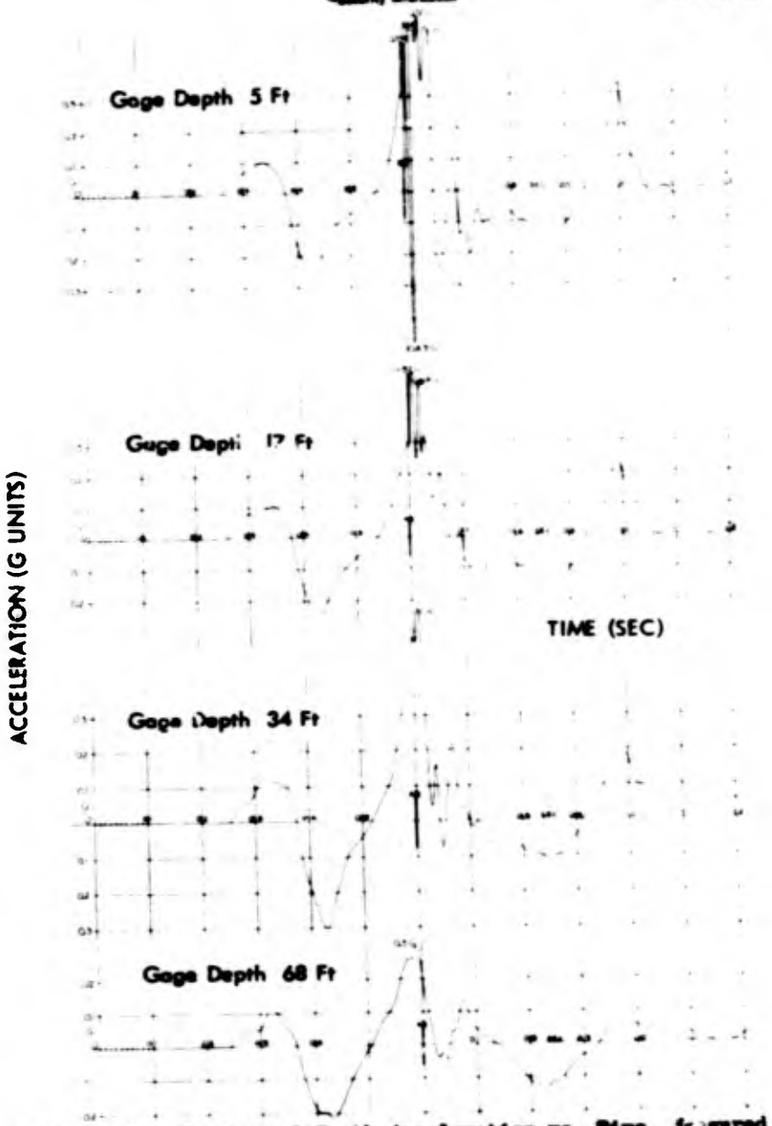

Fig. 4.8 Horizontal Earth Acceleration vs. Time, Measured at Various Depths for the Underground Test, R = 1025 ft

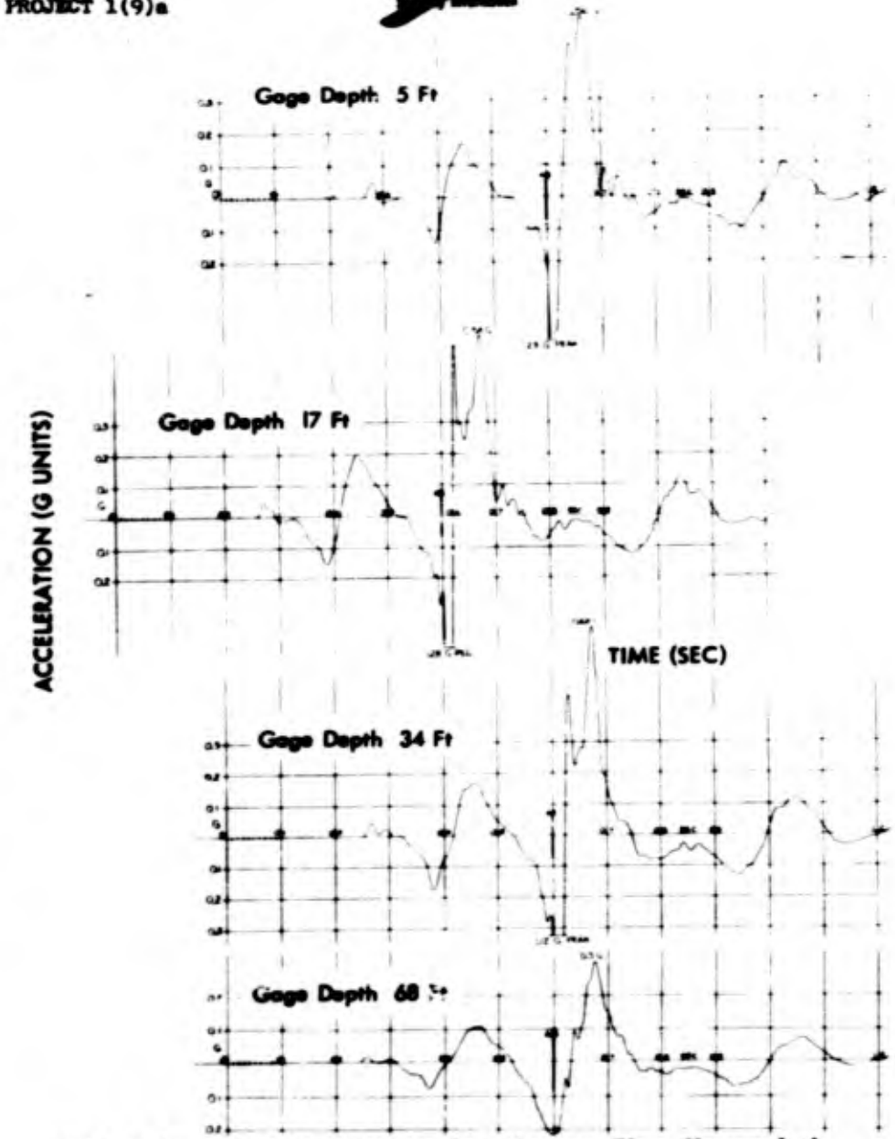

Fig. 4.9 Vertical Earth Acceleration vs. Time, Measured at Various Depths for the Underground Test, R = 1025 ft

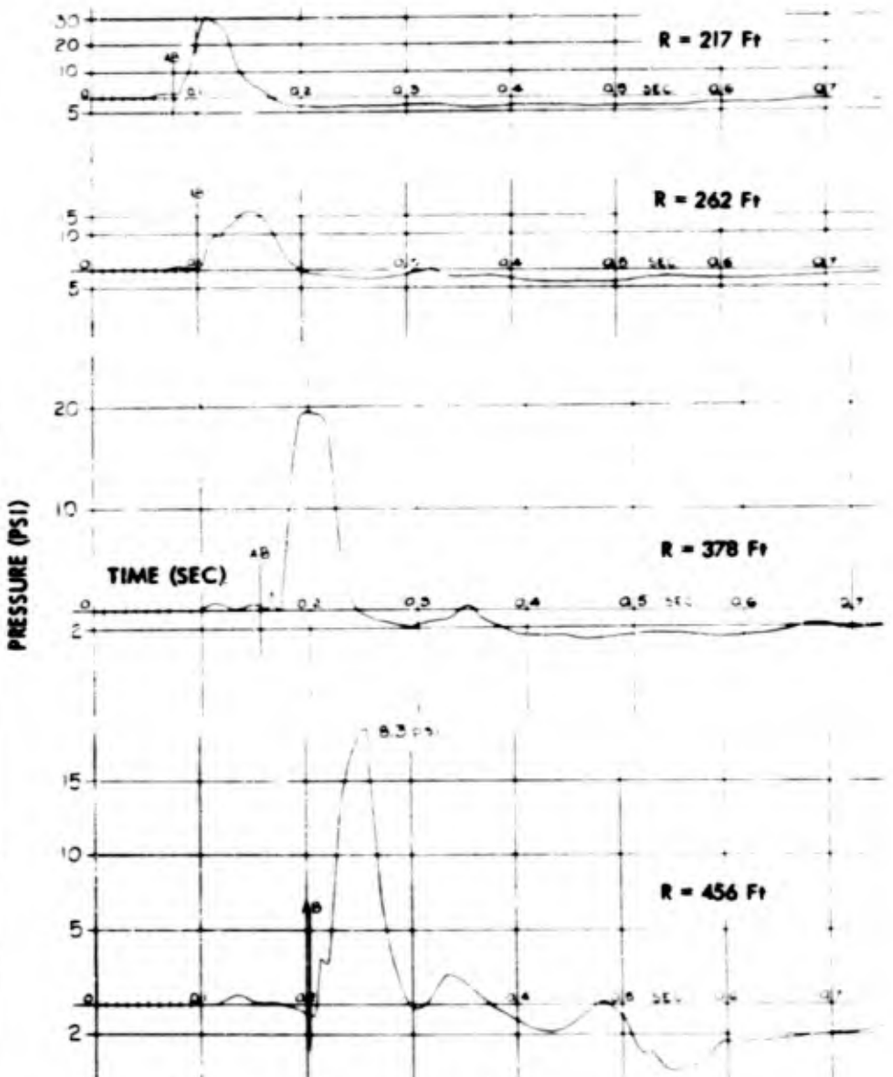

Fig. 4.10 Earth Pressure v. Time for the Underground Test. Gage depth, 10 feet

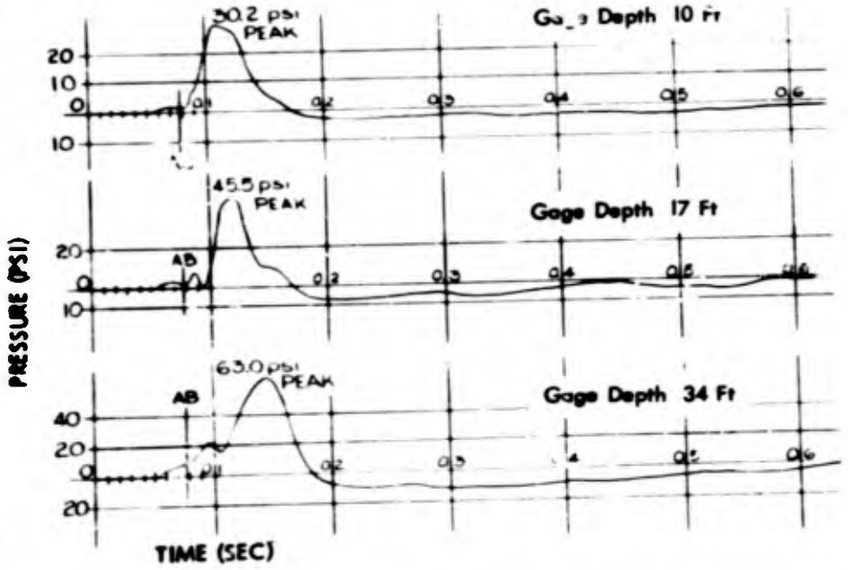

Fig. 4.11 Earth Pressure vs. Time Measured at Various Depths for the Underground Test, R = 217 ft

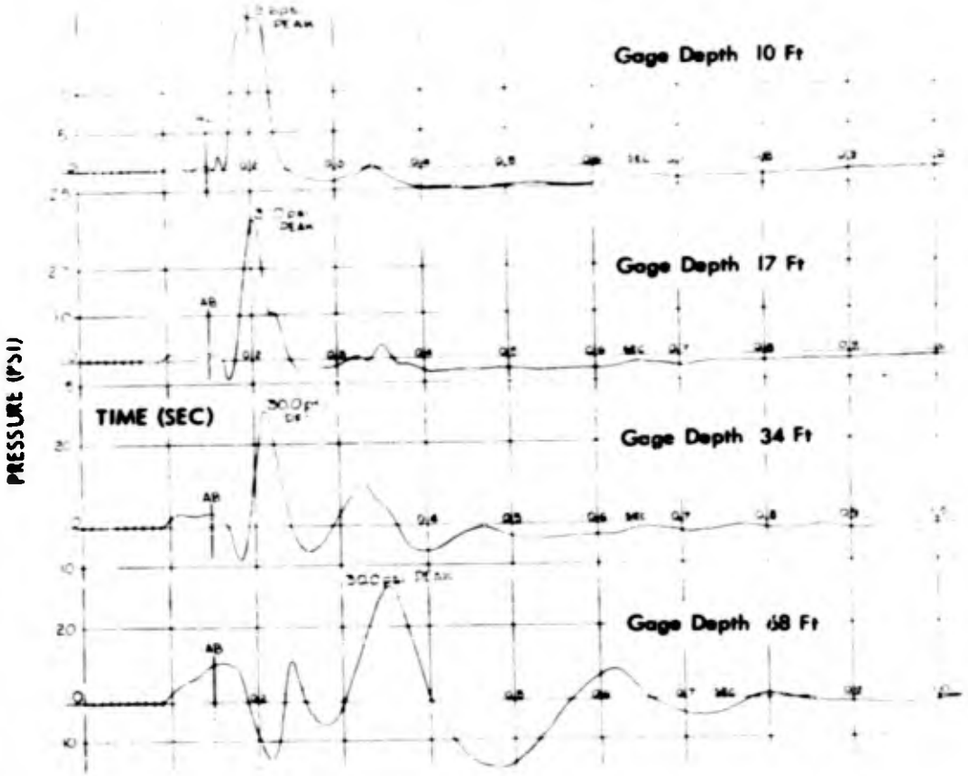

Fig. 4.12 Earth Pressure vs. Time Measured at Various Depths for the Underground Test, R = 378 ft

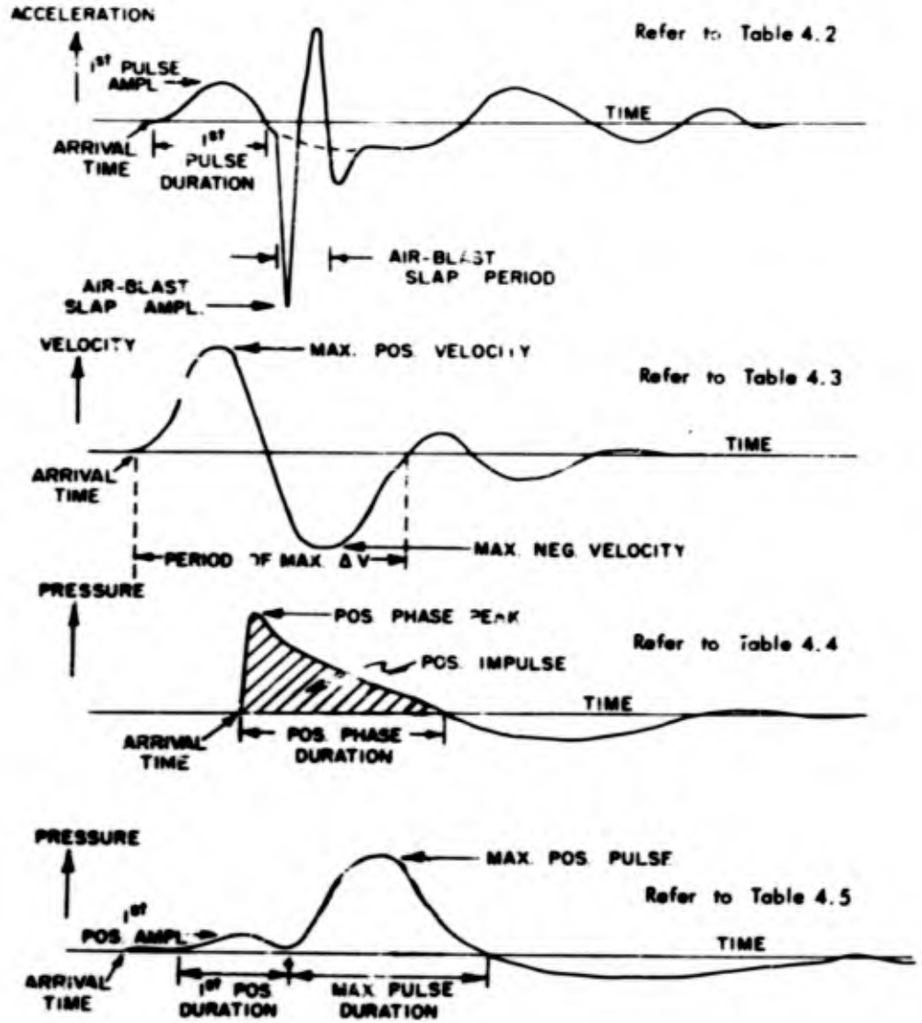

Fig. 4.13 **Quantities Measured from Transient Records for the Underground Test**

TABLE 4.2

Earth Acceleration

Gage Code No.	Gage Rating (G)	Horizontal Radius (ft)	Horizontal Radius λ	Arrival Time (sec)	First Pulse Ampl. (G)	First Pulse Durat'n (sec)	Air-Blast Slap Ampl. (G)	Air-Blast Slap Period (sec)
Horizontal								
2H	5	262	2.08	0.068	0.59	0.120		
3H	5	314	2.49	0.084	0.49	0.110		
6H	5	456	3.62	0.114	0.28	0.092		
8H	5	542	4.3	0.138	0.28	0.093		
10H	5	655	5.2	0.165	0.19	0.092		
11H	5	788	6.25	0.195	0.16	0.100		
13H	5	945	7.5	0.243	0.12	0.105		
14H	1	1025	8.15	0.261	0.10	0.120		
16H	1	1230	9.75	0.318	0.030	0.138		
17H	1	1480	11.7	0.386	0.026	0.128		
19H	0.5	2130	16.9	0.560	0.011	0.100		
20H	0.5	3080	24.4	–	0.012	0.100		
Vertical								
2V	5	25[illegible]	2.08	0.068	0.33	0.025	[illegible].5	0.026
3V	5	31[illegible]	2.49	0.084	0.24	0.025	8.4	0.022
6V	5	456	3.62	0.115	0.125	0.025	6.6	0.020
8V	5	542	4.3	0.138	0.13	0.027	3.3	0.027
10V	5	655	5.2	0.164	0.134	0.025	2.7	0.031
11V	5	788	6.25	0.196	0.080	0.025	2.0	0.029
13V	5	945	7.5	0.241	0.067	0.026	2.1	0.034
14V	1	1025	8.15	0.262	0.050	0.035	1.3	0.040
16V	1	1230	9.75	0.313	0.034	0.048	0.86	0.033
17V	1	1480	11.7	0.382	0.033	0.051	0.92	0.036
19V	0.5	2130	16.9	0.556	0.014	0.092	0.26	0.040
20V	0.5	3080	24.4	–	0.013	0.085	–	–

TABLE 4.3

Horizontal Earth Velocity

Gage Code No.	Horizontal Radius (ft)	Horizontal Radius λ	Peak Vel. (fps) Max. Pos.	Peak Vel. (fps) Max. Neg.	Aver. Ampl. (fps)	Period (sec)
2H	262	2.08	1.8	2.1	1.95	0.360
3H	314	2.49	1.7	2.0	1.65	0.345
6H	456	3.62	0.75	1.2	0.98	0.315
8H	542	4.3	0.85	0.94	0.90	0.305
10H	655	5.2	0.15	1.15	0.65	0.300
11H	788	6.25	0.45	0.60	0.53	0.360
13H	945	7.5	0.45	0.45	0.45	0.455
14H	1025	8.15	0.90	0.30	0.60	0.505
16H	1230	9.75	0.30	0.35	0.33	0.490
17H	1480	11.7	0.30	0.55	0.43	0.495
19H	2130	16.9	0.13	0.15	0.14	0.640

TABLE 4.4

Air-Blast Pressure

Gage Code No.	Gage Rating (psi)	Horizontal Radius (ft)	Horizontal Radius λ	Arrival Time (sec)	Positive Phase Peak (psi)	Positive Phase Durat'n (sec)	Positive Impulse (psi-sec)
3B	100	314	2.49	0.122	29.2	0.097	0.700
8B	10	542	4.3	0.255	14.3	0.174	0.725
13B	10	945	7.5	0.534	7.06	0.220	0.660
17B	10	1480	11.7	0.946	4.16	0.295	0.490
19B	10	2130	16.9	1.476	2.67	0.330	0.373

SECRET
Security Information

PROJECT 1(9)a

TABLE 4.5

Earth Pressure

Gage Code No.	Gage Rating (psi)	Horizontal Radius (ft)	Horizontal Radius λ	Arrival Time (sec)	First Pos. Pulse Ampl. (psi)	First Pos. Pulse Dur. (sec)	Max. Pos. Pulse Ampl. (psi)	Max. Pos. Pulse Dur. (sec)
1P	100	217	1.72	0.055	1.77	0.036	30.2	0.088
2P	100	262	2.08	0.068	0.99	0.035	16.5	0.095
5P	100	378	3.0	0.096	0.64	0.033	19.6	0.072
6P	10	456	3.62	0.116	0.67	0.045	18.3	0.087
8P	10	542	4.3	0.138	0.58	0.059	16.1	0.095
10P	10	655	5.2	0.165	0.43	0.092	17.7	0.076
11P	10	788	6.25	0.197	0.43	0.063	15.0	0.091
13P	10	945	7.5	0.238	0.27	0.037	9.8	0.090
16P	10	1230	9.75	0.312	0.17	0.050	9.05	0.080
17P	10	1480	11.7	0.383	0.13	0.052	8.7	0.770
19P	1	2130	16.9	0.555	0.070	0.050	---*	---*
20P	1	3080	24.4	0.815	0.020	0.085	---*	---*

*Galvanometer trace is off the oscillograph record; data are questionable.

CHAPTER 5

DISCUSSION

5.1 GENERAL

The discussion of the results of Project 1(9)a will cover seven main topics: air pressure; earth acceleration; damage; time of arrival; earth pressure; comparison with the scaled HE tests; and comparison with the Dugway dry clay tests in 1951.

The Project 1(9)-1 report[1] on the HE tests includes several predictions for the underground nuclear test. The HE-1 and HE-2 test results were examined and definite predictions were made for the experimental quantities which scaled properly for these TNT explosions. It will be one purpose of this discussion to compare these predictions with the underground test results.

The foregoing predictions were made assuming the underground nuclear charge to be equivalent to 1.0 KT of TNT energy release. Wherever possible, the equivalent TNT energy release of the underground nuclear charge will be computed for the particular phenomenon concerned, using HE-2 data[1] as the reference for TNT, assuming the normal explosive model laws.

5.2 AIR PRESSURE

The transient records of the air pressure measurements on Project 1(9)a are presented in Figure 4.2 of the previous chapter. Reference to this figure shows that the wave forms were very similar to those obtained in the HE-1 and HE-2 tests of Project 1(9)-1.[1] The shock fronts, or the initial abrupt pressure rises, are seen to be devoid of extraneous disturbances. In particular, there is no "front perch" effect such as was observed in the HE-3 test, which is what would be predicted from the fact that the nuclear charge burial depth was shallow. The reader is referred to the report on Project 1(9)-1[1] for a more detailed discussion of this "front perch" effect. The records in Figure 4.2 further illustrate that the duration of the positive phase increases with increasing distance from the charge.

The most important aspects of the air pressure records are the peak pressure, the positive phase duration, and the positive impulse. These quantities are shown plotted against the horizontal distance

from ground zero for the underground nuclear test in Figures 5.1, 5.2, and 5.3 respectively. In addition to the empirical curves, the figures also show the predictions for each of these quantities that were made in the Project 1(9)-1 report.[1] These predictions were scaled from the HE-2 test, assuming the underground nuclear test to be a scaled experiment and the charge energy release to be equivalent to 1.0 KT of TNT.

When comparison is made between the results of the underground nuclear test and the predictions for peak air pressure (Figure 5.1) it is observed that the curves are slightly different in form. The predicted pressure curve droops at small scaled distances, following HE-2. However, it was noted that for HE-1 the droop started at a larger value of λ. If this is a real effect of charge size, the net effect is to improve the curve fit at small λ.

At large ranges, the slopes of both curves of Figure 5.1 become constant, indicating a relation of the form

$$p \quad \frac{A}{R^n}, \tag{5.1}$$

where A is a constant and -n is the slope of the log log plot. The exponent n is 1.4 and 1.25 for the predicted and observed curves, respectively. Thus the attenuation laws for peak pressure are about the same for the underground nuclear and HE-2 tests.

Figure 5.2 shows the experimental and predicted values of the duration of the positive phase as a function of the experimental range. The curves have essentially the same form, with the predicted values lying above the experimental points shown. Similar behavior is exhibited in the positive impulse curves of Figure 5.3.

The scaling for air pressure between HE-1 and HE-2 was excellent, and the wave forms and attenuation laws observed on the nuclear test are similar to those from HE-2. Consequently there is justification for the calculation of equivalent yields for the various aspects of air-blast phenomena. Methods for doing this have been outlined in Section 5.2 of the report on Project 1(9)-1[1] and Section 5.1 of this report. With air pressure phenomena it is possible to get five scale factors (cube root of the yield ratio) by adjusting the curves for best fit. With a log log plot, as for peak pressure (Figure 5.1), only one adjustment is needed when the slopes are the same. Data for positive phase duration and positive impulse may be presented to advantage on a semi-log plot, in which two factors are used to match the curves. The five scale factors resulting for air blast, then, are as below

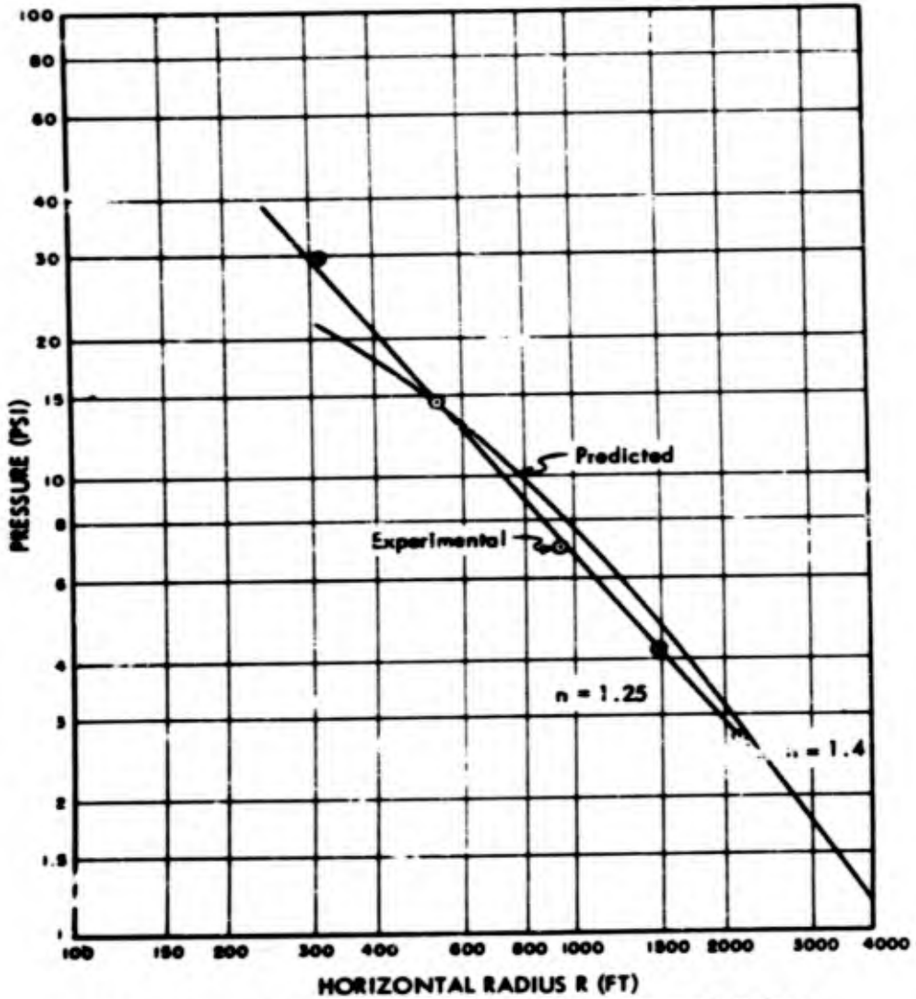

Fig. 5.1 Air-Blast Peak Pressure vs. Horizontal Radius for the Underground Test, with Curve Predicted for 1 KT of TNT

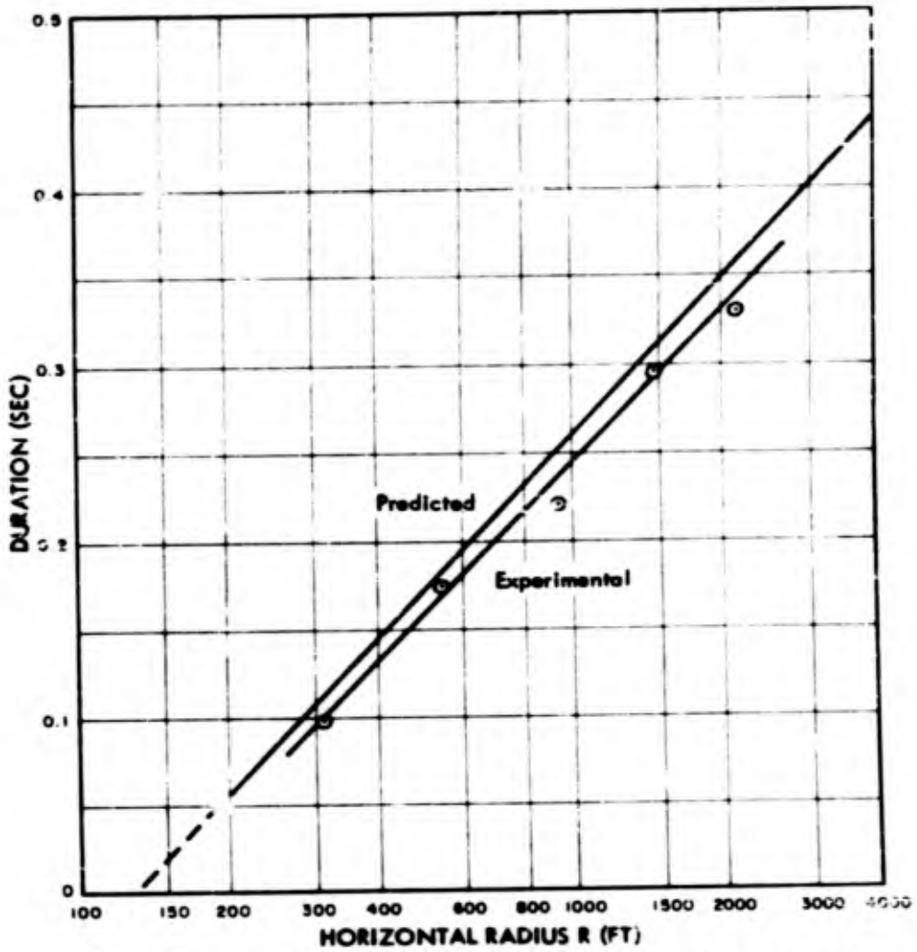

Fig. 5.2 Air Blast Positive Pulse Duration vs. Horizontal Radius for the Underground Test with Curve Predicted for 1 KT of TNT.

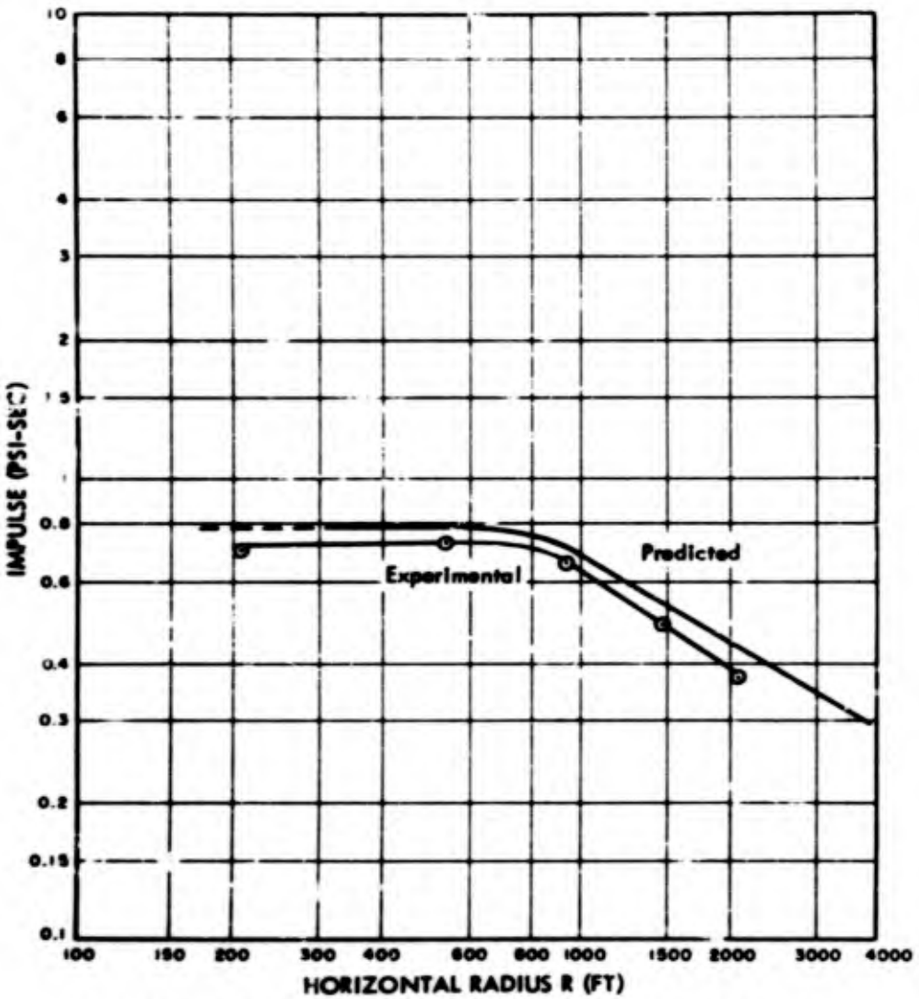

Fig. 5.3 Air Blast Positive Impulse vs. Horizontal Radius for the Underground Test, Curve Predicted for 1 KT of TNT

Quantity	Method	Scale Factor $\left(\frac{W_N}{W_{HE-2}}\right)^{1/3}$
Peak pressure	Curve fitting	3.5
Positive phase duration	Slope	3.4
	Intercept	3.6
Positive impulse	Slope	3.2
	Intercept	3.8

The arithmetic mean of the above values is 3.5, with a mean deviation of 0.16, or about four per cent. This air-blast scale factor corresponds to an equivalent yield of 0.85 KT of TNT, as judged by the ability of the underground charge to produce air blast. Of course, it must be pointed out that this yield is based upon the results of the air pressure measurements alone and it would be unwise, without further investigation to state that the underground nuclear charge of Project 1(9)a performed in all respects as a 0.85 KT charge of TNT would have performed under similar circumstances. The small deviation is an indication of the reliability of this yield calculation for air pressure. Since the radiochemical yield was announced to be 1.2 KT, the equivalent TNT efficiency was 70 per cent with respect to production of air pressure.

Figures 5.4, 5.5, and 5.6 show how well this scale factor of 3.5 holds between HE-2 and the underground nuclear test. The air pressure positive peaks, positive phase durations, and positive impulses are plotted in that order for both tests. In Figure 5.4 the curve represents the results of the nuclear test where the λ values have been computed on the basis of a charge equivalent of 0.85 KT of TNT. The points represent the HE-2 results. Except for low λ values, the fit is very good. The positive phase duration is treated in Figure 5.5. Since the time variable between two tests scales directly as the scale factor, it was necessary to multiply the HE-2 results by 3.5 to show the graphical correspondence. Here again, the underground test curve is drawn assuming a charge of 0.85 KT of TNT and the points are from HE-2 data. The curve appears to represent the plotted points very well. The positive impulse, shown in Figure 5.6, is treated in the same way. The curve, in this case, fits the plotted points for all λ values.

The preceding analysis gives a clear insight into the factors that must be considered when applying the model or scaling laws. A physical quantity, in this case air pressure, cannot be said to scale from one test to another unless its variation with respect to both radius (R) and time (t) are considered in detail. If, for any reason, the

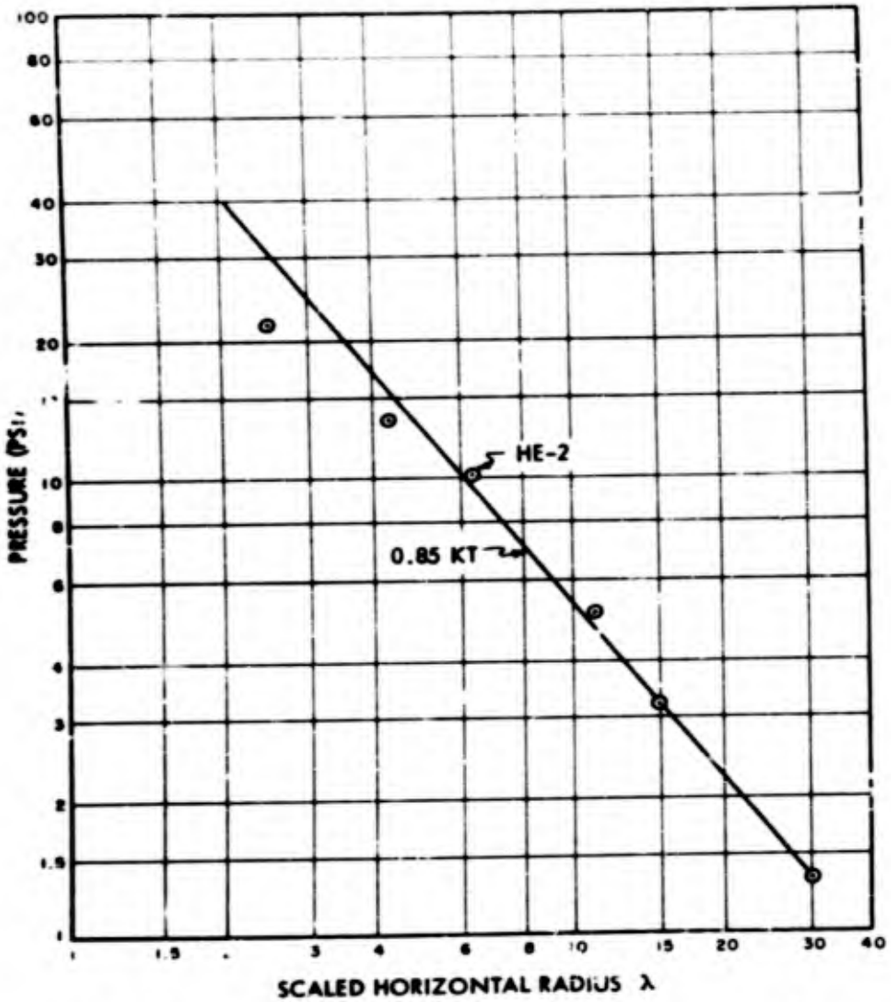

Fig. 5.4 Air Blast Peak Pressure vs. Scaled Horizontal Radius for 0.85 KT of TNT and HE-2 Test. Plotted points refer to HE-2

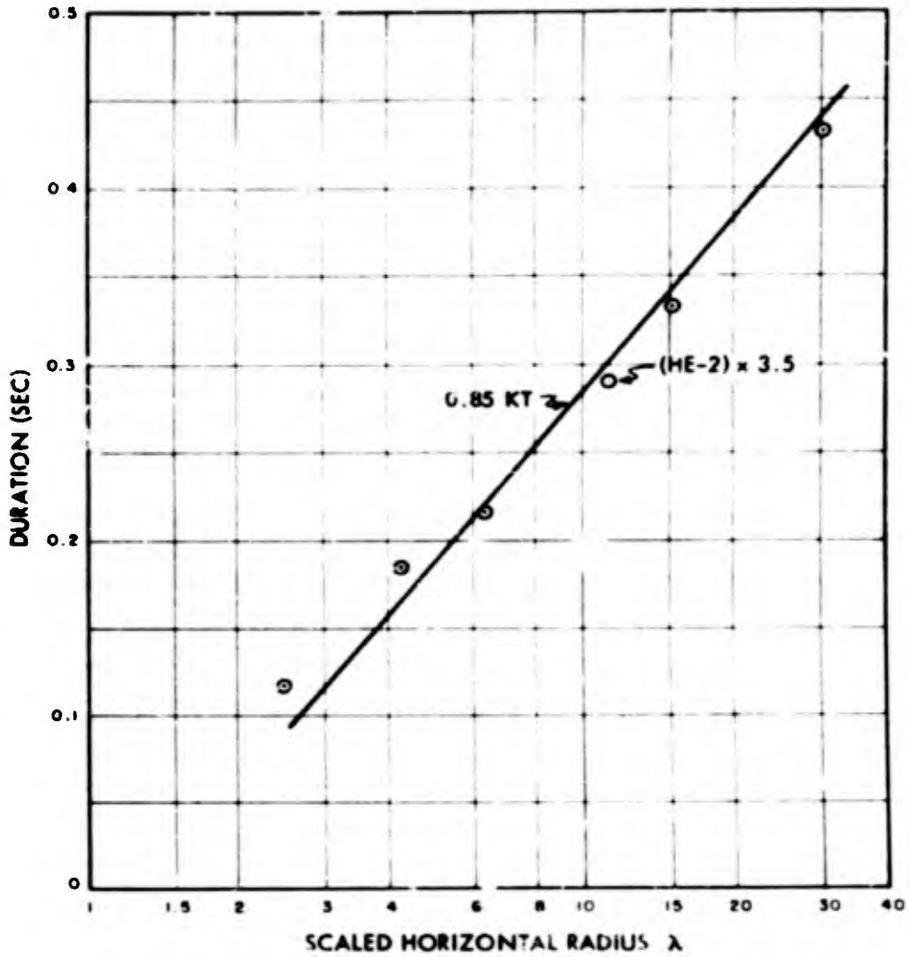

Fig. 5.5 Air Blast Positive Pulse Duration vs. Scaled Horizontal Radius for 0.85 KT of TNT and HE-2 Test. Plotted points refer to HE-2

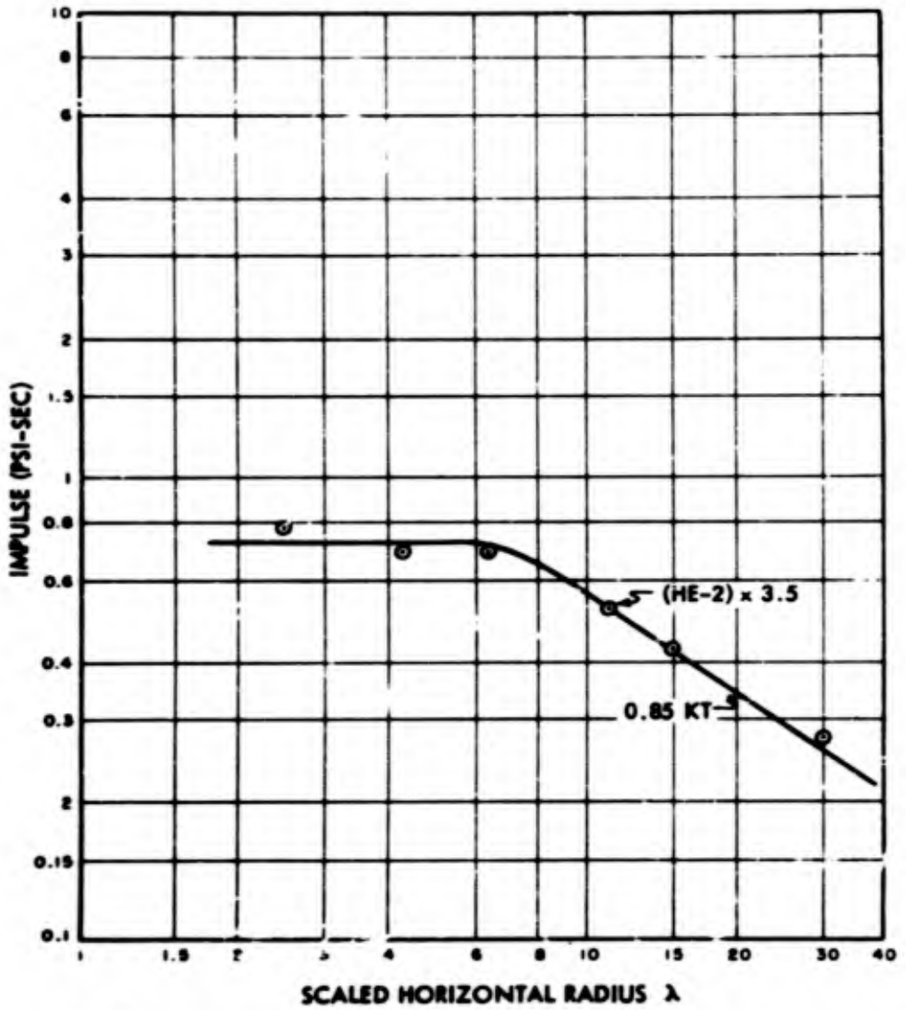

Fig. 5.6 Air Blast Positive Impulse vs. Scaled Horizontal Radius for 0.85 KT of TNT and HE-2 Test. Plotted points refer to HE-2

computed scale factors had been widely different, there would have been no basis upon which to compute an air-pressure equivalent yield of the nuclear test charge. To compute a different equivalent yield for peak pressure, for positive phase duration, and for positive impulse would have little practical meaning. This very problem presents itself when the phenomenon of earth motion is considered and it will be discussed later in this report.

Figure 5.7 presents air pressure records for the HE-1, HE-2, and underground nuclear tests at a constant λ value. The time scales have been scaled down appropriately, where the nuclear charge is assumed as 1.0 KT of TNT equivalent. The bottom graph shows a composite of all three records. According to the model laws, the pressures (at the same λ) should be equal. The composite graph shows that the three tests scaled quite well both in pressure and in time. One reason that the arrival times are different is that the velocity of the shock front in air is a function of the magnitude of the peak pressure. Since the nuclear charge gave rise to higher pressures near ground zero than did the other charges, the velocity of the shock front would be higher at first and the front would arrive earlier at the same scaled radial distance.

The time of arrival graph of the air-blast pressure (Figure 5.8) illustrates that the velocity is a function of pressure. The slope of the curve in the figure starts out low and increases up to a constant value. The low slope corresponds to a high velocity near ground zero where the pressures are high. The final velocity of 1220 feet per second would be expected for a shock overpressure of 3.4 psi for the atmospheric pressure (12.8 psi) and sound velocity (1100 feet per second) prevailing at the time of the test. This agrees very well with the mean pressure of about 3.5 psi over the outer range of the blast line.

For direct comparison to other nuclear tests the underground nuclear peak air pressure measurements have been normalized to standard conditions of 1.0 KT (radiochemical yield) at sea level. Using the announced yield of 1.2 KT and the ambient barometric pressure of 864 millibars, the distance correction factor becomes

$$\left[\frac{(864)(1.0)}{(1013)(1.2)}\right]^{1/3} = 0.89 \qquad (5.2)$$

and the pressure correction factor is

$$\left(\frac{1013}{864}\right) = 1.17 \qquad (5.3)$$

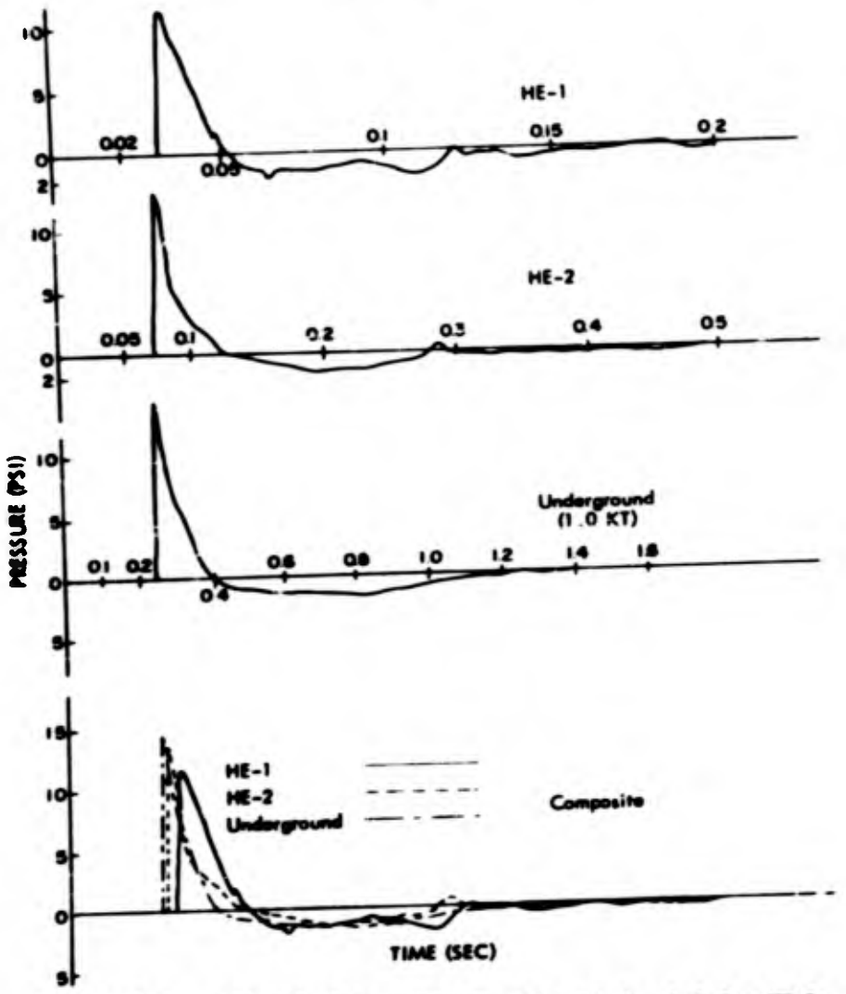

Fig. 5.7 Air Blast Pressure vs. Time at $\lambda = 4.3$ for HE-1, HE-2, and Underground Tests. Note that the time axes have been altered to correspond to scaling laws. The bottom graph is a composite of the three tests

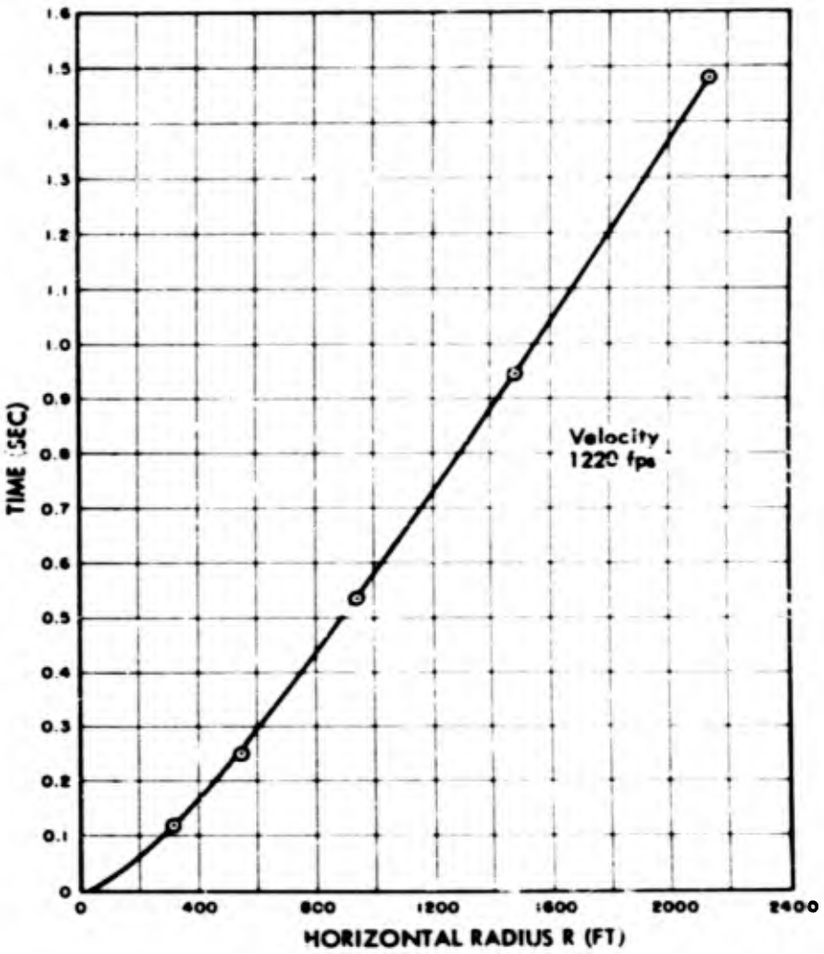

Fig. 5.8 Air Blast Pressure, Time of First Arrival vs. Horizontal Radius for Underground Test

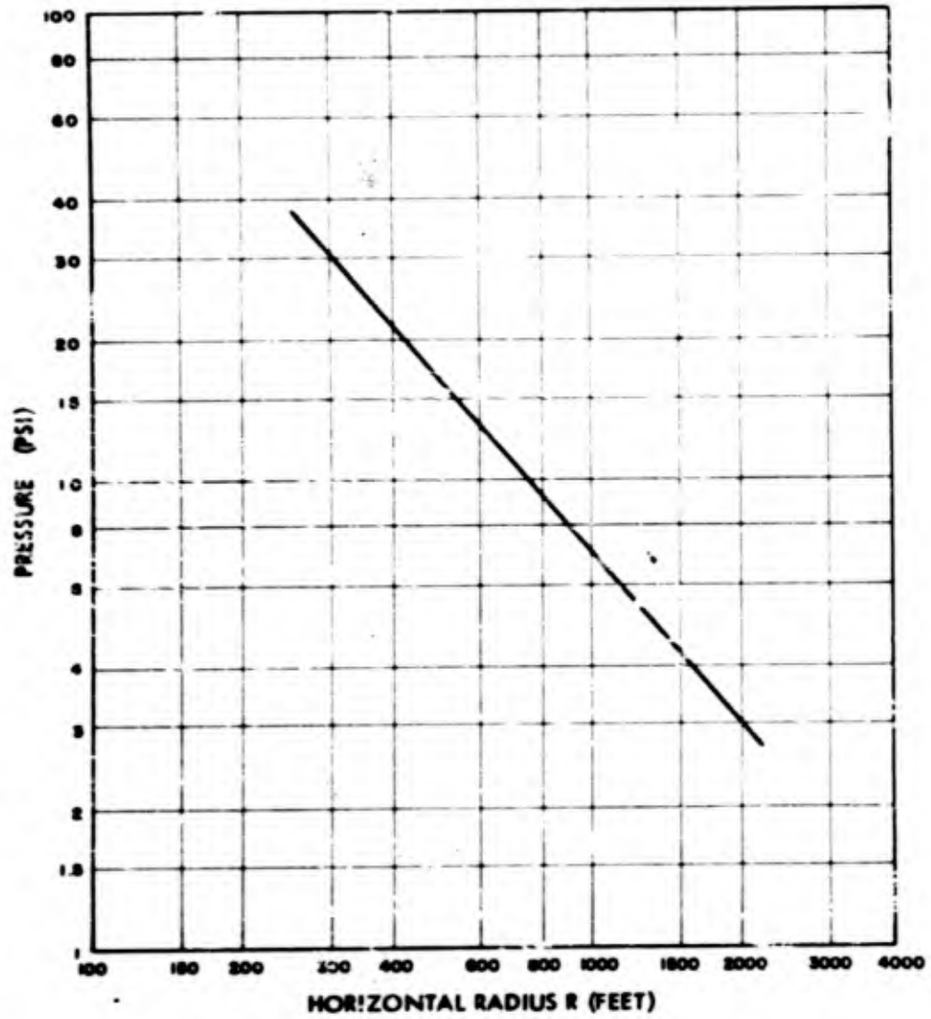

Fig. 5.9 Air-Blast Peak Pressure vs. Horizontal Radius for a 1 KT Nuclear Explosion. Detonated at a depth of 17 feet in JANGLE soil at sea level

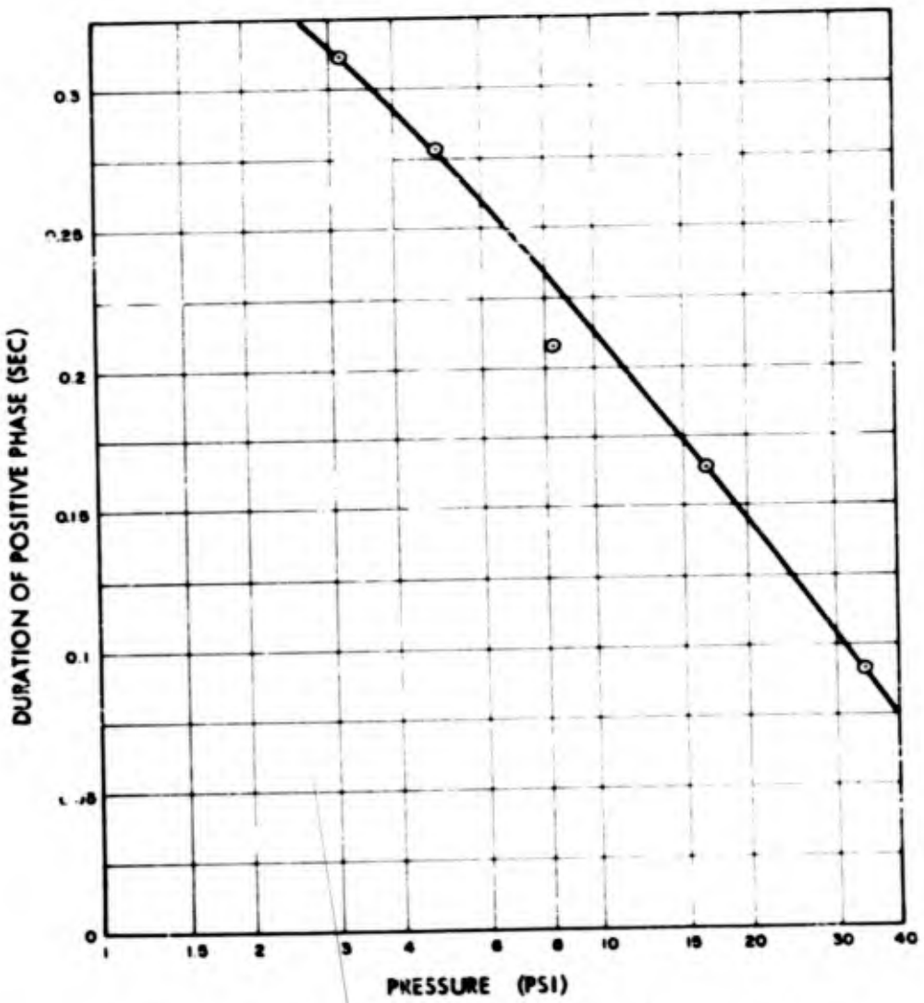

Fig. 5.10 Duration of Air-Blast Positive Phase vs. Peak Pressure for a 1 KT Nuclear Explosion at a Depth of 17 Feet in JANGLE Soil at Sea Level

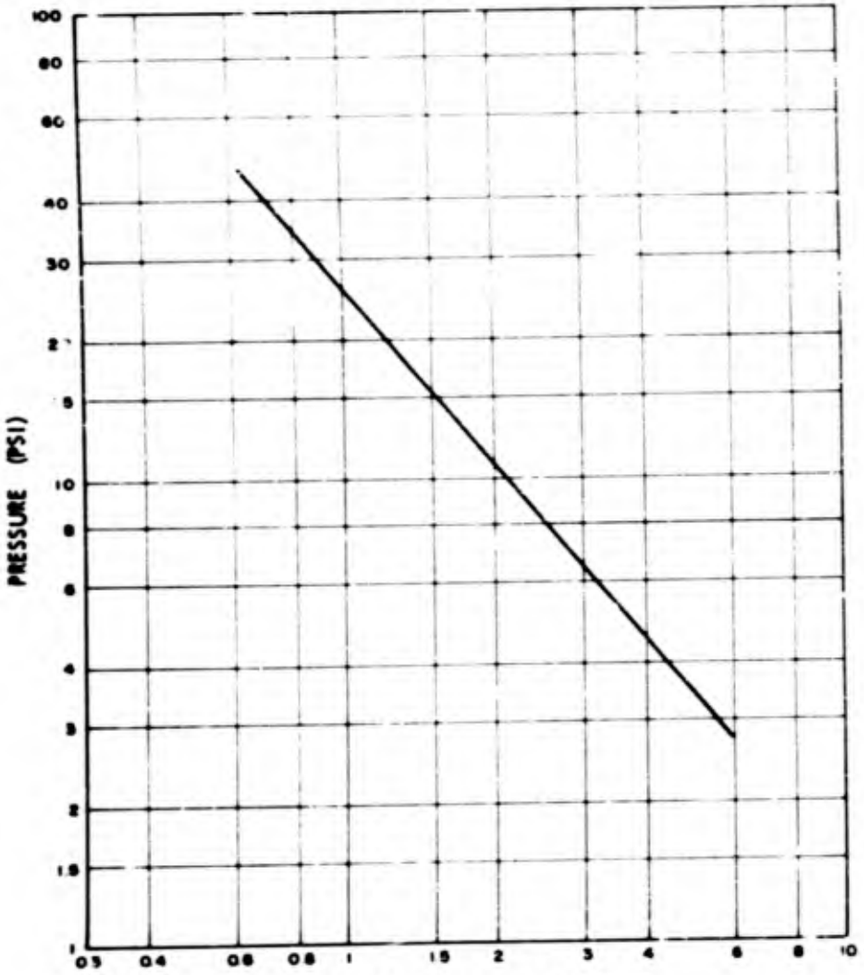

Fig. 5.11 Air-Blast Peak Pressure vs. Horizontal Radius for a 23 KT Nuclear Explosion at a Depth of 17 Feet in JANGLE Soil at Sea Level

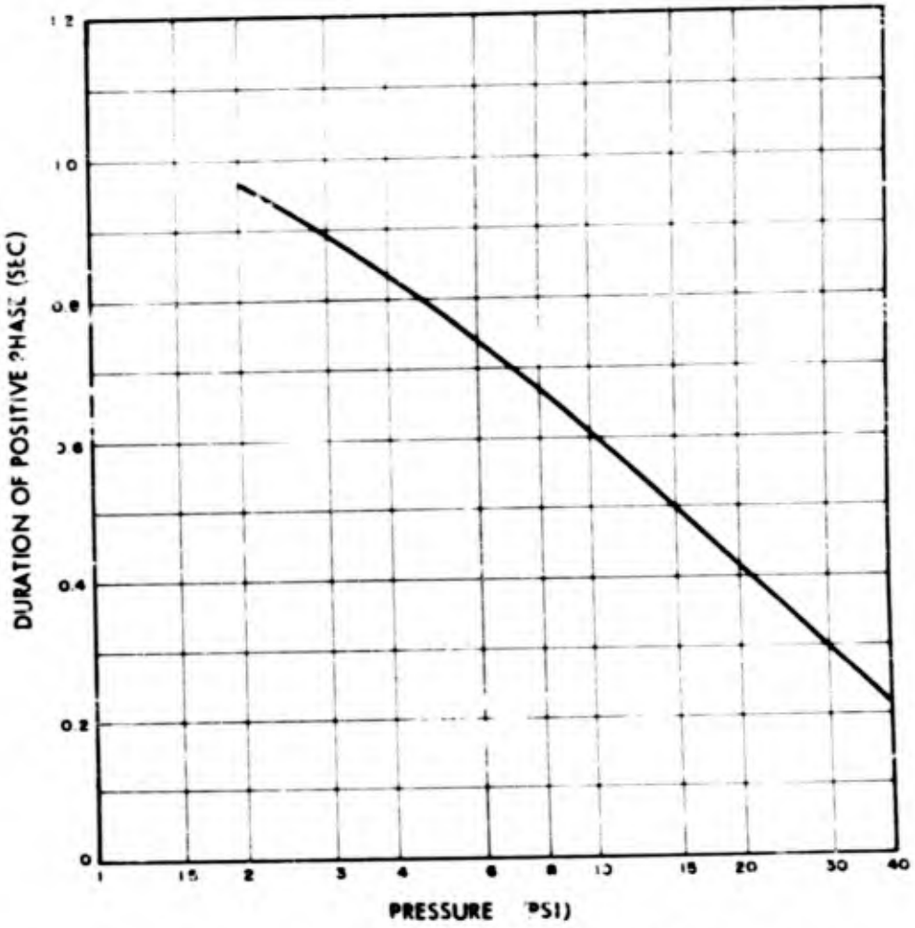

Fig. 5.12 Duration of Air-Blast Positive Phase vs. Peak Pressure for a 23 KT Nuclear Explosion at a Depth of 17 Feet in JANGLE Soil at Sea Level

The resultant normalized peak pressure data are shown in Figure 5.9, while Figure 5.10 presents the positive phase duration as a function of normalized peak pressure.

The excellent model law behavior for air pressure makes it possible to predict the results for a scaled 23 KT experiment at the same test site with good reliability. The predicted peak air pressure vs. distance curve for a 23 KT weapon at a depth of 46 feet is shown in Figure 5.11, while Figure 5.12 shows the predicted positive phase duration as a function of peak pressure.

From comparisons between the scaled HE tests and the tests at the Dugway dry clay site, there is some indication that the air pressure produced by an underground explosion is a function of the soil characteristics. It is believed that this effect is relatively small for the shallow burial depth, $\lambda_B = 0.135$, used for the underground nuclear test. However, very limited experimental data are available for the air pressure effects produced by buried charges, and the effect of soil type cannot be estimated or neglected with certainty.

5.3 EARTH ACCELERATION

The transient records of the earth acceleration measurements on Project 1(9)a are presented in the previous chapter. Figures 4.3 and 4.4 present the horizontal earth acceleration at a depth of 5 feet as a function of time as measured at various distances from the charge. Reference to these figures shows some large high-frequency pulses superimposed upon the low-frequency variations of acceleration. Since these short pulses are initiated very soon after the arrival of the air-blast shock at all gage stations (this arrival is denoted by the AB designation), it is concluded that the air-blast pressure is the cause. These results indicate that there is some energy being fed into the earth medium from the air. The amount of this "feed-back" energy does not appear to be insignificant. The first low-frequency acceleration pulse is probably most representative of the direct earth transmitted effects.

Concerning the horizontal earth acceleration data, Figure 5.13 presents the first pulse amplitude and duration as a function of horizontal radius. The amplitude values indicate a slope of about 1.25 out to 1000 feet. This is the same attenuation as shown in Figure 5.1 for the air-blast peak pressure. At larger radii, the amplitude drops off abruptly. These results are compared with the predicted values in Figure 5.14. It is at once obvious that one cannot proceed with an analysis similar to that developed in the case of the air-blast pressure. The two curves in Figure 5.14 take different

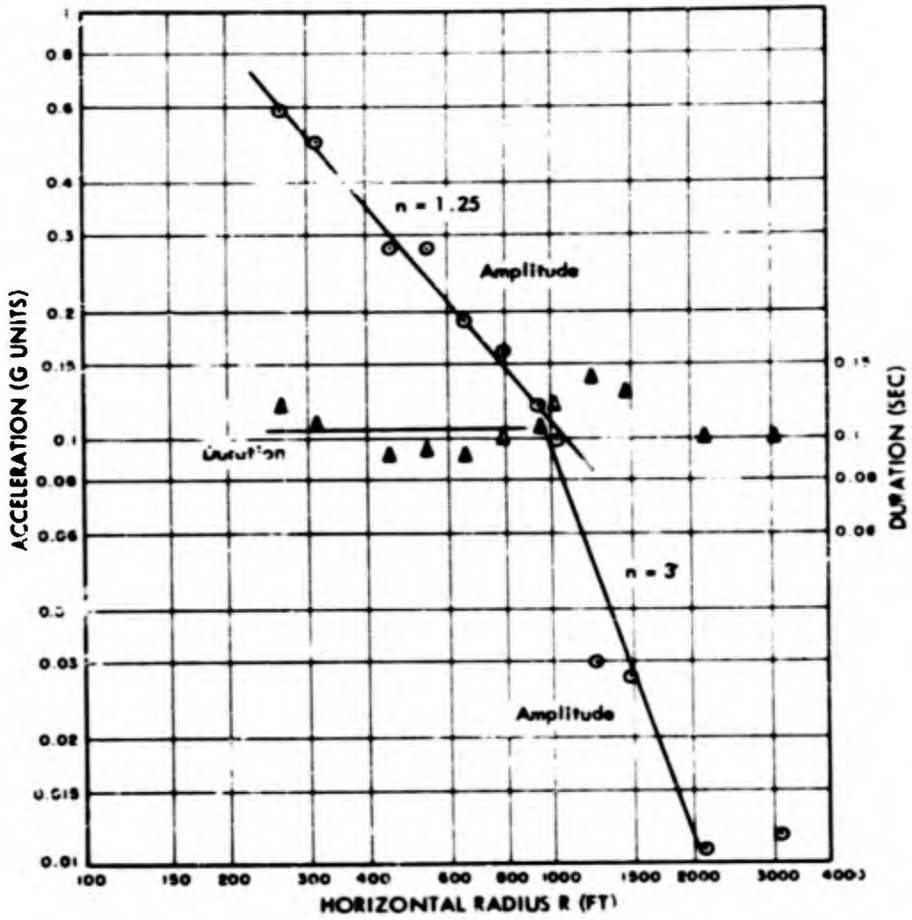

Fig. 5.13 Horizontal Earth Acceleration, First Pulse Amplitude and Duration vs. Horizontal Radius for the Underground Test. Gage depth, 5 feet

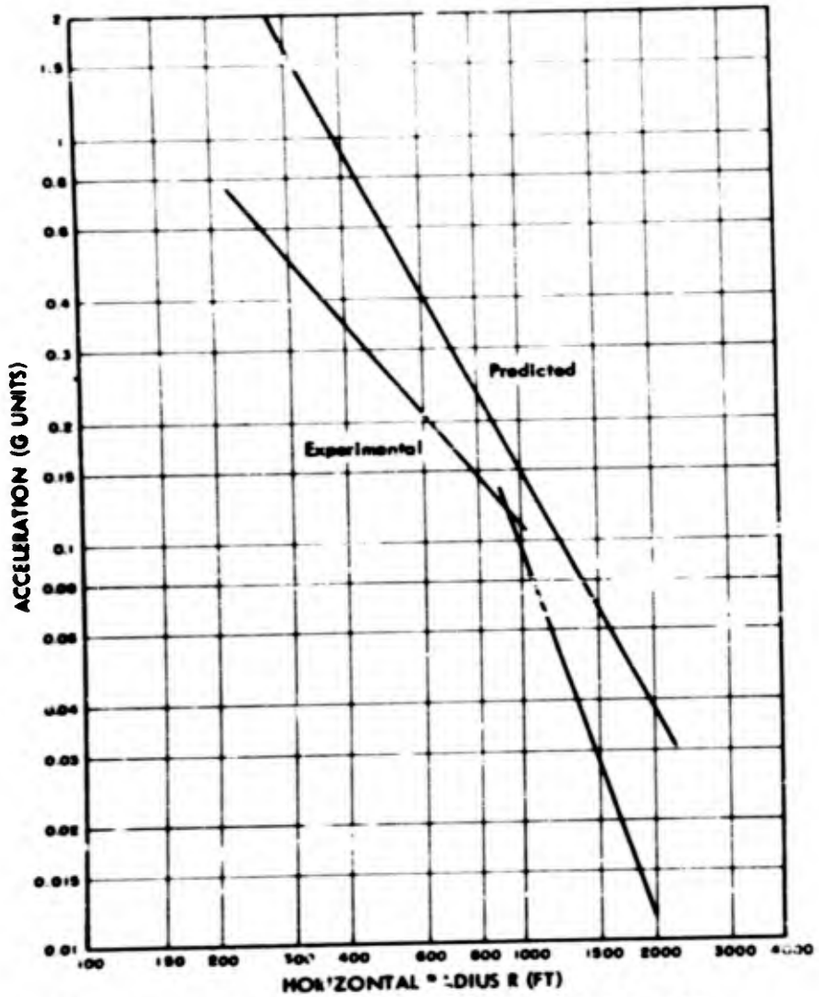

Fig. 5.14 Horizontal Earth Acceleration, First Pulse Amplitude vs. Horizontal Radius for the Underground Test Curve Predicted for 1 KT of TNT. Cage depth 5 feet

forms and it is not possible to regard them in toto. The predicted curve being above the empirical one indicates that the energy equivalent for horizontal acceleration is everywhere less than 1.0 KT of TNT.

When two curves are not of the same form, as is the case in Figure 5.14, the energy equivalent is a function of the magnitude of the measured quantity (in this case, acceleration), or of the distance chosen for comparison. This problem can be presented in a more general way by referring to Figure 5.15. Here the curves for two hypothetical tests, 1 and 2, have decidedly different forms and it would be impossible to calculate one scale factor between them which would hold for all values of the ordinate (independent variable). Let us assume that the energy release in equivalent pounds of TNT is known for Test 1 and is to be computed for Test 2. According to the scaling laws, pressure and velocity are the same at the same scaled horizontal distances for all tests. Therefore, if the curves in Figure 5.15 were plots of pressure or velocity vs. horizontal radius (using the same coordinate axes for both curves), then the scale factor at point P,v is given by the ratio between R_1 and R_2. However, it is evident from the figure that this ratio will be different for different values of the ordinate (labeled "Physical Quantity" in the figure). If the ratio or scale factor were a constant for all values of the ordinate, then the two curves would necessarily have the same form and a unique energy equivalence could be computed for Test 2.

Another possible approach would be to plot the curves on their own respective coordinate axes and then slide the axes relative to one another, maintaining ordinates parallel, until the curves intersect at the desired ordinate value, here labeled P,v. Again, if the curves take different forms, this will yield a scale factor (R_1/R_2) which is a function of the ordinate value chosen.

For an acceleration vs. distance graph, both the ordinate and abscissa are scaled quantities. Therefore, the Test 2 curve is moved along a 45-degree line (on log log paper) as indicated in Figure 5.15. This yields an acceleration scale factor which is valid for the one point that is labeled A on the ordinate. This procedure corresponds to sliding the separate graphs (for Test 1 and Test 2) over one another so that the point labeled "Acceleration" moves along the 45-degree line indicated in Figure 5.15. In a like manner, the time variable associated with an explosion test may be used to compute the scale factor as is shown in the figure. It must be pointed out that this graphical method is particularly useful when the results of two tests plot as a scatter of points through which a smooth curve cannot be drawn. In this case, the same general procedure of sliding the graphs over one another can be employed, matching the results where

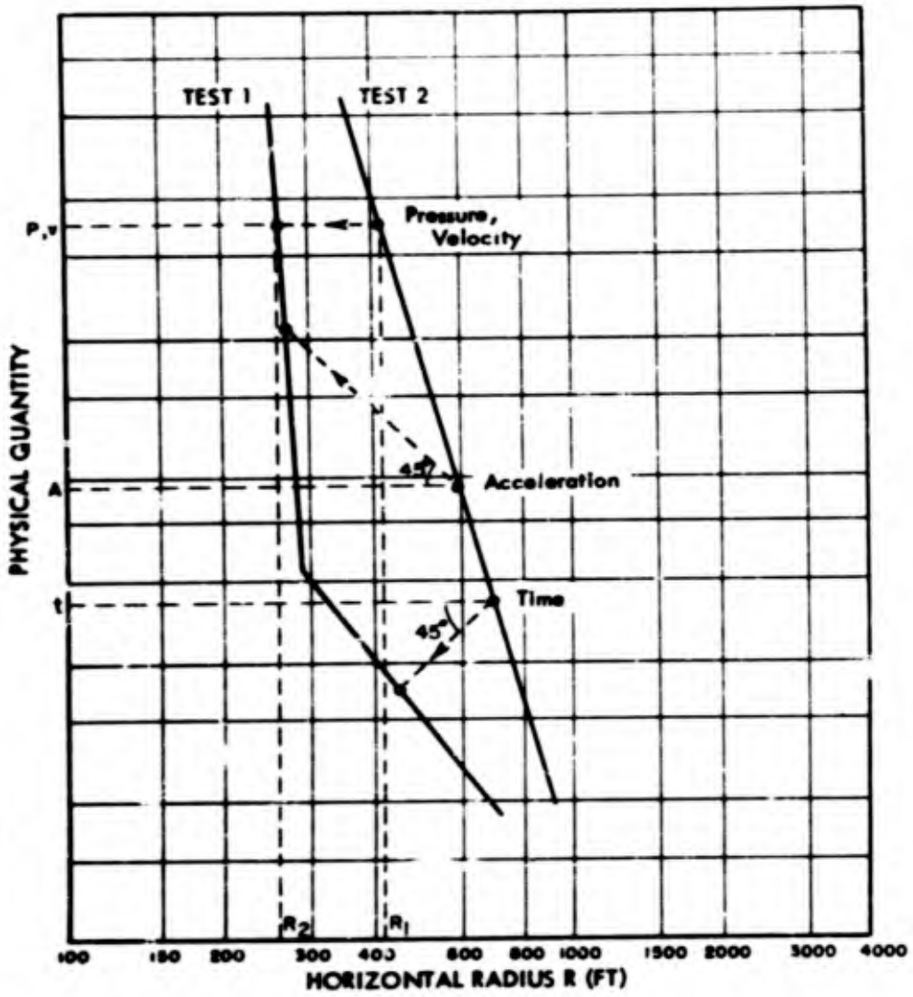

Fig. 5.15 A Graphical Method for Computing the Scale Factor between Two Explosion Tests when the Phenomenon Curves are not of the Same Form

the points appear to intermesh the best.

Using this graphical method on the curves in Figure 5.14, we can compute the energy equivalent for the underground nuclear test (first peak, horizontal acceleration) at any desired acceleration level. At the 0.60 G level (250 - 500 foot range), the equivalent is 0.02 KT of TNT, and at 0.20 G (600 - 900 foot range) the equivalent is 0.12 KT of TNT. At the 0.1 G level (1000 - 1250 foot range), where the nuclear test results seem to approach the predicted values most closely, the equivalent underground nuclear charge is about 0.33 KT of TNT.

The vertical component of the earth acceleration should be examined in a similar manner. Figures 4.5 and 4.6 show that the vertical transient acceleration records are in many ways similar to the horizontal records. The verticals show stronger air-blast induced effects and weaker first pulse amplitudes than the horizontals. The first pulse amplitudes and durations are plotted in Figure 5.16. This figure shows that the amplitude attenuation follows an inverse square law with a break in the attenuation curve from about 450 feet to 700 feet. This break is not inconsistent with the vertical acceleration results of the HE-1 and HE-2 tests of Project 1(9)-1.[1] On both these HE tests a similar break in the curve was observed at about 450 feet. As is pointed out in the Project 1(9)-1 report,[1] this result indicates that the effect is characteristic of the medium, rather than of the charge size. It is also postulated that the jog in the curve is due to an abrupt variation of seismic velocity with depth in the ground. The presence of a high velocity substratum would explain the effect adequately. The dotted curve in Figure 5.16 represents the air-blast pressure attenuation and is included for comparison.

Figure 5.17 presents the comparison between the nuclear test results (from Figure 5.16) and the predicted results. For values of R less than about 400 feet the experimental and predicted curves are quite close. In this region, the graphical method indicates that the equivalent underground nuclear energy release was about 0.75 KT of TNT.

Predictions were not made for the durations of the first pulse of acceleration because this quantity did not follow the model laws for the HE-1 and HE-2 tests.[1] The HE tests results could only give an idea of the limits to be expected on the nuclear test. As shown in the previous figures, the first pulse durations for the horizontal acceleration are about four times larger than those for the vertical acceleration. The significance of this result will be dealt with later in this section in connection with damage criteria.

It is quite possible that the "feed-back" effect referred to

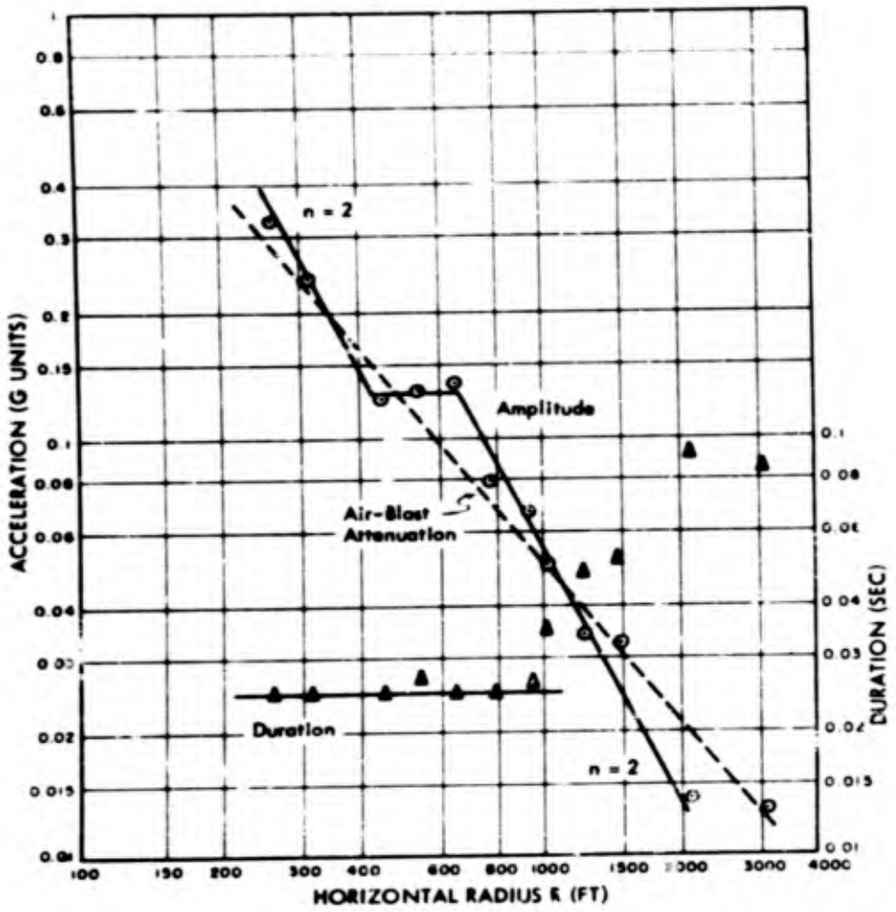

Fig. 5.16 Vertical Earth Acceleration, First Pulse Amplitude and Duration vs. Horizontal Radius for the Underground Test, Gage depth, 5 feet

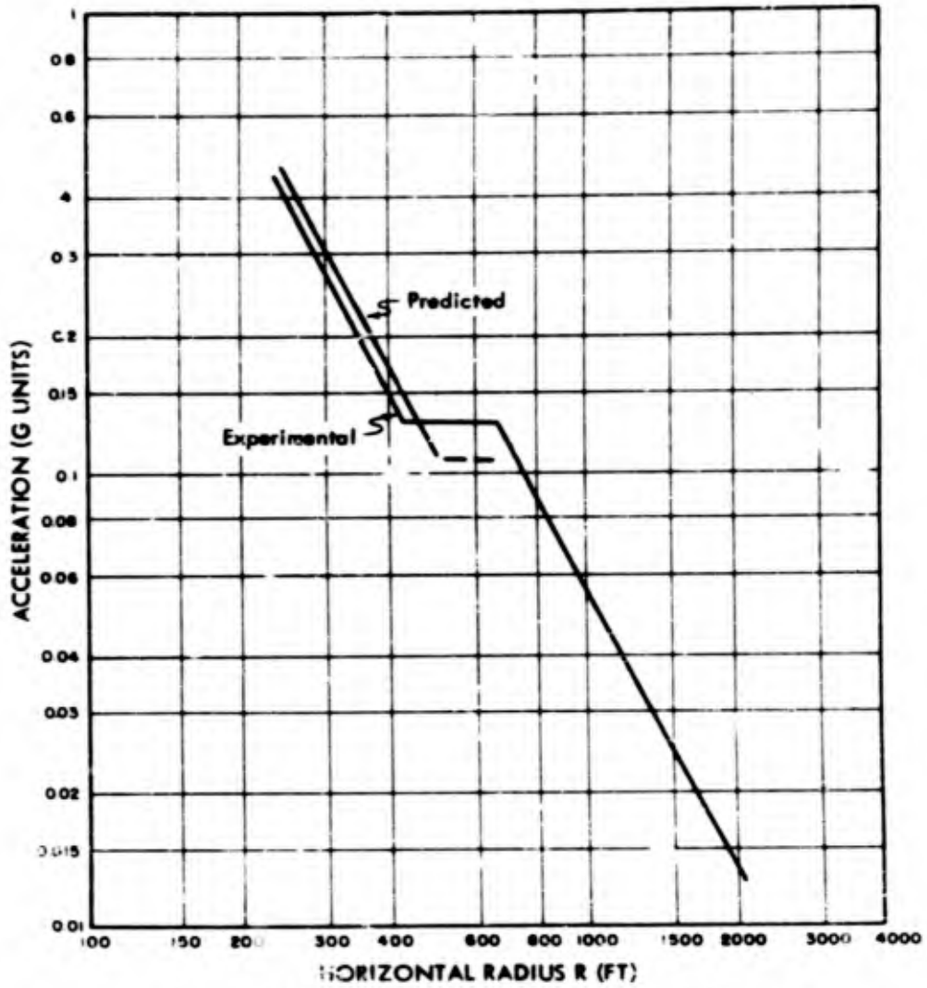

Fig. 5.17 Vertical Earth Acceleration, First Pulse Amplitude vs. Horizontal Radius for the Underground Test, with Curve Predicted for 1 KT of TNT. Gage depth 5 feet

previously could be responsible for deviations from model law behavior in the case of earth phenomena. Under extreme conditions two different types of scaling, air and earth, may be encountered. In fact, if energy fed back from the air predominates, we should expect scaling appropriate to air to determine the earth phenomena.

These "feed-back" phenomena, if they truly exist, make data analysis quite complex. The air-blast pressure and the direct earth acceleration scale differently, and the two quantities obey different attenuation laws. In addition, one must consider that the air disturbance travels more slowly in air than it does when transmitted through the earth.

It would be worthwhile to attempt to separate the air-blast induced effects from the direct earth effects. Since the air-blast effect was more consistent and predominant on the vertical component of the earth acceleration, this separation was performed on the vertical records. The separation process involves a smoothing of the acceleration record in the region of the air disturbance (see dotted portion on the top curve of Figure 4.13). The smoothed curve is taken as the "true" earth acceleration and the high frequency acceleration superimposed upon it is called the air-blast "slap" acceleration. The wave form corresponding to one of these slaps is shown in Figure 5.18. The wave is characterized by a strong negative onset (corresponding to a downward acceleration) and a highly damped, high-frequency oscillation.

If all other factors are maintained to scale, it is evident that the induced "slap" acceleration becomes more dominant (with respect to amplitude) as the charge size is increased. This arises since, for scaled tests at the same λ range, air pressure is constant, while acceleration is inversely proportional to $W^{1/3}$.

Figure 5.19 shows the plot of the negative peak air-blast slap acceleration against horizontal radius. The curve drawn through the points represents the air-blast pressure attenuation shown in Figure 5.1 where $n = 1.25$. If the slap acceleration for the underground nuclear test is compared with that predicted from scaling the HE-1 and HE-2 tests, then one obtains the plot shown in Figure 5.20. The curve is the predicted slap amplitude on the basis of 1.0 KT equivalent energy release and the plotted points refer to the experimental results. Close to the charge, out to a radius of about 500 feet, the nuclear test gave air-blast slap accelerations exceeding the predictions, undoubtedly because the blast pressures were greater in this region than for HE-2. However, at larger horizontal distances the empirical values fall off more rapidly with distance than do the predictions. This is illustrated by the fact that at the 7.0 G level the underground nuclear charge energy equivalent for the slap is about 4.0 KT of TNT,

Fig. 5.18 Wave Form of Air Blast Slap in Vertical Acceleration for the Underground Test, R = 788 ft. Gage depth, 5 ft.

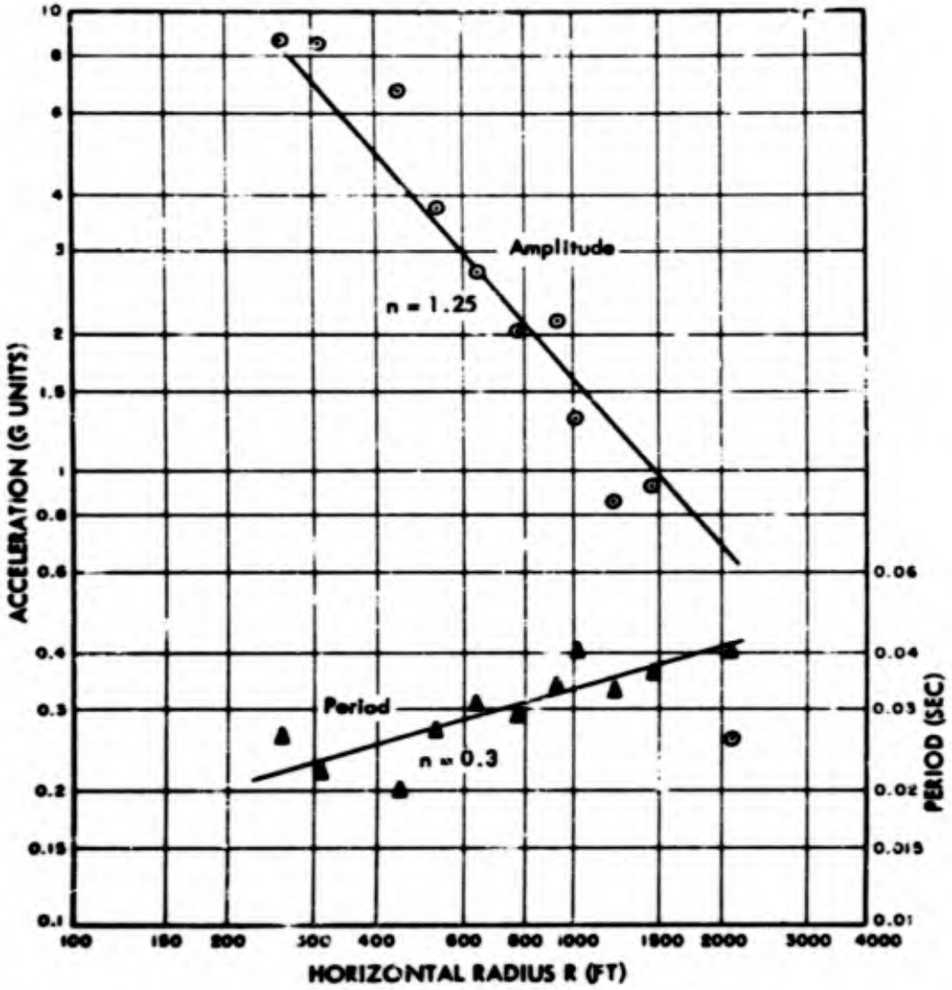

Fig. 5.19 Negative Peak in Vertical Earth Acceleration Due to Air Blast Slap. Amplitude and estimated period vs. horizontal radius for the underground test. Gage depth, 5 feet

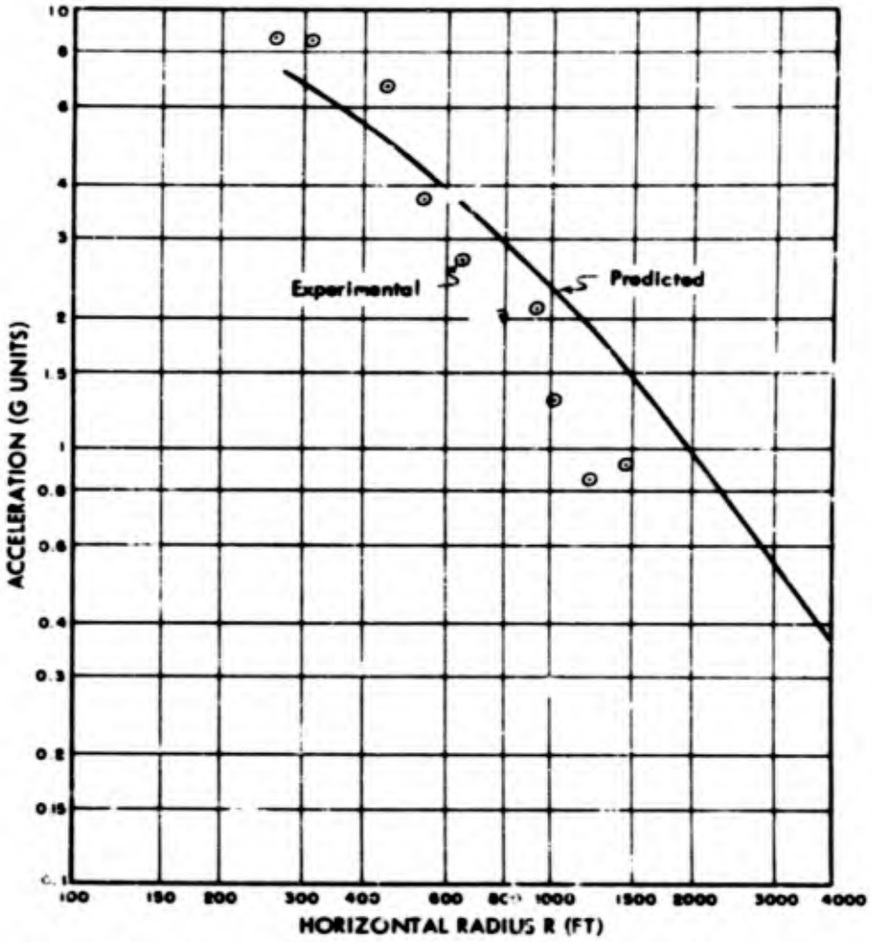

Fig. 5.20 Negative Peak in Vertical Earth Acceleration Due to Air Blast Slap. Amplitude vs. horizontal radius for the underground test, with curve predicted for 1 KT of TNT. The plotted points refer to underground test results. Gage depth, 5 feet

while at 1.0 G the equivalent is approximately 0.2 KT of TNT.

The acceleration measurements taken at depths greater than five feet were presented in Chapter 4 in the form of reductions of the traced records. The horizontal and vertical deep accelerations are shown in Figures 4.8 and 4.9. The records show that the general wave form and amplitudes are not altered appreciably as the gage is buried deeper. However, it is observed that the effect of the air blast is much reduced beyond the 34-foot depth. This reduction of the air-blast slap effect at the 68-foot gage is evident in both the horizontal and the vertical components of earth acceleration.

5.4 COMPARISONS WITH SCALED HE TESTS

By way of summarising the comparisons between the underground nuclear test and the scaled HE tests, the earth acceleration records at two radial distances are presented showing the transient records from the HE-1, HE-2, and nuclear tests. The curves have been normalised in the sense that the time and acceleration coordinates have been scaled according to the model laws. This means that if the three tests obeyed the model requirements in every respect the three records at a single scaled radius should appear exactly alike. For uniformity, the nuclear charge has been assumed to be an equivalent of 1.0 KT of TNT. Therefore the scale factors are HE-1 : HE-2 : nuclear as 1 : 2.5 : 9.2. These normalised records are shown in Figures 5.21 and 5.22 (horizontal components) and Figures 5.23 and 5.24 (vertical components).

Looking at the horizontal components, it is noted that the air-blast slap acceleration is insignificant on the HE-1 record, while it reaches huge proportions on the underground test record. The $\lambda = 2.08$ records for HE-1 and HE-2 show very similar wave forms (excluding the air-blast slap on HE-2). However, the nuclear test record show a time "squeeze" of this wave form, bringing out how poorly the time quantity followed the $W^{1/3}$ model law in the nuclear test. At λ 5.2 much the same analysis applies. In addition, the first pulse amplitudes show a marked deviation from scaling and HE-1 exhibits a large second positive pulse that is not measured on the other tests.

The vertical accelerations presented in Figures 5.23 and 5.24 show that the air-blast effects grew far out of proportion to the charge scaling factors when the nuclear test results are considered. Here again we find that the time quantity scales poorly from HE-2 to the nuclear test and it becomes increasingly more difficult to separate the "true" earth effects from the air-blast induced effects.

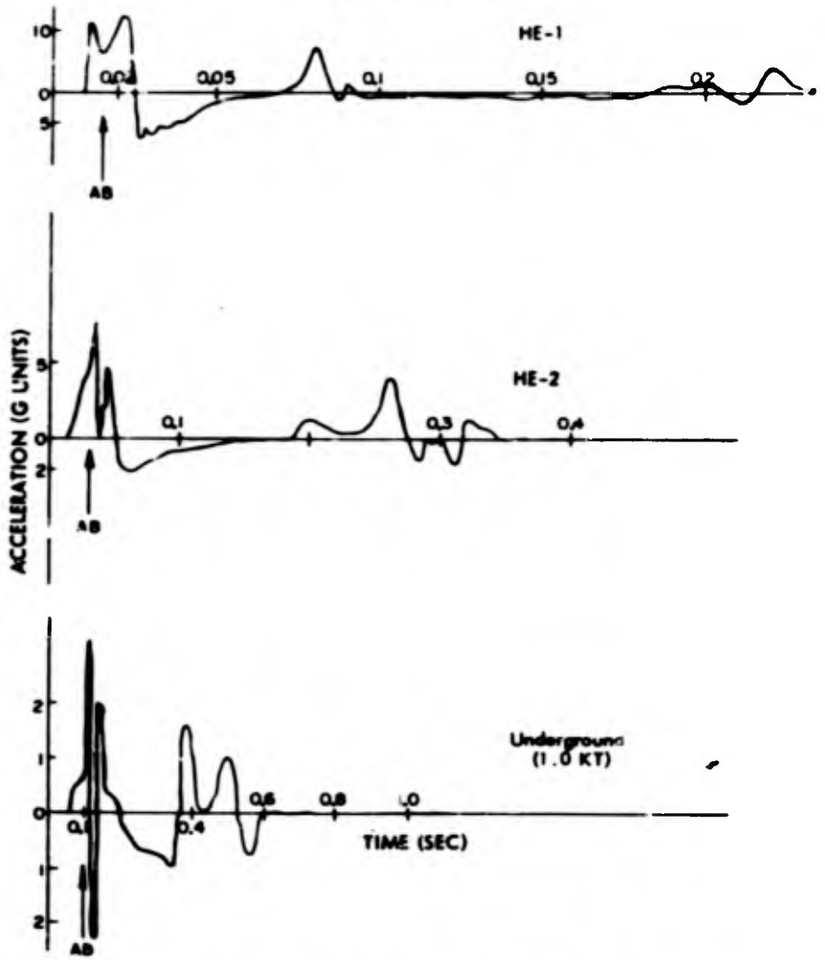

Fig. 5.21 Horizontal Earth Acceleration vs. Time at $\lambda = 2.08$ for HE-1, HE-2, and Underground Tests. Note that the coordinates have been normalised assuming model law conditions. Gage depth, 5 feet

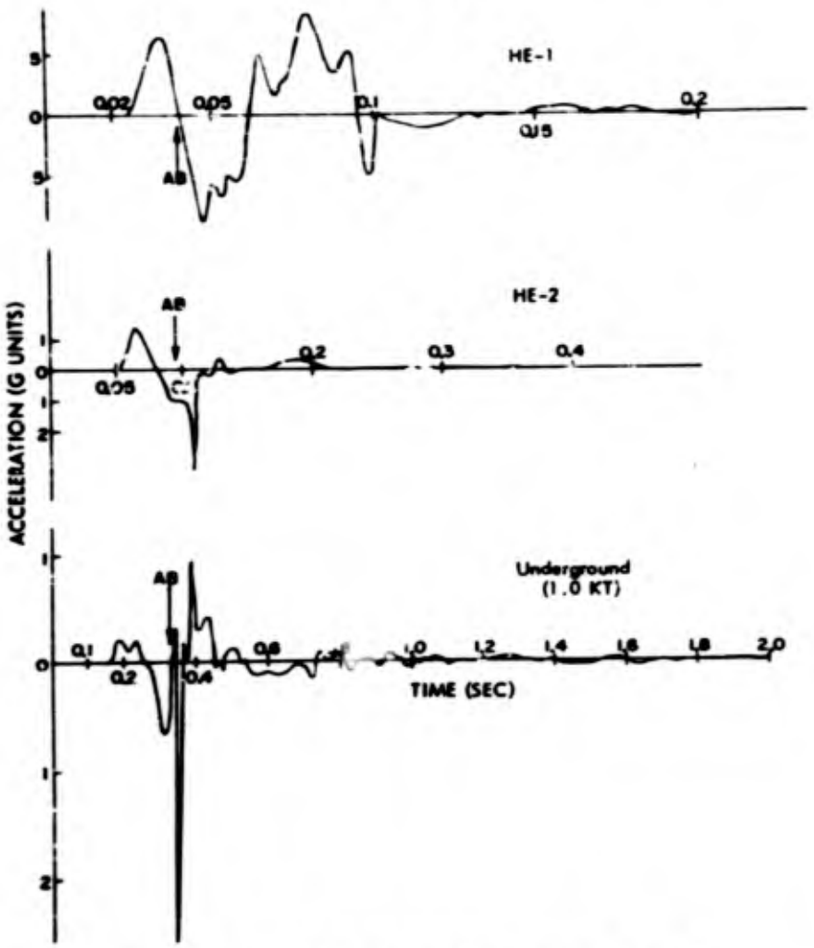

Fig. 5.22 Horizontal Earth Acceleration vs. Time at $\lambda = 5.2$ for HE-1, HE-2, and Underground Tests. Note that the coordinates have been normalized assuming model law conditions. Gage depth, 5 feet

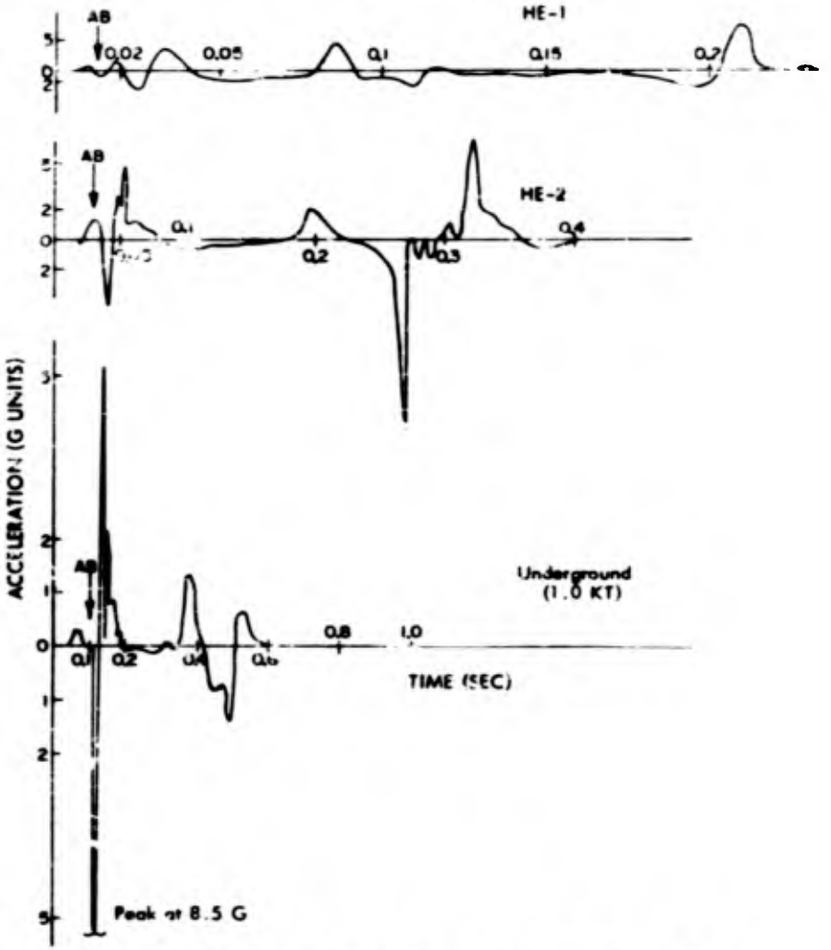

Fig. 5.23 Vertical Earth Acceleration vs. Time at $\lambda = 2.08$ for HE-1, HE-2, and Underground Tests. Note that the coordinates have been normalized assuming model law conditions. Gage depth, 5 feet

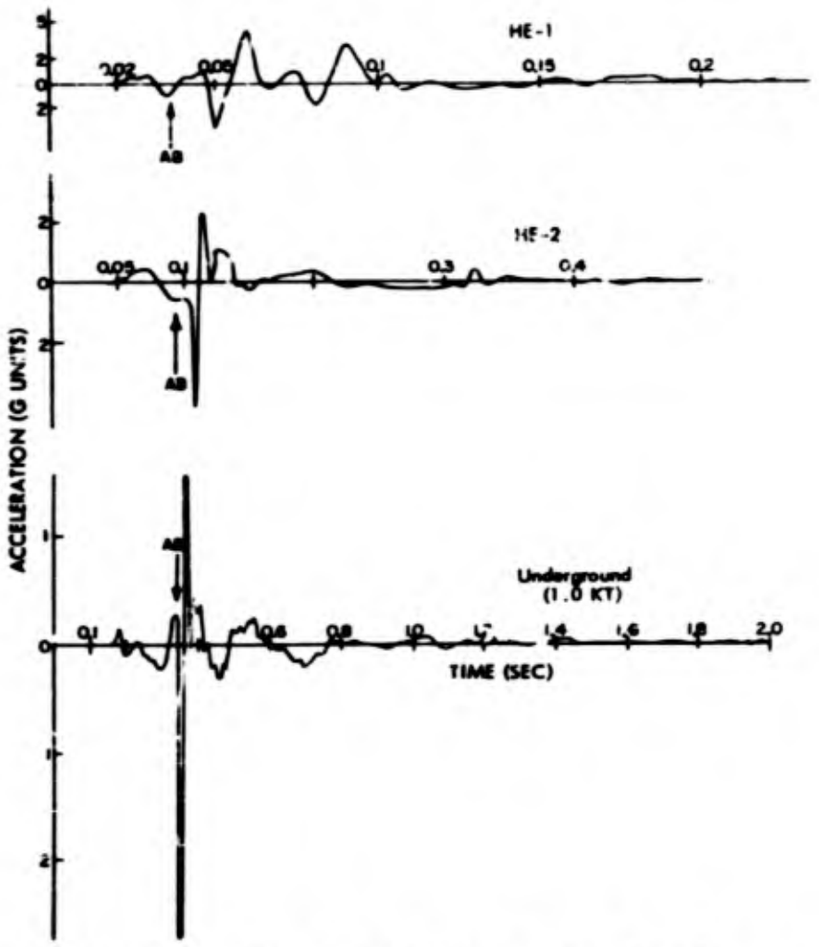

Fig. 5.24 Vertical Earth Acceleration vs. Time at $\lambda = 5.2$ for HE-1, HE-2, and Underground Tests. Note that the coordinates have been normalized assuming model law conditions. Gage depth, 5 feet

Figure 5.25 presents the time of first arrival of the horizontal earth acceleration plotted against horizontal radius for the Project 1(9)a underground nuclear explosion test. From this curve it is possible to compute the average seismic velocity for the test medium, where it is recognized that the seismic velocity varies with depth. The velocity turns out to be 3730 ft/sec. This result must be compared with the 3500 ft/sec and 3400 ft/sec obtained for HE-1 and HE-2 respectively. A discontinuity in the curve of Figure 5.25 near ground zero is not unlike the result obtained in the JANGLE HE tests. It is thought that this break indicates some anomaly in the subsurface geology.

5.5 DAMAGE

The damage to a surface structure whose foundation is well coupled to the earth is more or less proportional to the deformation of the structure. The choice of the earth motion phenomena most closely correlated to such damage depends essentially upon the ratio of the characteristic period of the earth motion to that of a typical structure being attacked. For small charges this ratio is much less than unity, and a simple analysis indicates that earth displacement is the principal factor influencing structure deformation. As this ratio approaches unity, earth particle velocity becomes the principal factor determining structure deformation. Furthermore, as the ratio increases to values much larger than unity, the earth acceleration more nearly governs damage.

Results of damage obtained from the surface structure tests at the Dugway Proving Ground[4] seemed to indicate that satisfactory damage criteria were (1) the maximum peak-to-peak particle velocity and (2) the period associated with this maximum velocity oscillation. In addition, it was found that the horizontal component of the earth motion was the most significant in damage analysis, since structures are least strong in the horizontal direction. The Dugway explosion tests gave rise to longer periods in earth than was the case in the nuclear test. This fact, in the light of the analysis above, would make the earth displacement data of the underground nuclear test more significant from a damage standpoint than it was at Dugway. However, on the nuclear test the largest acceleration was almost always caused by the air-blast slap passing over the gage. This slap acceleration has such a short period that the structure deformation would be governed by the resulting earth displacement. Since the earth displacement is roughly proportional to the product of peak acceleration and the period squared, it is evident that this direct air-blast effect contributes little to structure damage, because of the short period of the air-blast slap.

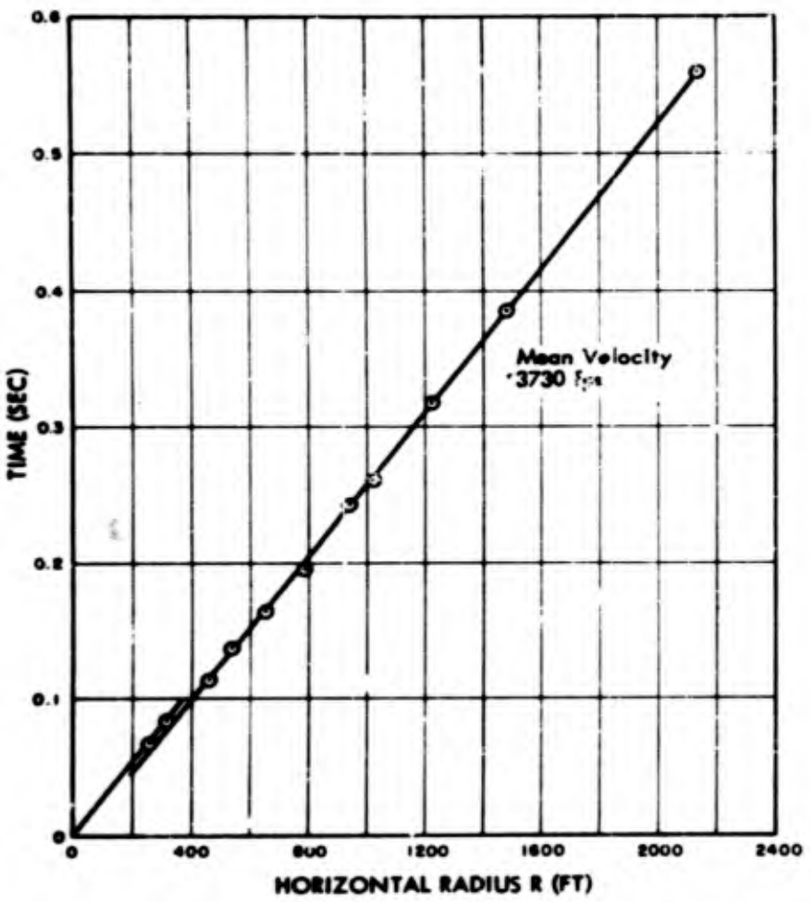

Fig. 5.25 Horizontal Earth Acceleration, Time of First Arrival vs. Horizontal Radius for the Underground Test

Since the horizontal particle velocity is of interest from a damage standpoint, it was decided that the horizontal acceleration records from the nuclear test should be integrated, if only roughly. Some of these integration curves are presented in Figure 4.7, where the label AB designates the arrival time of the air-blast pressure at the gage station. Figure 4.13 illustrates the data that were taken from these integration curves. In Figure 5.26 are shown plots of the average amplitude of the maximum velocity wave and the period associated with this wave. With the exception of two points, the amplitude data follow the same decay with horizontal radius as that for air pressure. The period which characterizes the maximum velocity wave is reasonably constant at 0.33 second for measurements out to about [illegible] feet. For larger distances the period increases abruptly.

Because the horizontal velocity data from the HE-1 and HE-2 tests[1] did not follow the model law, it was not possible to make predictions for this quantity for the nuclear test. However, it proves interesting to consider the characteristic periods of the velocity phenomenon in more detail. Figure 5.27 shows this period (mean) plotted on semi-log paper where the abscissa is the scale of the explosive charge. The HE-2 test is used as a reference with its scale equal to unity and the underground nuclear charge is assumed to be equivalent to 1.0 KT. The mean deviations of the velocity period are indicated for each plotted point on this graph. When the straight line drawn through the points is extrapolated to the scale factor 10 (corresponding to a 20 KT operational weapon), the period corresponds to a value between 0.4 and 0.5 second. This period is in the range of the natural period of many surface structures; therefore this analysis appears to lead to a significant result. That is, in the type of medium encountered at the Nevada Test Site, the horizontal particle velocity is the measured quantity which best determines structural damage.

When the results obtained at the Nevada site are compared with those from the Dugway dry clay tests, some significant differences are observed. Figure 5.28 shows representative horizontal acceleration records from the Dugway Round 315 test, the HE-2 test at Nevada, and the underground nuclear test, also at Nevada. The Round 315 and the HE-2 test charges both used 40,000 pounds of TNT; however, the Dugway charge was buried deeper than the HE-2 charge, while the HE-2 charge was at about the same scaled depth, λ_0, as the underground nuclear test. The Project 1(9)-1 report shows that the effect of this change in λ_0 (0.5 to 0.150) upon the periods of the low-frequency earth acceleration is small. This means that differences in durations of acceleration between Dugway Round 315 and HE-2 are due mainly to the different soil characteristics at the two sites.

Reference to Figure 5.28 shows that the first pulse duration at

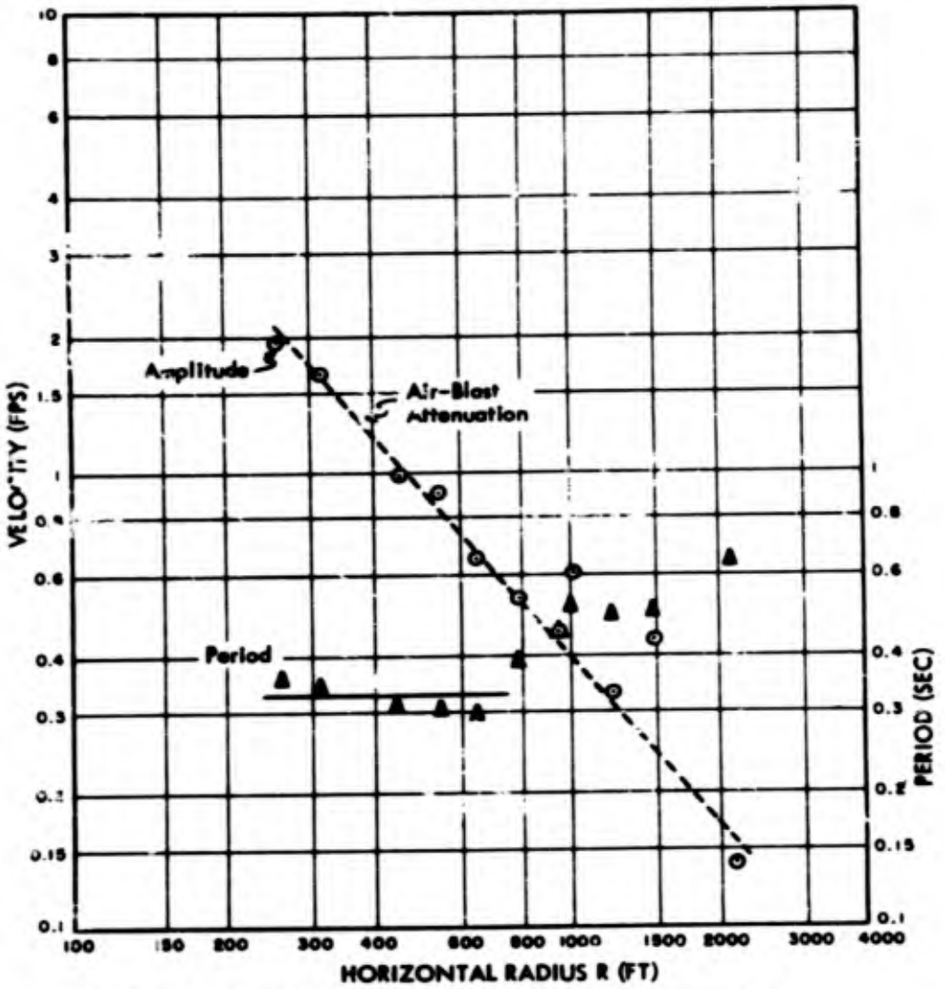

Fig. 5.26 Horizontal Earth Velocity, Maximum Peak-to-Peak Amplitude (Average) and Period vs. Horizontal Radius for the Underground Test. Dotted line indicates air blast attenuation. Gage depth, 5 feet

Fig. 5.27 Horizontal Earth Velocity, Period of Maximum Velocity Wave vs. Scale of Charge for HE-1, HE-2, and the Underground Tests (Scale of HE-2 taken as unity). Charge depth, 5 feet

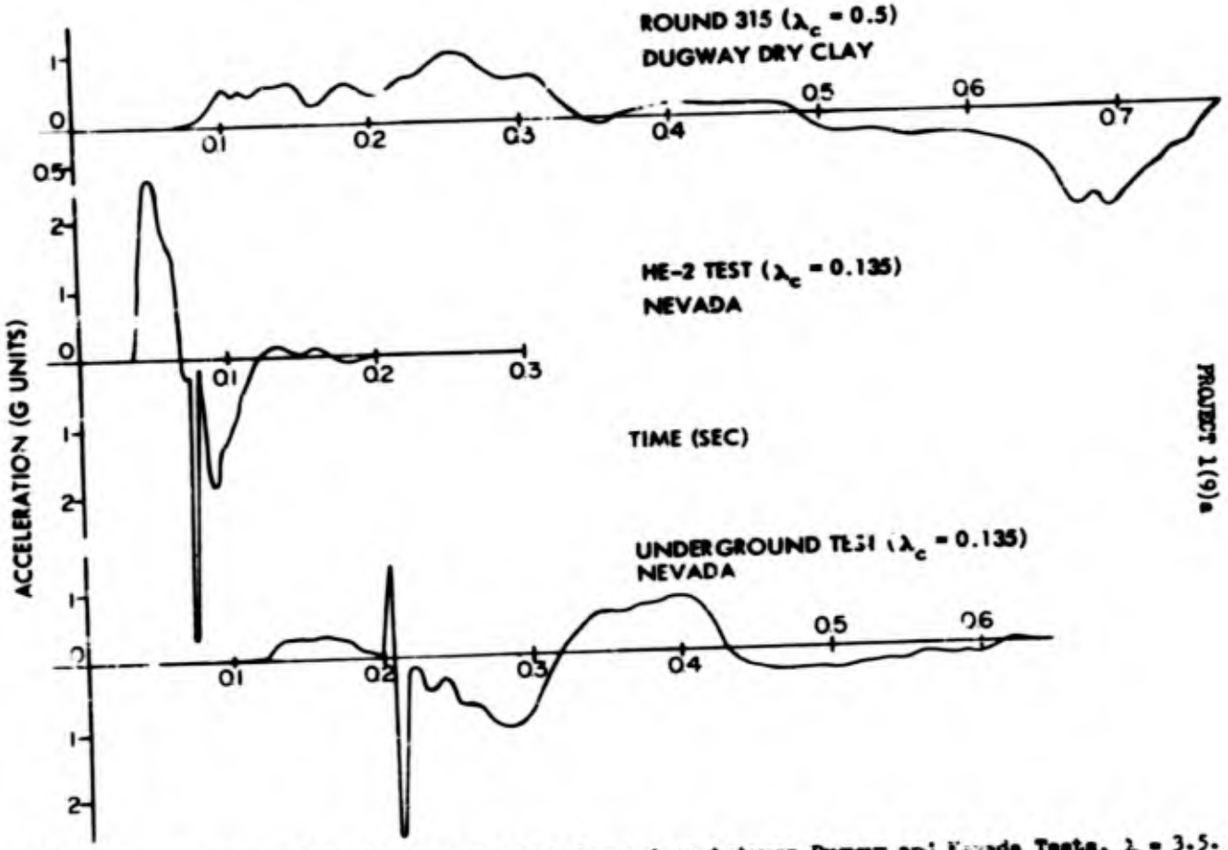

Fig. 5.28 Horizontal Earth Acceleration, Comparison between Dugway and Nevada Tests, λ = 3.5. Cage depth, 5 feet

Dugway is almost ten times longer than that at Nevada (HE-2). As would be expected on the basis of charge size, the durations corresponding to the nuclear test are longer than those observed on the HE-2 test, even though the $W^{1/3}$ time scaling law was not satisfied. However, the nuclear test durations are still shorter than those measured in the Dugway dry clay. When these acceleration records are integrated to obtain particle velocity and displacement, these differences in durations become very significant.

The Project 1(9)-1 report[1] includes detailed comparisons between Dugway and the scaled HE tests. The general conclusions are that the first pulse velocities are approximately the same at the two sites, which means that the displacements depend directly on the durations of the velocity pulse. It was found[1] that the permanent displacements (for identical tests) were ten to fifty times larger in Dugway dry clay than in Nevada desert soil (HE tests).

Although the permanent displacement data for the underground nuclear test are not yet available, the acceleration record comparisons in Figure 5.28 indicate that the displacements for the nuclear shot were less than those measured at Dugway for a considerably smaller charge (1.0 scale was 0.16 KT of TNT on Round 318). This would indicate that at equal distances from ground zero the damage to surface structures due to earth motion would have been less for the Nevada underground nuclear test than it was for the much smaller Dugway Round 318. Of course, to make statements concerning final damage, factors such as throwout and air-blast pressure would have to be considered.

The reader is reminded that the soil type may have a very marked effect on the ground motions produced by an underground explosion.[3,10, 11,12] The soil type can change the time scale of the phenomena by large amounts, yielding damage differences which would not be apparent from a casual study of peak accelerations produced. It appears safe to conclude that the 1.0 KT underground explosion would have had far greater damage effects on structures if it had been fired at the Dugway dry clay site. It is not safe to judge the effects of underground nuclear explosions by the results of the single test reported here, since there is insufficient information to estimate the effect of terrain on the characteristics of the various output phenomena which cause the principal damage to structures.

These are conclusions drawn from a rough and incomplete analysis of the earth motion data taken for Project 1(9)a. More precise integrations of the earth acceleration records are planned for the future in order to obtain accurate velocity and displacement data at all gage stations. With these data, it should be possible to make a more detailed analysis of damage to surface structures.

5.6 EARTH PRESSURE

The transient records from the 10-foot earth pressure gages are presented in Figure 4.10 in Chapter 4. All of these records exhibit the same general characteristics, a small first positive pulse followed by a relatively large second positive pulse. In every case, the large pulse seems to occur shortly after the arrival of the air-blast pressure at the gage location (designated by AB on the records). This would indicate that the large pulse is caused by the air-blast pressure. However, this pulse does not appear to decay appreciably with increasing horizontal radii out to 800 feet.

A plot of the first (small) pulse amplitude and duration is shown in Figure 5.29. The curve drawn through the points has the same decay as the air-blast pressure, that is, the slope is 1.25. However, it is not believed that this first earth pressure pulse is caused by the air blast. The points corresponding to pulse duration are scattered so much that no sensible curve could be drawn. No predictions were made for the earth pressure in the Project 1(9)-1 report, because the phenomenon was quite erratic and did not obey the model laws for the HE tests.

Transient records from the deeper earth pressure gages are shown in Figures 4.11 and 4.12, where the first figure gives results obtained at the closest station to ground zero. For this close station, the effect of depth upon the general wave form was slight. As the depth of measurement was increased, the amplitudes also increased. It is noted that the maximum positive pressure recorded at the 34-foot deep gage was about twice the same pressure measured at the 10-foot gage. The records at the 375-foot station show slightly different depth effects. The wave form shows a tendency to change for the 34-foot depth and then a marked difference is observed in the form of the pressure wave at 64 feet. At the 64-foot depth, there appears to be a build-up of pressure after the more shallow pressures have almost disappeared. Unlike the observations at the closer-in station, these pressure measurements show no marked build-up of amplitude with increasing depth.

As has been stated in previous reports,[1,5] the significance and operational techniques concerning earth pressure measurements are rather vague. For this reason, no attempt is made in this report to use the earth pressure data for predicting damage to underground structures.

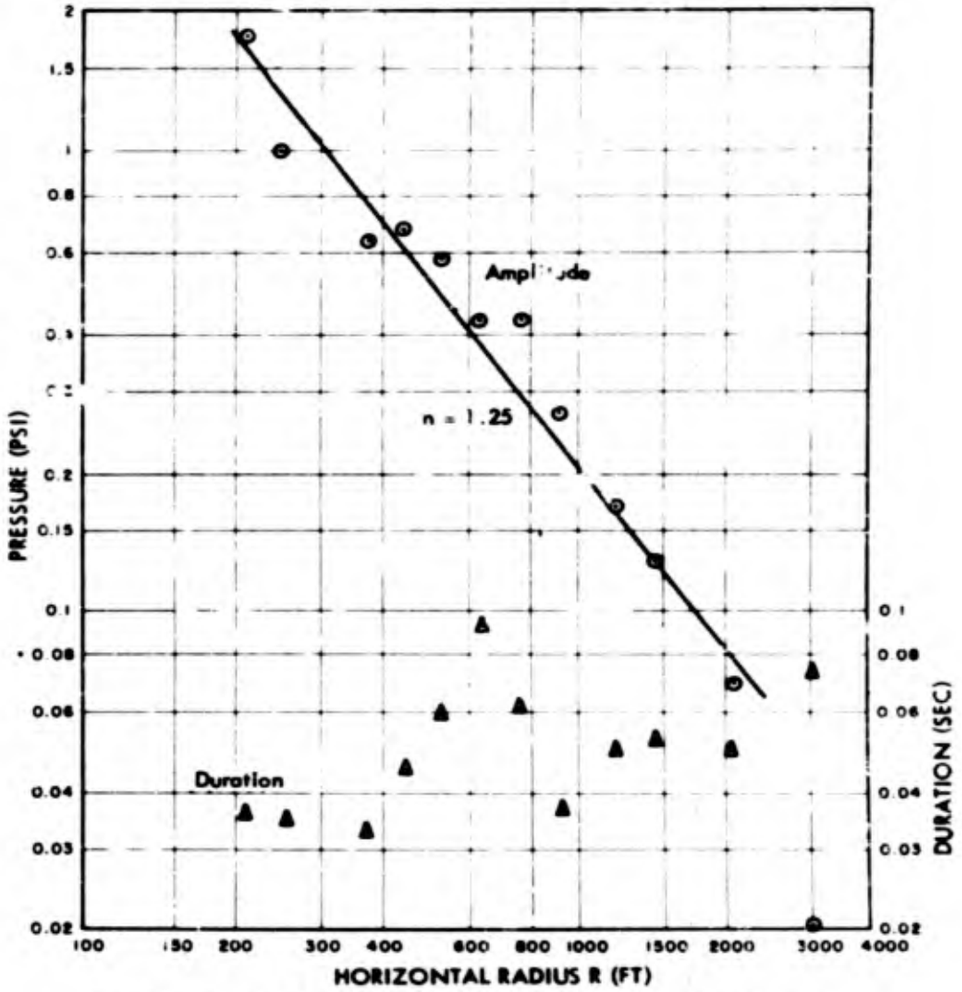

Fig. 5.29 Earth Pressure, First Pulse Amplitude and Duration vs. Horizontal Radius for the Underground Test. Gage depth 10 feet

CHAPTER 6

CONCLUSIONS AND RECOMMENDATIONS

6.1 AIR PRESSURE

Considered as a function of both distance and time, the air pressure phenomenon followed the conventional model laws quite closely on the scaled HE-1 and HE-2 tests. The air pressure vs. time measurements for the underground nuclear test could be scaled in a consistent manner to those of HE-2. As a consequence, it is possible to draw the following conclusions concerning air blast with reasonable certainty.

1. The air pressure from the underground nuclear test was equivalent to that from 0.85 KT of TNT at the same burial depth at the JANGLE test site. Thus the equivalent TNT yield (for air pressure) was 70 per cent of the radiochemical yield (1.2 KT).

2. Scaling to a 23 KT weapon at a depth of 46 feet appears justified. At sea level a peak overpressure of 10 psi should occur at a distance of about 2100 feet, with a positive phase duration of about 0.6 second. At sea level the peak pressure vs. distance should follow the relation:

$$p = \frac{150{,}000}{d^{1.35}} \qquad (6.1)$$

where the units are psi and feet

3. It is expected that air blast will be affected by the type of soil, but the influence of soil type should decrease as the scaled depth of burial decreases.

Two recommendations are made.

1. In future underground tests, both HE and nuclear, the air blast phenomenon should be measured. This is particularly true for shallow scaled depths of burial, where air blast can be a major cause of damage to surface targets.

2. More information is needed on the effects of soil type and depth of burial. Because of excellent scaling with HE, relatively small charges may be used in scaled experiments.

6.2 EARTH ACCELERATION

Earth acceleration as a complete phenomenon exhibited many departures from the conventional model laws. This could be attributed to several possible causes: (a) departure from conventional model laws due to gravity effects, requiring a different but analytically consistent set of model laws; (b) the inability to conduct truly scaled experiments in a uniform test medium or in a test medium where the variations are scaled; (c) the effects of air-pressure induced phenomena, involving different scaling factors; (d) other unknown causes. As a consequence, relatively few scaling conclusions are presented in this report.

1. The earth acceleration measurements are a combination of direct and air-pressure induced effects. The air pressure produces a local effect by its action on the ground surface directly above the gage location. There is an additional distributed air-coupled effect due to the earth transmission of the effects of the air pressure acting on the ground surface at distances remote from the gage location. The direct effects are defined as those similar to what would be produced if the charge were buried so deeply that no significant air blast would be produced. The first of these three effects can be readily separated from the acceleration gage records for large charges. No suitable technique has been developed for differentiating between the latter two effects.

2. The local air-pressure induced acceleration (slap) appears as a damped wave train of relatively high frequency as compared to the other frequency components of the earth acceleration. This frequency should become a function only of the soil type and the gage depth for explosive yields large enough so that the positive phase duration for air pressure is long compared to the natural period of vertically compressed earth.

3. For large charges the slap acceleration will produce the maximum peak amplitudes, and these peaks will become more dominant in the earth acceleration records as the charge size is increased, except for very great gage depths. The slap is more evident and consistent in the vertical component of earth acceleration. For large charges the peak vertical slap amplitude is determined by the peak air pressure above the gage location. The ratio was 0.25 for the underground nuclear test and 0.3 for HE-1 and HE-2, in G units per psi for a gage depth of five feet.

4. The slap acceleration is attenuated with depth. The vertical component at a depth of five feet is about ten times greater than at a depth of 68 feet.

5. No technique has been developed for separating the direct earth effects from the distributed air-pressure induced effects, since they seem to have somewhat similar wave forms. A simple examination of the conventional model laws demonstrates that the relative importance of the two could be a function of the charge size for scaled experiments, with the air-pressure effects becoming more significant for large charges. This may explain, in part, the apparent departure of the earth acceleration phenomena from the accepted model laws.

Since there are pronounced differences between the nuclear test earth acceleration wave forms and those recorded for the scaled HE experiments, it is difficult to obtain consistent tabular data for direct scale comparisons. It would be improper to attempt scale comparisons between the HE tests and the underground nuclear test by the comparison of non-corresponding parts of the acceleration records. As a consequence, particular attention has been paid to the first acceleration pulse, which may give the most representative indication of the direct earth effects. Because of possible importance with respect to military effects, some attention has been paid to the maximum earth acceleration defined as the maximum peak-to-peak difference between successive pulses, along with the duration of the corresponding complete cycle, after the slap acceleration has been separated.

The following conclusions concern the earth acceleration after the local air-pressure induced effect (slap) has been separated.

6. In general the amplitude of the first peak of earth acceleration showed no consistent scale relationship to the scaled HE-1 and HE-2 tests. Whereas for the HE tests the first pulse was generally the maximum pulse, for the underground nuclear test following acceleration pulses were frequently considerably greater than the first pulse.

7. The maximum peak-to-peak horizontal earth acceleration for distances greater than 500 feet followed the approximate relation:

$$pp^{A}_{H} = \frac{63,000}{R^{1.7}} \qquad (6.2)$$

for R in feet and A_H in G units (peak-to-peak). Two stations closer to the charge (310 and 260 feet) gave values approximately the same as for 500 feet. Direct application of the conventional model laws[9] yields a similar expression of

$$pp^{A}_{H} = \frac{130,000}{R^{1.7}} \qquad (6.3)$$

for a 23 KT weapon at a scaled depth of 46 feet at the JANGLE site, since the scaling between HE-1 and HE-2 for this parameter was fairly good.

8. The mean period of the cycle of maximum horizontal acceleration was about 0.5 second. Direct upward scaling ($W^{1/3}$) to a 23 KT weapon would give a mean period of 0.86 second. However, a $W^{1/4}$ time scale relationship would give a mean period of 0.63 second, which may be the more dependable estimate. The limited experimental data indicate an empirical $W^{1/4}$ time scaling factor, although a consistent use of this factor would require different model laws for the other aspects of the phenomena, for which no theoretical or experimental foundation has yet been established.

9. The maximum peak-to-peak vertical acceleration followed the approximate relation:

$$pp^{A}_{V} = \frac{1800}{R^{1.25}} \qquad (6.4)$$

It was considerably less than the horizontal component except at large distances, where the military effects would be unimportant. It is to be noted that this attenuation law is the same as that for peak air pressure, indicating that air-blast induced effects may be of principal importance even after the local slap is separated. No estimate is made for a 23 KT weapon, since the scaling for this parameter between HE-1 and HE-2 was not good.

10. At the one radius of measurement (1025 feet) the earth acceleration (less slap) was reasonably constant in both amplitude and wave form to a depth of 68 feet. At very small distances from the charge a depth effect could be expected, due to simple geometry considerations. On the HE-2 test little variation in depth was experienced where the 68-foot deep gage string subtended an angle of eight degrees at the charge center, corresponding to a radius of about 400 feet for the underground nuclear test.

11. The amplitude of the first pulse of vertical earth acceleration exhibited a step or shelf in the distance attenuation curve at a distance of about 450 feet. This result was observed in the [illegible] test series and is consistent with calculations based on the presence of a subsurface layer of higher seismic velocity at the JANGLE site.

12. Inconsistent scale factors were obtained for various aspects of the earth acceleration phenomenon when comparisons were made to the results of the HE-2 test. Consequently, no reliable estimate can be made of the equivalent TNT yield for earth acceleration for the underground nuclear test. There is some evidence that the equivalent TNT yield was considerably less than 1 KT. The equivalent TNT yield for earth acceleration would not necessarily be the same as that for air pressure, since the energy partition between the air and earth effects for an underground nuclear explosion could be different from that for TNT.

13. Upon comparing the scaled HE tests and the underground nuclear test with the Dugway dry clay tests,[2,3,4] it is evident that the soil type had a profound effect on earth acceleration. The JANGLE acceleration periods (durations) were far less than those obtained at Dugway for identical tests. The pronounced variation of the time scale of earth acceleration with soil type indicates that earth motion damage criteria could be affected much more by soil type than a study of peak acceleration amplitudes would indicate. For the JANGLE site the permanent and transient earth displacements were much less than those for identical tests in Dugway dry clay. No quantitative explanation of this effect of soil type has been attempted for this report. It is likely that a simple propagation type soil constant is inadequate to explain the significant differences between soil types with respect to earth shock phenomena. Perhaps such factors as cohesiveness, plastic flow, and dynamic stress-strain relations are of major importance in determining the earth effects of underground explosions.

The work of Project 1(9)a was not completed at the time this report was prepared. Further analysis is planned prior to the preparation of the final contract report.[8] This analysis will include a more complete study of the earth acceleration phenomena, with particular attention given to the complete records obtained and to their first and second integrals, yielding transient earth particle velocity and displacement information. At the time this report was prepared the surveyed permanent displacement data were not available to assist in these integrations.

It is apparent that more information is needed concerning model law behavior for large shallow underground explosions, with consideration given to possible model law variations, both empirical and analytical. Extensive additional studies are required on the influence of soil types and test medium variations on the underground effects of shallow underground explosions. The additional analysis planned includes correlation of the results of the JANGLE experiments with those from other extensive underground explosion test programs,[9,10,11,12] where

possible. The material contained in References 10, 11, and 12 was not available at the time this report was prepared. Insufficient information has been made available to include any symmetry effect studies in this report.

Until the further studies outlined above have been completed, only the following recommendations are made with regard to earth acceleration on future large shallow underground explosion tests.

1. Extensive measurements should be made at depths corresponding to those for underground targets of military interest. Such depths would probably markedly reduce the local air-pressure induced effects (slap) and present the distributed air-coupled effects in their proper proportion for military usefulness.

2. More attention should be given to "close-in" measurements where earth motion is of real importance in producing damage to underground and surface targets. In particular, measurements should extend to the edge of the true crater, and a sufficient number of instrument points should be included in the region of military interest so that the interpretation is not influenced by the results at larger distances having no apparent damaging usefulness.

6.3 EARTH PRESSURE

There exists a real uncertainty in the relation between the true earth pressure and the quantity measured as earth pressure by the experimental techniques used for this project. No systematic pattern was obtained when comparisons were attempted with the measurements obtained on the scaled HE test series. The few conclusions presented apply to the records obtained for the quantity measured as earth pressure, with no interpretation as to the significance of this quantity with respect to military usefulness.

1. The earth pressure measurements include a mixture of direct effects and air-pressure induced effects, as described for earth acceleration. The largest recorded earth pressures appear to be the result of the action of the air pressure on the ground immediately above the gage locations or on the liquid columns in which the hydrostatic pressure gages were immersed. Although these principal peaks do not bear a consistent amplitude relationship to the corresponding peak air pressures, the time of their occurrence correlates with the air blast phenomena.

2. Certain portions of the earth pressure records appear unrelated to the local air-induced effects in that they have the same

propagation velocity as the direct earth acceleration, this velocity being nearly equal to the known seismic velocity. These direct earth-pressure effects were very small and were probably insignificant and unimportant with respect to military damage. If significant direct earth-pressure effects existed, they were masked by the action of the air-blast phenomena.

3. The effect of depth on the quantity measured as earth pressure was a function of the horizontal distance from the charge. At a small radius (217 feet) the peak earth pressures increased markedly with depth (to 34 feet), although the general wave forms changed only slightly. However, at a larger radius (378 feet) a change in wave form occurred between the 34- and 68-foot depths, with no marked increase in pressure below 17 feet. Although no deep acceleration measurements were obtained at these two radii, a comparison with the HE-2 results indicates completely different behavior of the earth acceleration. No explanation is advanced for this discrepancy, although it is expected to lie, in part at least, in the uncertainties of the instrumental techniques used for earth pressure measurement.

Additional studies are planned prior to the preparation of the final contract report.[8] It is evident that attention must be given to the extensive measurements obtained at the Dugway explosion tests in soils.[10,11,12] Only after such extended study can specific recommendations be made. However, it does appear that particular emphasis should be placed upon the development of techniques for the measurement of the phenomena known as earth pressure, which will permit direct correlation with the damage inflicted on representative underground targets. Attention should be given to the directional properties of pressure in a medium capable of supporting shear stresses. Such work is strongly recommended in advance of any future large scale underground explosion tests, to permit a better understanding of the test results that might be obtained. It is likely that analytical support will aid in the interpretation of existing experimental data and in the development and design of future experimental techniques.

For future large underground explosion tests the recommendations for deep measurements and extensive close-in measurements made for earth acceleration are also made for earth pressure.

6.4 DAMAGE CRITERIA - SURFACE STRUCTURES

1. For large shallow underground explosions at the JANGLE type site, it is believed that air blast will be the major factor in determining damage to conventional surface structures. For greater

burial depths and/or for nuclear explosions in different soil types, it is possible that both earth motion and throwout could be major contributors to the damage of structures of this type. Of course, if air blast damage alone is desired, the underground detonation is far from optimum.

2. Depending upon the size of the explosion, the soil type, and the target type, either earth acceleration, particle velocity, or displacement can be the principal criterion for judging the damaging effect of earth motion on surface targets. For a 23 KT weapon at a depth of 46 feet at the JANGLE site, it is estimated that the earth particle velocity will be the most dependable criterion of damage to conventional surface structures, since its estimated period of 0.5 second is within the region of the natural periods of two- to four-story structures.

3. For large nuclear charges in more cohesive soils, such as at the Dugway dry clay site, earth acceleration would probably be the best single earth motion parameter for judging surface structure damage, exclusive of air blast.

4. Since the time characteristics of the driving forces can be of dominant importance in determining the marginal damage limits for certain types of structures, it is of extreme importance to have a better understanding of the wave forms of the earth motion phenomena produced by underground explosions. Methods for predicting the peak values alone of acceleration, velocity, and displacement for different charge sizes in different soil types are insufficient, and a means is necessary for estimating the time scale of the complete earth motion phenomena.

5. It is conceivable that a more complex subsurface stratigraphy could produce significant earth motion damage to surface structures at larger distances than would be predicted for an essentially uniform test medium. Subsurface reflection and refraction of energy back toward the surface could give reinforcement under certain conditions to produce this effect.

6. Because of the potential importance of transient earth particle velocity and transient earth displacement in establishing damage criteria, it is recommended that efforts be directed toward the direct measurements of these quantities on future tests, if such direct measurements can give more reliable information than would be available from the single and double integration of accelerometer records.

6.5 DAMAGE CRITERIA - UNDERGROUND TARGETS

In this report the underground nuclear test results have not been evaluated with respect to damage criteria for underground or buried targets. The factors governing damage to underground targets are not clearly understood by the authors, and the results of previous extensive underground explosion tests[9,10,11,12] must be evaluated before major conclusions or recommendations can be made. Pending such an evaluation, the following tentative conclusions and recommendations are presented.

1. It is likely that the strong local air-induced phenomena are of negligible importance in damaging buried targets, due to their short periods and their apparent attenuation with depth.

2. Earth motion can be a contributing factor to the damage of underground targets. The target characteristics, plus the time scale of the earth motion, will determine the relative importance of acceleration, velocity, and displacement as damage criteria. For a 23 KT weapon the principal earth motion wave lengths should be long compared to the dimensions of many representative buried targets, and damage could be estimated by considering the response of the target and its contents when the target moves as a whole with the surrounding earth. However, the interval of differential movements when the earth-motion wave is passing over the target is far more complex and could be of major importance.

3. If a buried target can be considered as a rigid body, compared to the surrounding earth, it is possible that the flow of earth material around the target could be of major significance in determining damage. In addition to the normal pressure forces developed, friction forces due to the slippage of earth along target surfaces could be important.

4. It is likely that earth pressure is of major significance in determining damage to buried targets. Crushing and fracturing of external walls of such targets could be the result of pressure forces transmitted by the earth.

5. As noted above, under Earth Pressure, more information is required in order to permit the measurement of "free earth" phenomena which can be directly translated into damaging effects on buried targets. Particular attention should be given to this problem in advance of any future large underground explosion tests, after the results of previous tests[9,10,11,12] have been evaluated in connection with the JANGLE underground nuclear test.

6. It is likely that the region of major importance for damage to underground targets is confined to the region of important rupture and permanent displacement in the earth medium surrounding the underground explosion. As a consequence, the region of important damage should be located relatively close to the crater boundaries.

PROJECT 1(9)a

APPENDIX A

PERSONNEL

Project 1(9)a of Operation JANGLE was performed by Stanford Research Institute under Contract No. N7onr-32104 with the office of Naval Research, Washington. Mr. J. W. Smith and Mr. J. Kane served as Project Officers for ONR.

All Stanford Research activities on Project 1(9)a were under the direction of Dr. E. B. Doll. Dr. Doll supervised the initial planning for the test program and directed the field activities, with Mr. L. M. Swift serving as field party chief. Additional members of the field party were L. H. Inman, W. E. Krakow, C. C. Hughes, S. C. Ashton, and W. N. Stewart. This report was prepared by Dr. Doll and Dr. V. Salmon, with typing and drafting assistance from Miss Blanche Shoemake and Mrs. Jane Simons, respectively.

LCDR D. C. Campbell USN of Program One coordinated the activities of this project with the remainder of Operation JANGLE.

PROJECT 1(9)a

BIBLIOGRAPHY

1. Stanford Research Institute, "Scaled HE Tests - Operation JANGLE," April 1952. Prepared for the Office of the Chief of Engineers, Department of the Army, Contract DA-49-129-eng-119. SECRET.

2. Office, Chief of Engineers, Protective Construction Branch, Engineering Division, "Underground Explosion Tests; Program 'A' Tests in Soils" Revised November 1950. RESTRICTED.

3. Stanford Research Institute, "Underground Explosion Tests at Dugway," Interim Report, July 1951. Prepared for Sacramento District Office, Corps of Engineers, U. S. Army, Contract DA-04-167-eng-379. CONFIDENTIAL.

4. Stanford Research Institute, "Underground Explosion Tests at Dugway, Surface Structure Program," Final Report, March 1952. Prepared for Sacramento District Office, Corps of Engineers, U.S. Army, Contract DA-04-167-eng-379. CONFIDENTIAL.

5. Stanford Research Institute, "HE Tests - Operation JANGLE," Interim Report, October 1951. Prepared for the Office of the Chief of Engineers, Department of the Army, Contract DA-49-129-eng-119. CONFIDENTIAL.

6. Stanford Research Institute, "HE Tests - Operation JANGLE," Interim Report, Part II, October 1951. Prepared for the Office of the Chief of Engineers, Department of the Army, Contract DA-49-129-eng-119. SECRET.

7. Stanford Research Institute, "Predictions - U Test - Operation JANGLE," Technical Report No. 4, November 8, 1951. Prepared for Office of Naval Research, Contract N7onr32104. SECRET, RESTRICTED DATA.

8. Stanford Research Institute, "Project 1(9)a - Operation JANGLE," Final Report (to be prepared). Office of Naval Research, Contract N7onr32104.

9. C. W. Lampson, "Final Report on Effects of Underground Explosions," OSRD No. 6645, February 20, 1946.

10. Engineering Research Associates, Inc., "Instrumentation of Underground Explosion Test Program, Interim Technical Report No. 1, Dry Clay," 1 August 1951. CONFIDENTIAL.

PROJECT 1(9)a

11. Engineering Research Associates, Inc., "Instrumentation of Underground Explosion Test Program, Interim Technical Report No. 2, Dry Sand," 1 October 1951. CONFIDENTIAL.

12. Engineering Research Associates, Inc., "Instrumentation of Underground Explosion Test Program, Interim Technical Report No. 3, Wet Clay," 1 November 1951. CONFIDENTIAL.

OPERATION JANGLE

PROJECT 1(9)b

BASE SURGE ANALYSIS FOR NUCLEAR TESTS

by

George A. Young and Mary L. Milligan

5 JUNE 1952

U. S. NAVAL ORDNANCE LABORATORY WHITE OAK, MARYLAND

CONTENTS

ILLUSTRATIONS

TABLES

ABSTRACT

Base surge and related surface phenomena produced by underground TNT explosions at depths scaled to the JANGLE underground shot are described. Empirical formulas showing the effect of charge weight on column and jet are listed and a method of scaling base surge flow for various charge weights and depths is presented.

The cloud phenomena formed by the JANGLE surface shot are described briefly and compared with TNT results.

Measurements of the base surge, column, jet, and smoke crown produced by the JANGLE underground shot are presented. The data indicate that column size can be predicted on the basis of TNT measurements but that overall cloud heights do not scale because of the thermal energy of the fireball. Froude scaling of the JANGLE base surge data shows a slower rate of growth and smaller extent than the surges formed by scaled TNT explosions.

A method is presented for predicting the rate of growth and maximum extent of base surges formed by atomic weapons with different energies than the JANGLE one kiloton bomb, but scaled to the same depth.

INTRODUCTION

1.1 RESULTS WITH HIGH EXPLOSIVES

In the Operation JANGLE report on Project 1(9)-4, titled "Base Surge Analysis - HE Tests",[1] data were summarized on the behavior of the base surge and related surface phenomena produced by underground TNT explosions in three types of soil at Dugway, Utah in 1951 and by similar underground explosions in the Operation JANGLE HE Tests. Combining the two sets of results gave a total range of charge weight from 216 to 320,000 lb. For comparison of charges of different weights, a scaled depth, λ_c, was used:

$$\lambda_c = \frac{d}{W^{1/3}} \qquad (1.1)$$

where d = depth to center of charge, ft
W = weight of charge, lb (TNT)

The base surge radial growth curves presented for high explosives showed that dry sand is the most favorable of the three Dugway soil types for the formation of a base surge and wet clay the least favorable, with dry clay intermediate in effectiveness. The results at the Dugway dry clay site were generally similar to the HE results obtained at the Frenchman Flat and Yucca Flat sites.

1.1.1 Description of Surface Phenomena

Three TNT rounds at Nevada were fired at scaled depths similar to the JANGLE underground nuclear shot: Round HE-1, 2560 lb at $\lambda_c = 0.147$ ft/lb$^{1/3}$; Round HE-2, 40,000 lb at $\lambda_c = 0.135$ ft/lb$^{1/3}$; and Round HE-9a, 216 lb at $\lambda_c = 0.139$ ft/lb$^{1/3}$. These rounds were all fired with the top of the charge tangent to the ground surface; the differences in λ_c are due to differences in charge shape.

---

[1] G. A. Young, Base Surge Analysis - HE Tests, Operation JANGLE Project 1(9)-4, U. S. Naval Ordnance Laboratory, 20 May 1952.

At these scaled depths, the earth bulges upward at detonation and appears to explode radially into a roughly crown-shaped cloud of smoke and dust. A hollow conical column of earth, initially much smaller in diameter at the base than at the top, forms beneath the cloud and grows rapidly in height and width, becoming approximately cylindrical is shape. At about the same time, a broad jet appears at the center of the smoke crown, rising at a high velocity and expanding horizontally.

The column settles and a shallow surge cloud appears at its base, while the jet cloud continues to rise and expand. The assumption is made that the base surge is produced by the bulk subsidence of a suspension of soil particles in air, constituting the column, which falls at a rate considerably greater than the rate of fall of individual particles and flows outward along the ground. At this relatively shallow charge depth the base surge is tenuous and moves slowly. In the Nevada tests its initial formation was often obscured by radial throwout of earth clods and the lifting of a layer of surface dust by the passage of the shock wave in air.

The jet continues to rise because of its buoyancy and is gradually diluted by the surrounding air until it becomes an irregular diffuse cloud. Probably the lower portions of the jet and smoke crown flow downward and add material to the base surge, but this contribution is relatively slight at these depths.

The rate of radial growth of the base surge gradually decreases and the surge eventually rises in the form of a circular cloud which is difficult to distinguish from the remains of the jet and smoke crown. The entire diffuse cloud mass is transported by the wind and is dispersed by atmospheric turbulence.

Relatively shallow explosions, such as these, are not favorable for the formation of a large base surge. The optimum condition was attained at a scaled depth of about 1.0 ft/lb$^{1/3}$.

1.1.2 Formulas Obtained from High Explosive Data

Empirical formulas for the maximum dimensions of portions of the surface phenomena produced in the Dugway dry clay and in the Nevada soil were obtained in the study of high explosive results. Those pertinent to the JANGLE underground test are the following:

$$D_{max} = 8.38\ W^{0.304} \quad (\lambda_c = 0.135\ \text{ft/lb}^{1/3}) \tag{1.2}$$

$$C_{max} = 5.71\ W^{0.304} \quad (\lambda_c = 0.135\ \text{ft/lb}^{1/3}) \tag{1.3}$$

$$J_{max} = 116\ W^{0.224} \quad (\lambda_c = 0.512\ \text{ft/lb}^{1/3}) \tag{1.4}$$

where D_{max} = maximum column diameter, ft
C_{max} = maximum column height, ft
J_{max} = maximum jet height, ft
W = charge weight, lb (TNT)

Maximum column diameter (D_{max}) is defined as the greatest horizontal extent of the base of the column. The measurement is made before the column loses its relatively smooth appearance and radial throw-out appears. Column height (C) is measured to the base of the smoke crown. The maximum value (C_{max}) is used for scaling, assuming that any part of the column extending into the smoke crown can be neglected. Maximum jet height (J_{max}) is defined as the limit of the buoyant rise of the jet. The jet cloud that remains may subsequently rise or fall, depending upon atmospheric conditions. Formula 1.4 may be used at scaled depths between zero and 0.6 ft/lb$^{1/3}$ with a 15% possible error.

1.1.3 Froude Scaling of Base Surge Radial Growth

The radial growth measurements of the base surges from TNT charges in dry clay at Dugway and at the Nevada Test Sites were reduced according to Froude scaling with the following parameters:

$$r = \frac{R}{D_{max}} \tag{1.5}$$

$$\tau' = \frac{t\,(C_{max})^{1/2}}{D_{max}} \tag{1.6}$$

where r = scaled surge radius (dimensionless)
R = surge radius, ft
D_{max} = maximum column diameter, ft
τ' = scaled time, sec/ft$^{1/2}$
t = time, sec
C_{max} = maximum column height, ft

When scaled in this manner, measurements of the radial growth of the base surge formed by explosions at the same scaled depth fell on the same curve. As agreement could be obtained only if complete geometrical similarity existed between the columns formed by charges of different weights fired at the same scaled depth, the ratio of the diameter of the hollow core of the earth column to the outer column diameter (D_c/D) must be the same when the values of λ_c are equal.

Column cores have not been measured directly, but by assuming that the diameter of the true crater is equal to the diameter of the jet at the ground, and that the jet fills the entire core, estimates of D_c/D were obtained at different scaled depths.

Liquid model results were available with a wide range of column height, column diameter, column density, and core diameter. The simulated base surges formed by the collapse of the liquid model column had been measured and were scaled with r, as defined herein, and a more generalized Froude scaling parameter for reducing values of time:[2]

$$\tau^* = \frac{t\,(\sigma C_{max})^{1/2}}{D_{max}} \qquad (1.7)$$

where τ^* = scaled time, $sec/ft^{1/2}$

$\sigma = \frac{\rho - \rho_o}{\rho}$ (dimensionless)

ρ = density of moving fluid

ρ_o = density of ambient fluid

Combining 1.6 and 1.7 gives the following expression:

$$\tau^* = \sigma^{1/2}\,\tau' \qquad (1.8)$$

Using the estimated values of D_c/D, the scaled growth curves for base surges produced by underground explosions were compared with scaled results for the simulated base surges formed by liquid models with the same ratio of core to outer column diameter. As the ratio of column to atmospheric density was unknown for the earth columns, τ' values were multiplied by various assumed values of $\sigma^{1/2}$ and replotted against r to obtain a series of r vs τ^* curves for direct comparison. When consistent agreement was obtained between curves from the liquid model and prototype, it was assumed that the ratio of the bulk density in the earth column to atmospheric density was the same as the ratio of column to ambient density in the liquid model.

This procedure proved to be adequate at a scaled depth of about 0.5 $ft/lb^{1/3}$ and a density ratio of 1.9 was obtained. It was therefore possible to estimate the weight of soil in the earth column which contributed to the formation of the base surge.

The method could not be used successfully for very shallow and very deep explosions. It failed for a scaled depth of 0.135 $ft/lb^{1/3}$ because the slope of the assumed r vs τ^* curves was considerably less than the slope of liquid model r vs τ^* curves with the same D_c/D ratio and similar density ratios.

Physically, this would indicate that frictional drag becomes important at an early stage, retarding the radial growth of the base surge. The relatively slow growth of the base surge and its tenuous appearance at a scaled depth of 0.135 $ft/lb^{1/3}$ indicate that the bulk density of the column and surge is low. The ratio of column to atmospheric density is almost certainly less than the ratio at a scaled depth of 0.5 $ft/lb^{1/3}$, which was estimated to be 1.9.

A second factor contributing to the slow rate of surge growth is the relatively small contribution of the jet and smoke crown to the base surge. At scaled depths of 0.5 $ft/lb^{1/3}$, and at greater depths, virtually all of the jet and smoke crown drop and flow outward into the base surge, adding considerable material and energy. At a scaled depth of 0.135 $ft/lb^{1/3}$ almost all of the smoke crown and jet remain airborne.

1.2 SOURCES OF DATA FOR NUCLEAR TESTS

Ground-level photographic records of the Operation JANGLE surface and underground nuclear shots were analyzed by the Data Reduction Unit of the Sandia Corporation, Albuquerque, New Mexico.[3] Measurements of the height of the base and top of the cloud produced by the surface shot as a function of time are reproduced herein. The following Sandia

---

[2] A. B. Arons, G. A. Young, and M. L. Milligan, Further Investigation of the Base Surge, Interim Report No. 3 of NOL Project 152, NAVORD Report 2164, 1 June 1951, pp 1-3.

[3] J. J. Miller, Photographic Analysis, Operation JANGLE Project 4.1a, Sandia Corporation, 26 March 1952.

PROJECT 1(9)b

data from the underground shot are also used in this report: overall height and diameter of the cloud vs time, and height and diameter of the base surge vs time; these measurements were limited to one camera station.

Measurements of the crosswind radial growth of the base surge from the underground shot, obtained from aerial photographs, were provided by Cpl. Alvin A. Kraus of the Radiological Division, Army Chemical Center, Md.

CHAPTER 2

SURFACE SHOT

2.1 DESCRIPTION OF SURFACE PHENOMENA

The visible surface phenomena produced by the JANGLE atomic explosion on the ground can be separated into three distinct parts: the rapidly rising fireball, a large irregular dust cloud which rose beneath it, and a vertical pillar of ascending air and soil particles, which flowed from the ground surface into the irregular dust cloud. As the expanding fireball cooled, it formed a white cloud which merged with the dust cloud to form an elongated diffuse mass. Its subsequent behavior was determined by atmospheric conditions.

Considerable surface dust was raised by the passage of the shock wave. The thermal current created by the ascending ball of fire formed the rising pillar of air and soil, which had a diameter of about 480 ft. The main cloud mass continued to rise because of its buoyancy, and attained a maximum height of about 6400 ft.

The Sandia measurements of overall cloud height and distance of the cloud base as functions of time are presented in Fig. 2.1. Smoothed curves are given, as the data points from cameras at Stations 1 and 2 show some scatter.

No downward density flow was observed and no base surge was formed.

2.2 COMPARISON WITH HIGH EXPLOSIVE TEST

One surface high explosive test record is available for comparison: Round HE-4 at Nevada,[1] a 2560 lb TNT charge fired on the ground (scaled depth, λ_g = -0.149 ft/lb$^{1/3}$). The surface phenomena were similar, except for the absence of a fireball. An irregular particulate cloud formed and rose into the air, while a narrow current of air and dust ascended beneath it, flowing from the ground surface into the base of the upper cloud. No base surge was formed.

---

[1] G. A. Young, Base Surge Analysis - HE Tests, Operation JANGLE Project 1(9)-4, U. S. Naval Ordnance Laboratory, 20 May 1952.

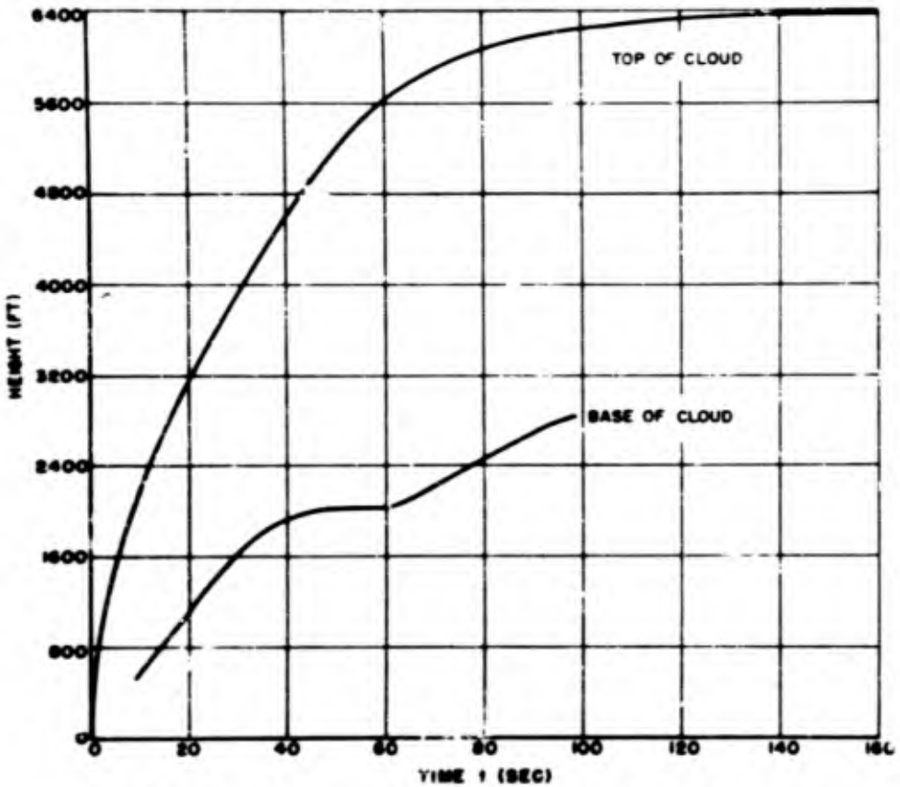

Fig. 2.1 Height of Top and Base of Cloud vs Time - Surface Shot

CHAPTER 3

UNDERGROUND SHOT

3.1 MEASUREMENT OF SURFACE PHENOMENA

In general, the surface phenomena produced by the JANGLE underground shot were similar in appearance to the surface effects from TNT explosions at the same scaled depth (λ_c), except for the emergence of the fireball after the nuclear explosion.

The smoke crown formed at the initial breakthrough was irregular and of great lateral extent, with several jet-like "arms" which grew radially for a long period.

The earth column beneath the smoke crown was similar to those formed by shallow TNT explosions, reaching a maximum diameter of 660 ft at its base prior to the appearance of radial throwout. Maximum column height, measured to the base of the smoke crown, was 420 ft.

The rounded top of a broad irregular central jet rose above the top of the expanding smoke crown at about 18 seconds. A plot of overall height vs. time is presented in Fig. 3.1, the first part of the curve representing the rising smoke crown. The jet expanded and merged with the smoke crown to form an irregular "cauliflower" cloud. Initially, the diameter of the cauliflower cloud increased at a greater rate than its height. (See Fig. 3.2.)

While the jet rose, radial throwout was observed, giving a spikey appearance to the column. The material in the column then fell, and a surge cloud appeared at the base. The initial growth of the base surge was obscured by dust trails from the radial throwout and by a layer of surface dust which rose to about 200 ft after the passage of the shock wave.

Sandia measurements of the cauliflower cloud diameter and surge diameter as functions of time are presented in Fig. 3.2. These measurements were obtained from Camera Station 2 (15,000 ft, S 20° W from ground zero). The surface wind at the time was from the south at 5 mph. As the measurements from different camera records do not coincide, mean curves are given. The Sandia measurements, however, extend only for 70 seconds and are subject to some doubt due to dust obscuration. Measurements of the crosswind radial growth of the base surge, obtained from aerial photographs at the Army Chemical Center, are reproduced in Fig. 3.3. The outline of the base surge was clearly visible from the air,

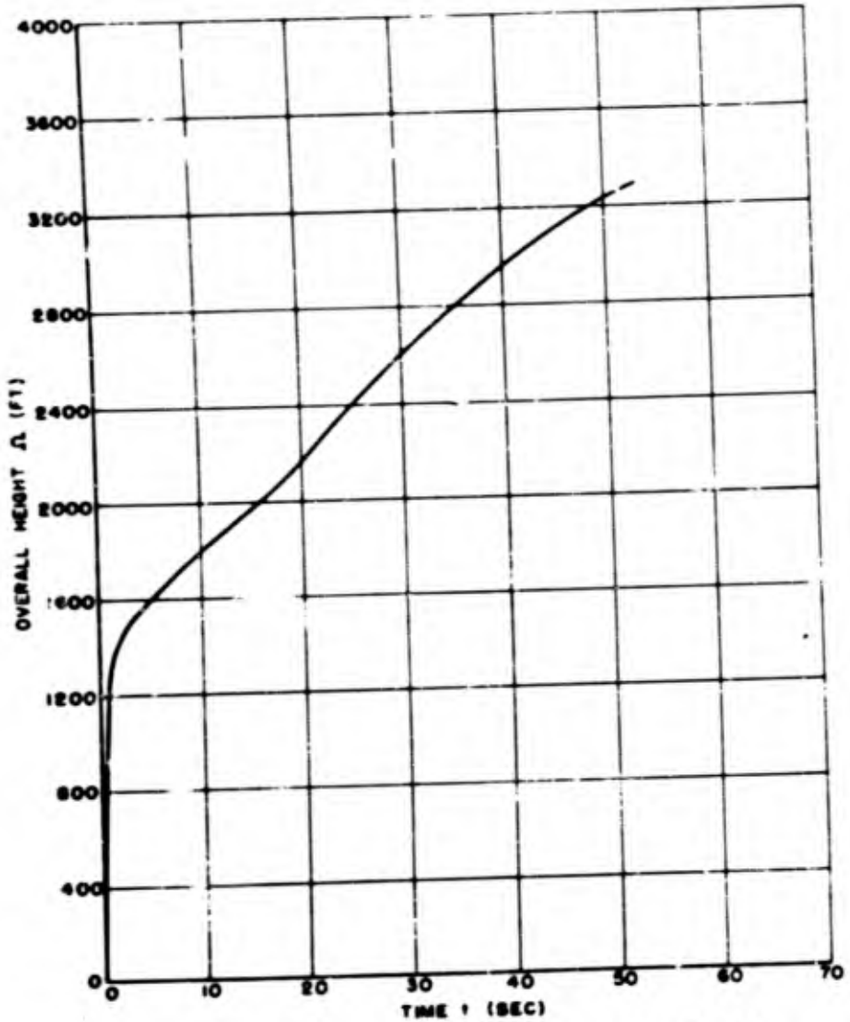

Fig. 3.1 Overall Height vs Time - Underground Shot

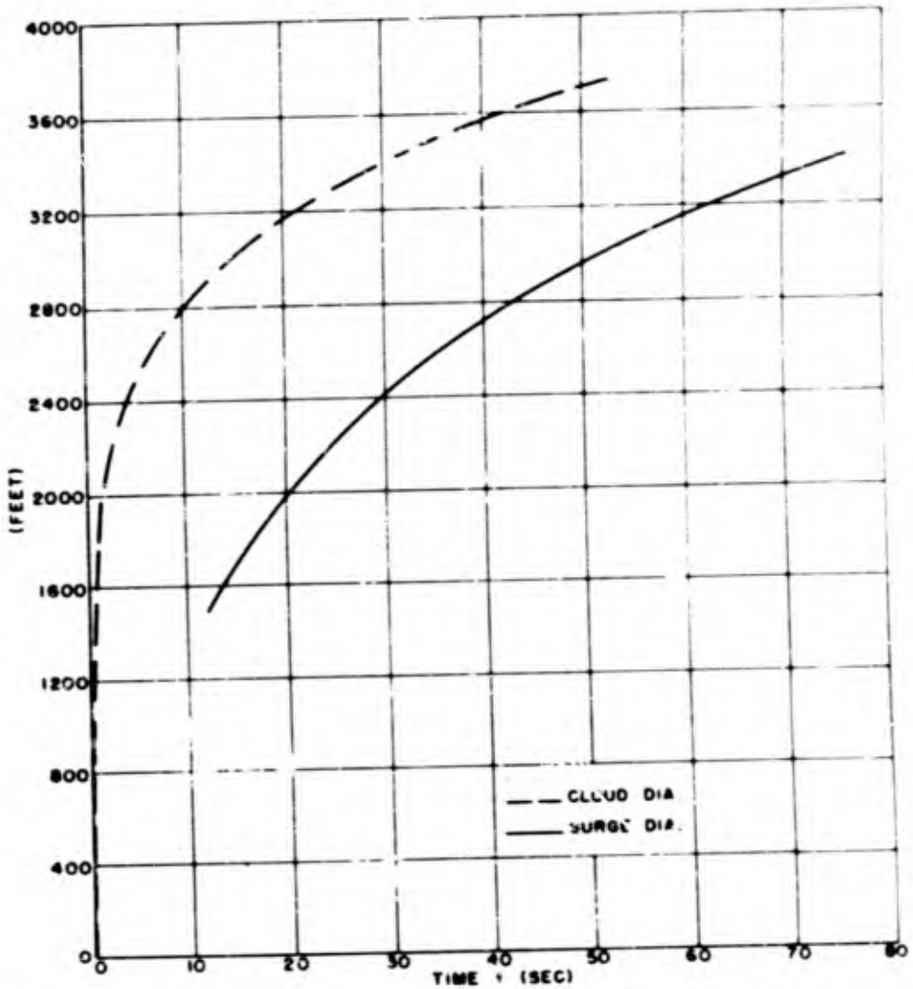

Fig. 3.2 Cloud and Base Surge Diameters vs Time from Camera Station 2 - Underground Shot

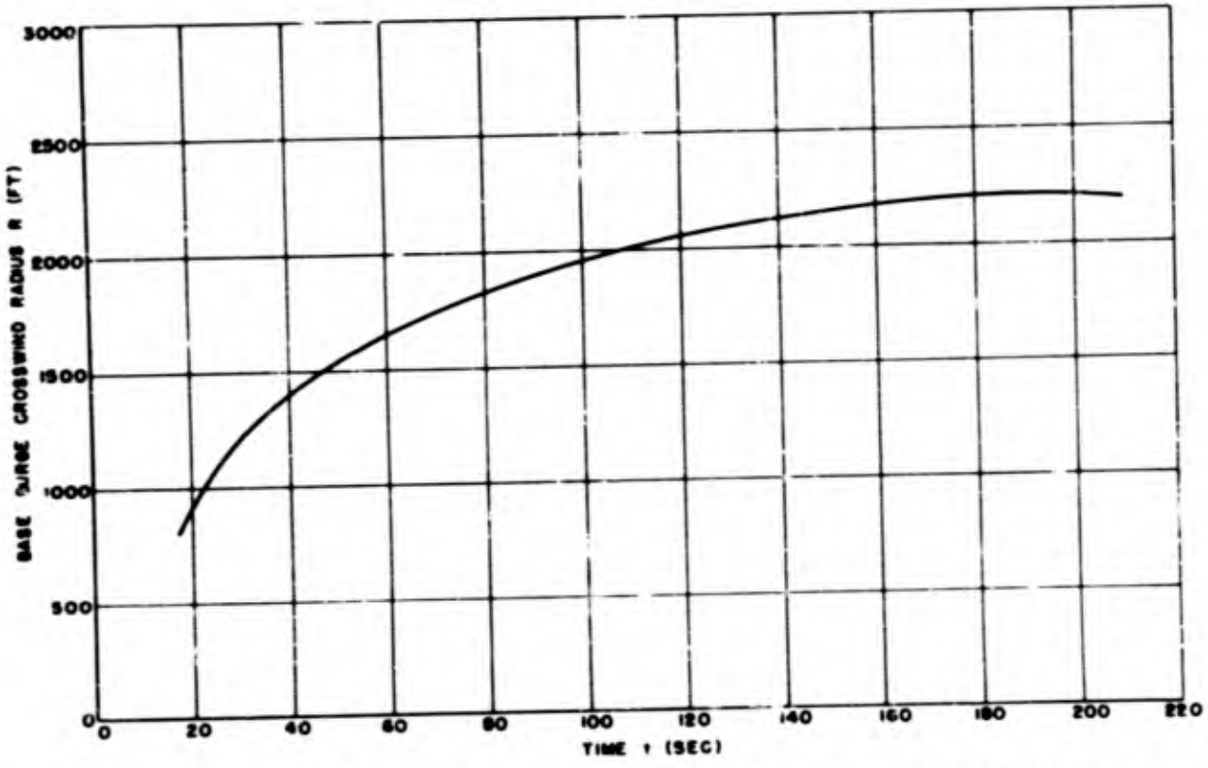

Fig. 3.3 Base Surge Crosswind Radius vs Time from Aerial Photographs - Underground Shot

and these measurements show that the base surge attained a maximum crosswind radius of about 2200 ft 3 minutes after detonation. Sandia surge height measurements from Camera Station 2 are given in Fig. 3.4.

Considerable fall-out from the cauliflower cloud into the base surge was observed. After 180 seconds, when radial growth of the surge had ceased, large quantities of material continued to fall into the surge, increasing the surge height but having little effect on surge diameter.

The upper part of the cauliflower cloud continued its buoyant rise until more than 200 seconds after zero time, reaching a height of about 5000 ft. It retained distinct outlines even after the lower part, containing the original smoke crown, became diffuse and started to settle. Surge height increased continually, due to mixing with the surrounding air. After about 10 minutes the surge and the remains of the smoke crown merged to form a roughly cylindrical diffuse cloud mass beneath the cauliflower cloud, which was rapidly distorted by the upper wind.

3.2 SCALING OF SURFACE PHENOMENA

3.2.1 Column and Jet

In order to test the applicability of the empirical formulas given in Chap. 1 to the results of underground atomic explosions, the maximum dimensions of the column and jet that would be produced by the explosion of one kiloton of TNT at a 47 ft depth in the soil at the Nevada Test Site have been computed. These estimates are compared with the NOL measurements of the JANGLE underground shot in Table 3.1.

TABLE 3.1

Computed and Observed Dimensions of Column and Jet
JANGLE Underground Shot

	Computed from TNT data (ft)	Measured at NOL (ft)	Percentage Difference (%)
Max Col. Diameter (D_{max})	690	660	4.5
Max Col. Height (C_{max})	470	420	11.9
Max Jet Height (J_{max})	2990	5000	40.2

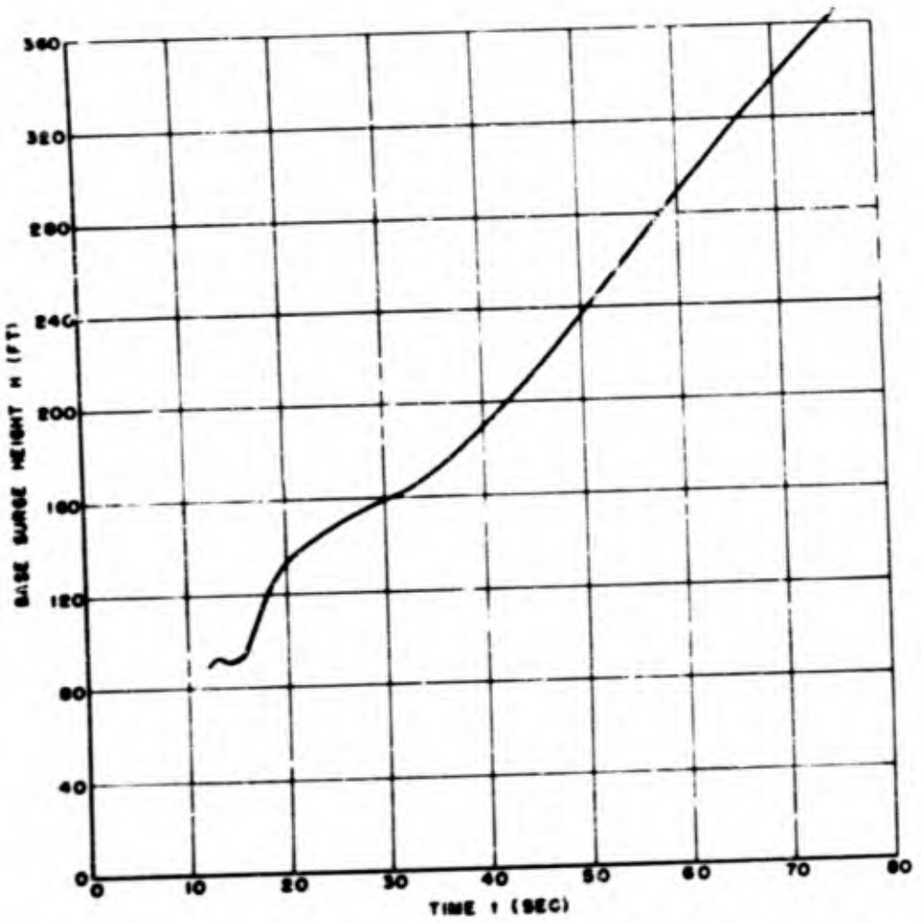

Fig. 3.4 Base Surge Height vs Time from Camera Station 2 - Underground Shot

The agreement between computed and observed values of h_{max} is good. As the scatter in measurements of column height is generally greater than in measurements of column diameter,[1] the agreement between the computed and observed values of h_{max} can also be considered reasonably good. The greater observed jet height is due to the high temperature attained in the atomic explosion, and the consequent greater buoyancy of the jet.

In the study of HE results, the assumption was made that the rising and expanding jet pushes the earth column outward into the form of a hollow, approximately vertical cylinder and that the true crater diameter is equal to the jet diameter within the column. On this basis an average ratio of core to outer column diameter (D_c/D) of 0.46 was obtained for high explosive charges at a scaled depth of 0.137 ft/lb$^{1/3}$.

The diameter of the true crater formed by the JANGLE underground shot is unknown, but the apparent crater diameter at ground level was 280 ft. As the true crater would be somewhat larger, the ratio of core to outer column diameter is estimated as a value greater than 0.42.

From this it appears that the earth columns formed by underground atomic explosions are geometrically similar to the columns formed by TNT explosions with the equivalent energy at the same depths in the same type of soil. Therefore, column size can be predicted by extrapolating the results of experiments with TNT.

The jet produced by an underground atomic explosion rises higher than the jet formed by an equivalent TNT charge, due to the larger proportion of energy emitted as heat at the time of the explosion and the consequent greater buoyancy of the jet cloud. This thermal effect can not be reproduced with conventional high explosives.

3.2.2 Base Surge

The Army Chemical Center radial surge growth data, reduced according to Froude scaling parameters, is shown in Fig. 3.5, superimposed upon scaled curves for TNT charges fired in similar soil at scaled depths ranging from zero to 2.05 ft/lb$^{1/3}$. The initial part of the scaled JANGLE underground shot curve is similar to the curve for

---

[1] G. A. Young, Base Surge Analysis - HE Tests, Operation JANGLE Project 1(9)-4, U. S. Naval Ordnance Laboratory, 20 May 1952.

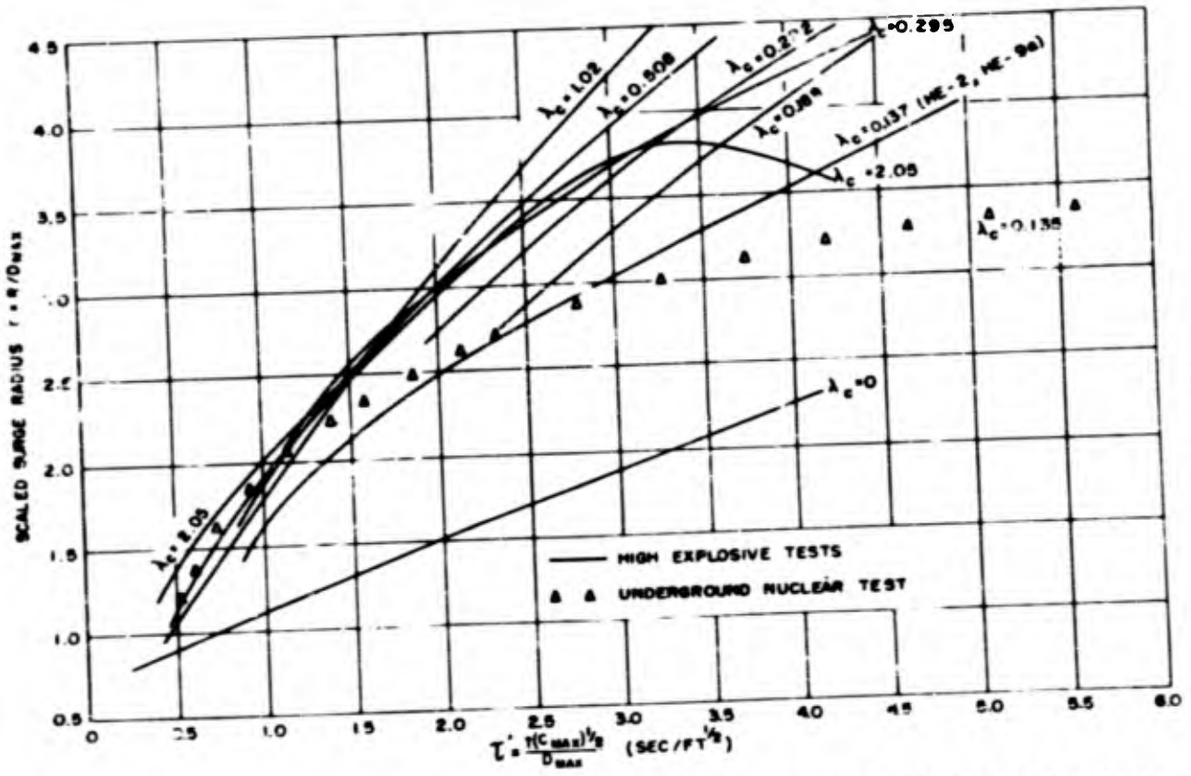

Fig. 3.5 Scaled Radial Growth of Base Surge from TNT Explosions at Different Scaled Depths

high explosives at a scaled depth of 0.508 ft/lb$^{1/3}$. However, the slope of the JANGLE curve decreases rapidly and the growth levels off at a scaled radius of ? 36.

TNT rounds at scaled depths ranging from zero to 1.02 ft/lb$^{1/3}$ did not produce base surges that behaved similarly. The surge clouds continued to grow in extent, first due to gravity flow and then as a result of eddy diffusion, until their limits could no longer be determined visually.

The initially rapid rate of radial growth of the base surge from the JANGLE underground shot indicates the possibility that the column density may be somewhat greater than the density of columns produced by TNT charges at the same scaled depth, though the column size can be scaled to TNT results. The similarity of the JANGLE curve to the HE curve for a λ_c of 0.508 ft/lb$^{1/3}$ is evidence that the ratio of the bulk density of the column to ambient density may also be about 1.9.

Making use of the observed values of column height and diameter, and assuming a cylindrical shape and a 304 ft diameter hollow core (D_c/D = 0.46), a volume of 113,000,000 cu ft is obtained for the column. The surface weather observation at the test site at 1200 PST, 29 Nov. 1951, indicates an atmospheric density of 0.0651 lb/cu ft. The bulk density of the column would therefore be 0.124 lb/cu ft. On this basis, the estimate can be made that the base surge was produced by 3310 tons of finely divided falling soil in the walls of the column. This result should be considered very approximate, because of the many assumptions that were necessary in the application of the scaling technique.

The leveling of the surge radial growth curve is partly due to the absence of any observable contribution of the jet material to the surge cloud. Because of its great heat, the jet cloud rose and expanded rapidly, remaining airborne and not falling into the surge.

3.3 PREDICTED SURGE RADIAL GROWTH FOR NUCLEAR EXPLOSIONS SCALED TO JANGLE

The success of Froude scaling for the comparison of surge flow from high explosives of different weights fired at the same scaled depth indicates that it would be reasonable to assume that atomic weapons with different energy yields, when fired at a scaled depth of 0.135 ft/lb$^{1/3}$, would produce base surges whose radial growth can be scaled with the same parameters. Data from explosions of different size, reduced in the form of r and T', should lie on the same curve if this assumption is valid. It is therefore possible to derive an expression for maximum surge radius as a function of equivalent charge

weight for nuclear explosions at a scaled depth of 0.135 ft/lb$^{1/3}$ in the Nevada soil. Combining equations 1.2 and 1.5 and using the scaled maximum radius of 3.36 shown in Fig. 3.5 gives the following result:

$$R_{max} = 28.2\ W^{0.304} \quad (\lambda_c = 0.135\ \text{ft/lb}^{1/3}) \tag{3.1}$$

where R_{max} = maximum surge radius, ft
W = charge weight, lb (TNT)

In a similar way, it is possible to combine equations 1.2, 1.3, 1.5, and 1.6, thereby deriving the following expressions:

$$R = 8.38\ r\ W^{0.304} \quad (\lambda_c = 0.135\ \text{ft/lb}^{1/3}) \tag{3.2}$$

$$t = 3.51\ \tau' W^{0.152} \quad (\lambda_c = 0.135\ \text{ft/lb}^{1/3}) \tag{3.3}$$

where R = surge radius, ft
r = scaled surge radius (dimensionless)
W = charge weight, lb (TNT)
t = time, sec
τ' = scaled time, sec/ft$^{1/2}$

By substituting equivalent weights of TNT in formulas 3.2 and 3.3, and using the values of r and τ' obtained in measurements of the JANGLE underground shot, it is possible to obtain a predicted curve for radial base surge growth for atomic bombs of different energy release at a scaled depth of 0.135 ft/lb$^{1/3}$. Curves derived in this manner for energy equivalents of 10, 20, 50 and 100 kilotons of TNT are presented in Fig. 3.6.

For convenience, r and τ' values for the JANGLE underground shot are listed in Table 3.2.

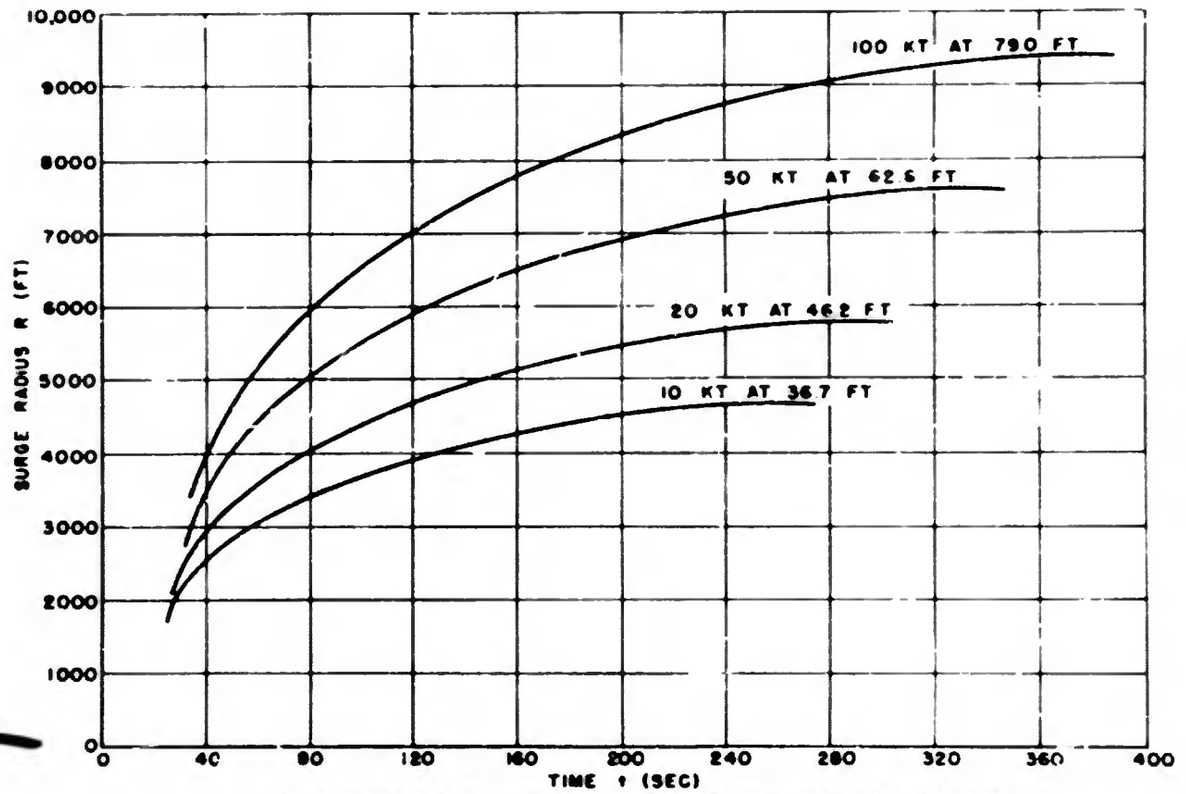

Fig. 3.6 Predicted Radial Growth of Base Surge for Atomic Weapons at a Scaled Depth of 0.135 Ft/Lb$^{1/3}$

TABLE 3.2

Base Surge Scaled Radius-Time Data
JANGLE Underground Shot

Scaled Surge Radius (r)	Scaled Time (τ')	Scaled Surge Radius (r)	Scaled Time (τ')
1.21	0.528	2.72	2.33
1.37	0.622	2.88	2.79
1.61	0.742	3.01	3.26
1.85	0.935	3.12	3.73
2.07	1.15	3.21	4.19
2.24	1.40	3.28	4.66
2.35	1.58	3.33	5.12
2.50	1.87	3.36	5.59
2.63	2.14	3.36	6.05

It is important to emphasize that the numerical results presented herein apply only to nuclear weapons fired at a scaled depth of 0.135 $ft/lb^{1/3}$ in a soil similar to the Nevada Test Site soil. Results with THF indicate that the largest, most rapidly-spreading surge clouds are formed by explosions at a scaled depth of about 1.0 $ft/lb^{1/3}$. The data also show that a base surge produced by an explosion in dry sand is larger and grows faster than the base surge produced by an equivalent explosion in the Nevada soil. The limited information available indicates that soils with low seismic velocities have the physical characteristics best suited for the formation of a base surge.

BIBLIOGRAPHY

A. B. Arons, G. A. Young, and M. L. Milligan, Further Investigation of the Base Surge, Interim Report No. 3 of NOL Project 152, NAVORD Report 2144, 1 June 1951.

J. J. Miller, Photographic Analysis, Operation JANGLE, Project 4.1a, Sandia Corporation, 26 March 1952.

G. A. Young, Base Surge Analysis - HE Tests, Operation JANGLE, Project 1(9)-4, U. S. Naval Ordnance Laboratory, 20 May 1952.

END